e-Zine for meteor observers meteornews.net

MeteorNews

ISSN 2570-4745 VOL 6 / ISSUE 1 / JANUARY 2021

Fireball recorded by Yuri Goryachko (Minsk, Belarus) at 02h44m UT on December 8, 2020 (Photo © and courtesy Yuri Goryachko)

Contents

Ursids (URS#015) major or minor shower, and another outburst in 2020?

Paul Roggemans

Pijnboomstraat 25, 2800 Mechelen, Belgium
paul.roggemans@gmail.com

The history of the Ursid meteor shower has been summarized and a case study based on video meteor orbits is presented. New mean orbits based on a large number of Ursid orbits for different thresholds of dispersion were calculated. The Ursids have a large diffuse radiant with a dense core caused mainly by Ursids recorded during or near the maximum activity. The activity profile based on 12 years video data displays an annual maximum at solar longitude 270.45° and a secondary maximum at 270.80° caused by occasional outbursts associated with dust trail encounters. The peak activity is rather sharp, about half a day for the annual maximum and only a couple of hours for the occasional outbursts. The orbital elements display a large spread which is also visible in the velocity distributions. The Ursids appear to be mainly faint meteors although the occasional outbursts produce some brighter meteors. Ursids ablate significantly higher in the atmosphere than the Geminids because of their fragile cometary composition. Lyytinen and Jenniskens (2006) predicted two possible dust trail encounters for 2020 December 22 with a possible high activity level. The parent comet 8P/Tuttle will return at its perihelion in August 2021 which means the 2020 Ursid activity occurs in a similar situation as in 1993 when very good ursid rates were observed.

1 Introduction

Although the Ursids appear in each shortlist of meteor showers as a major shower, it remains one of the poorest known major showers which remained unnoticed during many years. It was assumed that the Ursids escaped attention because of the often-unfavorable weather for most meteor observers in the northern hemisphere this time of the year. Apart from some outbursts the shower does not appear in observing reports or the activity remained below the detectability level, typical for minor showers.

The history of the Ursids has been summarized in this article and a case study has been made based on the publicly available video meteor orbit datasets. The video data can help to understand the structure of the Ursids as a meteoroid stream and whether this should be regarded as a major shower or rather as a minor shower with periodic outbursts.

2 Ursid history

The oldest mention of an Ursid outburst might have been recorded in Japan on 1795 December 20, the eve of the winter solstice (Imoto and Hasegawa, 1958). No details about the radiant are given but the date is close to that of possible Ursid activity, just five years after Pierre Méchain in Paris, France, had discovered the parent comet on 1790 January 9. Some historic reports about meteor rains from 1433 in Japan and 1532 in China at the solar longitude of Ursid activity may refer to past outbursts, but very little information is available.

First mention of possible meteor activity from the Ursids parent comet 8P/Tuttle were published in 1874 by A.S. Herschel in the British Association Report with a list of cometary radiants with the following data for Méchain-Tuttle's comet:

Méchain (1790 II)	$\alpha = 220°$, $\delta = +76°$	Dec. 20+
Tuttle (1858 I)	$\alpha = 221°$, $\delta = +77°$	Dec. 20+

This reference was cited by W.F. Denning (1916) mentioning that he had observed meteors from a radiant near β Ursa Minoris in various years between December 18–25 from a radiant at $\alpha = 218°$, $\delta = +76°$. The display had shown no special abundance and Denning called for further observations to recover this meteor shower. In 1923 W.F. Denning lists Méchain-Tuttle meteors with their radiant based on as few as 7 meteors plotted during "various" years (Denning, 1923). Probably the poor weather circumstances for this typical northern hemisphere meteor shower hampered observational efforts during the activity period as no distinct activity of Ursids can be found other than typical for any minor shower.

The Ursids didn't catch attention until observers at the Skalnaté Pleso Observatory (Slovakia) witnessed a meteor outburst in the early evening of Saturday 1945 December 22. Dr. Antonin Bečvář reported these observations as the discovery of a new, formerly unknown meteor shower (Bečvář, 1945). Antonin Bečvář (1901–1965) was one of the founders of the Skalnaté Pleso Observatory in the High Tatras mountains. In original publications the Ursids outburst of 1945 was referred to as Bečvář's meteor stream, Tuttleids and later as the Umids instead of Ursids.

Initially the outburst was reported with an activity level of 169 meteors per hour, which was often cited as a ZHR of 169. The number of meteors were a total of meteors counted

by 4 visual observers. In 1951 Dr. Zdeněk Ceplecha (1951) analyzed the observations again and obtained a much lower rate of 48 meteors per hour as an average for three observers. Looking at the rates in 10-minute intervals a peak of 108 meteors per hour was found at 18^h UT (mean value for 3 observers). The precise observing conditions aren't clear from literature, but the usual high meteor activity had been noticed right after twilight around 16^h30^m and further observations were hampered by the rising 84% illuminated Moon in Leo after 18^h30^m when also clouds disturbed when the high meteor activity had ceased.

Ceplecha (1951) also obtained photographic plates from Antonin Bečvář which allowed a more precise determination of the radiant position as well as an orbit for the Ursid meteors. It is not explained how the velocity was determined, this may have been assumed parabolic or the orbital period was assumed identical to that of the comet. The Ursid orbit was in perfect agreement with the orbit of comet Tuttle for return in 1939. The 1945 outburst occurred several years after the perihelion passage of 1940.0, when the parent comet was almost at the opposite side at its aphelion.

Alerted by the 1945 Ursids outburst, visual observations were organized at the Ondřejov observatory (Vanýsek, 1947) and the Skalnaté Pleso Observatory (Bochníček and Vanýsek, 1948). The observers concentrated on the determination of the radiant position while the actual hourly rates remained low in 1946. Further visual observations as well as radar observations did not detect any unusual activity for the Ursids. Prentice (1948) attempted visual observations of the Ursids on 1947 Dec. 22 and Dec. 23, first night had excellent conditions but only 1 possible Ursid was seen, the second night allowed only 25 minutes of observing under very unfavorable conditions, four of the eight meteors were possibly Ursids from which the author estimated an hourly rate of 20. The Ursids were also covered by radar observations at Jodrell Bank which confirmed low rates in 1947 (Clegg et al., 1948) and comparable low rates in all following years until 1953. In literature these radar hourly rates were quoted as representative for visual rates. However, because of the limitations of the radio techniques used and the lack of any decent calibration the only possible conclusion from these observations is that only low rates at best were observed in these years. It is important to know that radar monitoring was done during certain time intervals and not continuously, which means any unforeseen outburst could have remained unnoticed.

After 1953 until 1970, the Ursids were completely ignored, despite that this shower got included in the short lists of major meteor showers in most general astronomy books. When visual meteor observations were resumed in 1970 low hourly rates were reported throughout the 1970s. In general, low rates were confirmed by European, American and Japanese meteor observers and this continued during the first half of the 1980's. British radio observers reported enhanced activity on 1973 December 22 ($\lambda_\odot$ = 270.83°, eq.2000) lasting for 1 hour, unfortunately the exact source of the information is not known (Jenniskens, 2006).

The Ursids performed a great show in 1986. Radio observer Luc Gobin monitored radio echoes every day between 19^h30^m and 20^h30^m UT and on December 22 the number of echoes was about 2.5 times higher than other nights (Roggemans and Steyaert, 1987). The radio observations by Luc Gobin were soon confirmed by visual observers in the UK under unfavorable circumstances as well as by two Norwegian visual observers under good circumstances. "*On December 22, Kai Gaarder saw 94 Ursids in 4 hours from 17^h00^m–21^h00^m UT. Lars Trygve Heen saw 54 Ursids in one hour, 21^h00^m–22^h00^m UT. Several Ursid fireballs were counted*" (Hillestad, 1987). Kai Gaarder commented to the author: "*I was one of the few lucky to observe the great Ursid outburst of 1986. I was expecting to see about 5 Ursids an hour, but was stunned by the activity comparable to a modest Perseid maximum as I remember it.*". The maximum occurred on 1986 December 22, at 21^h30^m ($\lambda_\odot$ = 270.93° J2000) with a ZHR = 122 ±17. This is about 0.38° earlier in $\lambda_\odot$ than the 1945 outburst (Roggemans, 1987). The 1945 outburst was in progress when observers noticed it in twilight, no information is available of what happened before the 1945 observations could start because of the twilight in Slovakia. Another remarkable fact is that the 41 years between 1945 and 1986 represents almost exactly three times the orbital period of the comet. The 150 years between the possible first mention of Ursids in 1795 and the 1945 outburst is about eleven times the orbital period of the parent comet (Roggemans, 1987). Steyaert (1987) derived a period of 13.64 years. Unfortunately, no observational data seems to exist around the Ursid activity for some interesting years like1836 and 1904 to confirm this periodicity.

Both the 1945 and 1986 outbursts took place when the parent comet was near aphelion. Jenniskens et al. (2002) found that it takes 45 revolutions for the dust released from the comet to lag half an orbit relative to the comet and to get into the Earth's orbit while the comet's orbit is rather far from Earth's orbit.

In 1994 the Ursids displayed an outburst when the parent comet had passed through its perihelion in 1994. Ilkka Yrjölä recorded significantly enhanced radio echo rates around the Ursid time of maximum in both 1993, before the perihelion passage of the parent comet and in 1994 after the passage (Jenniskens, 2006). These outbursts were much broader than the aphelion outbursts of 1945 and 1986. The 1994 Ursids outburst was confirmed by Japanese visual observers (Ohtsuka et al., 1995). Poor weather hampered most Japanese, only H. Shioi could successfully observe visually although the limiting magnitude was poor (5.2) resulting in a maximum ZHR of more than 100 but with large error margins at $\lambda_\odot$ = 270.75° (eq. 2000.0), 200 days after the parent comet had passed through the descending node 0.06 AU outside the Earth orbit. The same report mentions that a similar Ursid outburst had been observed by Bob Lunsford on 1993 December 22 at $\lambda_\odot$ = 270.81° (eq. 2000.0), 165 prior to the parent comet's passage through the

descending node. Bob Lunsford wrote the author about this: "*My best Ursid year was 1993 when I counted 81 during 4.56 hours of observing on December 22nd. The limiting magnitude was excellent that night as it ranged from +7.11 at the start of the session (01:00 Local Time) to +5.70 at 06:00 local time. My best period produced 26 Ursids during 52 minutes of observing with an LM of +6.77. 21 Sporadics were also seen during this period which was twice as many as any other period*."

Ohtsuka et al. (1995) also refers to enhanced Ursid activity with several fireballs observed in Japan on 1981 December 22 at $\lambda_\odot = 270.82°$ when the parent comet had passed 394 days earlier through its descending node 0.08 AU outside the Earth orbit during its perihelion passage in 1980. Ohtsuka et al. (1995) concluded from these 1981, 1993 and 1994 observations that the Ursid meteoroid stream dust had spread at least over a range of $-12° < \Delta M < +28°$ where ΔM is the difference between the mean anomalies of the comet and the Ursid meteoroid stream. Also, in 1979 enhanced Ursid activity had been reported on December 22 by observers in Sogne, Norway, about 8 months before the perihelion passage in 1980 (Kronk, 1988).

Meteoroid stream modelers Esko Lyytinen and Peter Jenniskens discovered that the Ursid meteor shower displayed broad filaments with outbursts around the perihelion passage of parent comet 8P/Tuttle with isolated narrow outbursts with the parent comet at its aphelion. They applied the technique used for the Leonids to calculate the 8P/Tuttle dust trail encounters. This study explained the past observed outbursts and also predicted that the 1405 dust trail might be encountered on 2000 December 22 at 7^h59^m UT and as well as perhaps the 1392 trail at 8^h38^m UT (Jenniskens and Lyytinen, 2000).

A dedicated observing campaign was organized in California and observations started at 5^h25^m UT, initially just a single occasional Ursid was seen. After 7^h UT Ursids appeared more often and after 8^h UT it was obvious an outburst was in progress with relatively faint meteors of magnitude +3 and +5. The peak activity reached a ZHR of about 90 at $\lambda_\odot = 270.78°$ (J2000). The observed profile had its maximum between the predicted times for the 1405 and 1392 dust trails, indicating that both trails contributed to the activity profile (Jenniskens and Lyytinen, 2001).

More years with possible enhanced Ursid activity were predicted for 2002, 2004, 2006, 2014, 2016 and 2020. The 2002 predicted enhanced activity did not materialize. Visual observations were seriously hampered by an 89% illuminated Moon while radio data showed only weak activity during the 8 hours covering the time of theoretical peak activity (Boschin et al., 2003). These results were confirmed by the Dutch radio observer Peter Bus in Groningen. The 2004 prediction did not get conclusive observational evidence beyond the usual low or non-existence Ursid activity (McBeath, 2005). Also 2006 did not produce any significant activity and certainly nothing like an outburst (Jenniskens, 2006b).

Canadian meteor observer, Pierre Martin watched a modestly enhanced Ursid activity in 2009 when he saw 43 Ursids in 3.68 hours including a –5 Ursid fireball at a fairly nice sky on December 22 between 7^h20^m and 11^h30^m UT, $\lambda_\odot = 270.44°$ to 270.61°. This spectacle reminded him of a similar enhanced Ursid display seen in 1988 but not documented in a dedicated visual meteor watch. Both Ilkka Yrjola and Esko Lyytinen measured elevated rates using the technique of meteor forward scattering. From their data, the outburst peaked at Dec. $22^d09^h \pm 0.5$ hr UT, $\lambda_\odot = 70.51 \pm 0.02°$ (Jenniskens, 2010).

Video and forward scatter observations confirmed the predicted Ursid dust trail that crossed the Earth orbit at $\lambda_\odot = 270.84°$ on 2014 December 22–23, but hourly rates weren't comparable to the 1945 or 1986 levels (Moreno-Ibáñez et al., 2017). Also, Peter Brown, Western University, reported that a significant outburst of Ursid meteors was detected by the Canadian Meteor Orbit Radar (CMOR) between Dec. $22^d23^h15^m$ and $23^d00^h45^m$ UT. The apparent activity maximum occurred at Dec. 23^d00^h UT ($\lambda_\odot = 270.85 \pm 0.03°$, J2000) with a ZHR in excess of 50 (Brown et al., 2015). The 2014 enhanced Ursid activity was also confirmed in Slovakia (Gajdoš et al., 2015).

In 2016 the Ursids showed a high activity around 10^h30^m (UT) on the 22nd December ($\lambda_\odot = 270.78°$). Although a strong Ursid activity was also observed in 2014, the activity in 2016 was weaker than in 2014 (Ogawa, 2017). E. Lyytinen had calculated an encounter with the A. D. 1076 dust ejecta of 8P/Tuttle at 2016 Dec. $22^d10^h05^m$ UTC, at $\lambda_\odot = 270.760°$. P. Jenniskens reported that the Earth encountered the A. D. 1076 ejected dust of comet 8P/Tuttle on 2016 Dec. $22^d11^h35^m$ UTC, at $\lambda_\odot = 270.825 \pm 0.010°$ (J2000) (Jenniskens, 2017).

In 2019 the United Arab Emirates Camera Network, UACN, registered a significant Ursid activity during the night of December 22–23. They collected a nice set of orbits during the time interval of $270.40° < \lambda_\odot < 270.65°$, corresponding to December 22–23, at about 20^h00^m–02^h00^m UT. After this interval only few Ursids could be registered. (Roggemans and Johannink, 2020). Visual observer Pierre Martin in Canada observed 14 Ursids on December 23 between 0^h00^m and 10^h40^m UT (Martin, 2020). Also, SonotaCo reported only few Ursid orbits in 2019.

Ilkka Yrjölä from Finland has been monitoring the Ursids with radio forward meteor scatter consistently and he has detected high Ursid activity in years around the return of the comet, suggestive of an Ursid Filament (Jenniskens, 2020).

Other years the Ursid activity remained with low annual activity. The coverage with permanent radio and video monitoring makes it unlikely that any enhanced activity or short outburst would occur unnoticed. Visual observers were too few in number in the past across the planet to monitor activity around the clock. Specific about the Ursids, Norman W. McLeod, one of the most active visual observers in modern times commented these were like the Quadrantids in the sense that observers had to be within 12

hours of the maximum to see much (Kronk, 1988). This being said, it is obvious that several, if not many past Ursid outbursts must have passed unnoticed due to poor coverage and often very bad weather around the time of the year.

Table 1 – The median values for the mean Ursid orbit obtained by CAMS (2016) and SonotaCo (Koseki 2021) compared with the orbit of 8P/Tuttle.

	URS (2016)	URS (2021)	8P/Tuttle (2008)
$\lambda_\odot$	271.0°	270.5°	–
α_g	219.9°	219.0°	–
δ_g	+75.4°	+75.3°	–
v_g	32.9 km/s	33.0 km/s	–
a	4.87 A.U.	4.92 A.U.	5.70 A.U.
q	0.940 A.U.	0.940 AU	1.027 A.U.
e	0.807	0.809	0.8199
ω	205.6°	205.9°	207.5°
Ω	270.1°	270.5°	270.3°
i	52.6°	52.8°	54.98°
N	62	390	

For many years the number of known orbits for Ursid meteoroids was very low. For instance, a dedicated observing project for the Ursids in California in 1997 by Peter Jenniskens increased the number of available Ursid orbits at once from two to twenty-four orbits. Some major video meteor networks changed the picture a lot in past 12 years. The orbits published in literature are listed in *Table 1*.

3 The Ursids as observed by video camera networks

CAMS, EDMOND and SonotaCo together have 1101923 video meteor orbits publicly available covering the period 2006 to 2019. In this section we will extract all Ursid orbits from these datasets. Each network has its own criteria to identify the shower association but a quick verification proves that several obvious Ursid orbits were not identified as Ursids. In order to consider all the orbits with the same criteria the author applied an iterative procedure starting from some initial reference orbit to identify all orbits that form a concentration of similar orbits which define the meteor shower. This method has been described before (Roggemans et al., 2019).

To calculate a reference orbit for a collection of similar orbits we do not use the median or average values of the orbital elements, but we compute the mean orbit according to the method described by Jopek et al. (2006). To compare orbits on similarity researchers established different discrimination criteria, often abbreviated as D-criteria. The D-criteria that we use are these of Southworth and Hawkins (1963), Drummond (1981) and Jopek (1993) combined. The oldest and most popular D-criterion, the one established by Southworth and Hawkins or D_{SH} proved often too tolerant and unsuitable for short period orbits near the ecliptic. It is not unusual that orbits which are very similar according to D_{SH}, fail for another D-criteria such as that of Drummond or D_D.

In order to distinguish dispersed and compact orbits we define five classes with different threshold levels of similarity, kind of shells with comparable degree of dispersion. These should help to visualize the degree of dispersion and compactness within the meteoroid stream. The different classes of similarity are defined as follows:

- Low: $D_{SH} < 0.25$ & $D_D < 0.105$ & $D_H < 0.25$;
- Medium low: $D_{SH} < 0.2$ & $D_D < 0.08$ & $D_H < 0.2$;
- Medium high: $D_{SH} < 0.15$ & $D_D < 0.06$ & $D_H < 0.15$;
- High: $D_{SH} < 0.1$ & $D_D < 0.04$ & $D_H < 0.1$;
- Very high: $D_{SH} < 0.05$ & $D_D < 0.02$ & $D_H < 0.05$.

Removing the classes with better similarity for instance allows one to look at the shell with very dispersed orbits alone. To reduce the number of iterations in our procedure, we remove all orbits which are a priori excluded from being related to the Ursids meteor shower. To estimate the activity period, the radiant size and the velocity range, we take a sample reference orbit from literature and make a preliminary run to identify all possible Ursid orbits for this reference. The activity period, radiant size and velocity range are chosen slightly wider than obtained from this preliminary estimation.

- Time interval: $256° < \lambda_\odot < 283°$;
- Radiant area: $174° < \lambda_g - \lambda_\odot < 254°$ & $+62° < \beta_g < +83°$;
- Velocity: 25 km/s $< v_g <$ 40 km/s.

158576 orbits are available within the solar longitude interval, 2757 orbits have the ecliptic radiant within the above area and their geocentric velocity within the chosen range. Starting with the mean orbit as reference, the iterative loop converges with a selection of 1986 similar orbits for which a final mean orbit can be computed for the Ursids. Various researchers use different standards and criteria to define similar orbits. Some shower associations are based only on the radiant position and velocity, some consider very dispersed orbits and others select only very similar orbits to compute a mean orbit for a stream. The problem is that it is often not known how orbits were selected and which threshold has been used to compute a mean orbit. Therefore, the author defined the different classes of similarity in order to keep track of the dispersed particles as well as the dense concentration that makes up the core of the meteoroid stream. For each similarity class a mean orbit has been calculated. The results are listed in *Table 2*.

The 1986 low similarity orbits include 358 dispersed orbits with a slightly lower geocentric velocity of v_g = 32.0 km/s, a lower eccentricity and lower inclination. The advantage of this method is that we can remove or isolate dispersed orbits like shells of orbits with different degrees of dispersion. The more towards the core of the shower with very similar orbits, the higher the geocentric velocity, the higher the eccentricity and the inclination becomes.

Table 2 – The mean orbits calculated for each similarity class according to the threshold of the D-criteria for the Ursids based on the shower identification by the author.

	Low	Medium Low	Medium High	High	Very high
$\lambda_\odot$ (°)	270.48	270.48	270.49	270.53	270.6
α_g (°)	219.1	219.0	219.0	219.1	219.1
δ_g (°)	+75.8	+75.8	+75.8	+75.7	+75.7
$\Delta\alpha$ (°)	0.86	0.81	1.38	1.48	1.28
$\Delta\delta$ (°)	–0.57	–0.61	–0.57	–0.45	–0.26
H_b (km)	101.7	102.0	102.2	102.4	102.6
H_e (km)	89.4	89.7	89.9	90.1	89.8
v_g (km/s)	32.8	32.9	32.9	33.0	33.0
λ-$\lambda_\odot$ (°)	217.5	217.6	217.8	217.9	218.0
β (°)	+71.8	+71.8	+71.9	+72.0	+72.0
a (AU)	4.85	4.92	4.96	4.98	5.04
q (AU)	0.9297	0.9325	0.9354	0.9376	0.9388
e	0.808	0.811	0.811	0.812	0.814
ω (°)	206.5	206.7	206.4	206.2	206.0
Ω (°)	270.0	269.9	270.0	270.3	270.5
i (°)	51.8	51.9	52.3	52.6	52.6
Π (°)	116.5	116.6	116.5	116.5	116.5
Q (AU)	8.8	9.0	9.0	9.0	9.2
T_j	1.78	1.75	1.75	1.74	1.73
P (y)	10.7	11.1	11.1	11.1	11.3
N	1986	1628	1311	952	496

Table 3 – The mean orbits calculated for each camera network separately for the Ursids that fulfill the high threshold criteria based on the shower identification by the author.

	CAMS	EDMOND	SonotaCo
$\lambda_\odot$ (°)	270.69	270.49	270.49
α_g (°)	219.4	219.1	218.8
δ_g (°)	+75.7	+75.8	+75.6
H_b (km)	103.3	101.3	102.4
H_e (km)	92.8	88.1	89.2
v_g (km/s)	32.9	32.9	33.2
λ-$\lambda_\odot$ (°)	217.9	217.7	218.3
β (°)	+72.1	+72.0	+71.9
a (AU)	4.99	4.92	5.05
q (AU)	0.9382	0.9373	0.9376
e	0.812	0.810	0.814
ω (°)	206.1	206.3	206.2
Ω (°)	270.3	270.3	270.2
i (°)	52.4	52.5	52.8
Π (°)	116.4	116.6	116.3
Q (AU)	9.1	8.9	9.2
T_j	1.74	1.75	1.72
P (y)	11.2	10.9	11.3
N	300	334	318

The three main camera networks use different hardware. CAMS uses a standard of small FoV optics (30° × 22°) and has its own trajectory solver. SonotaCo uses the same Watecs as CAMS but mainly with larger fields of view and has its own detection software and trajectory solver. EDMOND uses the same software as SonotaCo but collects data with a large variety of different cameras and various optics. Question is if it is opportune to mix the data of all three networks for a single analysis? To test this, we calculated the mean orbits for the data of each network. To eliminate outliers, we use the high threshold similarity class ($D_D < 0.04$). The results are compared in *Table 3* and all the parameters are in very good agreement, far within the standard deviation of these values (not listed). The results listed in *Table 2* and *Table3* are in good agreement with the values previously published in literature (*Table 1*).

Note that our sample of CAMS is based on 300 Ursids, about 5 times more than used by Jenniskens (2016) on exactly the same dataset. It is not known how the orbits were selected for the result of CAMS in *Table 1*. Several perfect Ursid orbits were listed as sporadics in the CAMS dataset. In EDMOND and SonotaCo this occurs mainly for dispersed Ursids which were not recognized as shower meteors.

Note that the Ursids have about the same velocity as the Geminids (GEM#4), but the beginning heights of the Ursids are significant above that of the Geminids. For instance for the Geminids we obtained $H_b = 97.0 \pm 2.5$ km and $H_e = 85.5 \pm 4.4$ km, roughly 4 to 5 km deeper in the atmosphere. The reason for this is the composition of the Ursid meteoroids which consists of fragile cometary material that interacts differently with the high atmosphere than the more compact Geminid meteoroids (Roggemans, 2017).

4 The Ursid radiant

In most astronomical literature meteor showers are listed with equatorial coordinates for their geocentric radiants. For most inexperienced readers this is confusing as the position in right ascension and declination refers to a point source. When the 1945 Ursid outburst happened, visual observers at Skalnaté Pleso plotted Ursids on star maps in an attempt to define the Ursid radiant. The results led to some controversy as the plotted Ursids failed to fit the assumption to have a point source or at least very narrow radiant position (Ceplecha, 1951). Of course, plotting errors were problematic but in that time visual plottings were the only way to define radiant positions. Moreover, radiants were assumed to be very narrow in size. How big is a meteor shower radiant at the sky? The size depends upon the meteor shower velocity as well as on the nature of the meteor shower. Very slow velocity meteor showers produce meteors from a widely scattered radiant area. Old and dispersed meteor showers display meteors over a long activity range from diffuse radiants. The Ursid meteoroids that manage to encounter our planet needed as long as about 600 years to get far enough inside the Earth orbit and therefore got dispersed by gravitational and other forces.

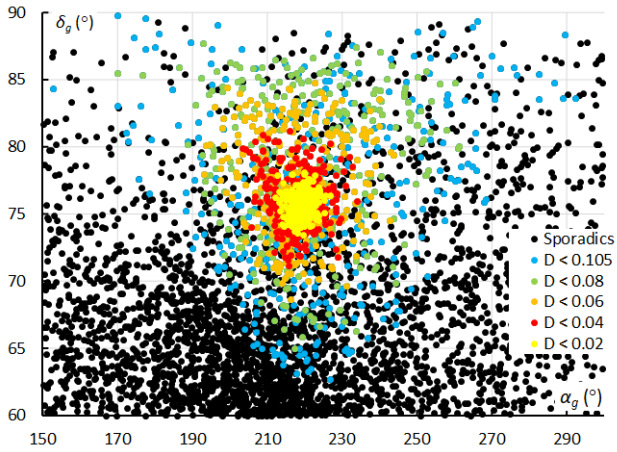

Figure 1 – The geocentric Ursid radiant in equatorial coordinates.

The Ursids may be expected to display a diffuse radiant unless some compact dust trail encounters the Earth. The geocentric radiants in equatorial coordinates for sporadic orbits and for the Ursids are displayed in *Figure 1*. As can be seen, the low threshold radiants are widely dispersed (blue dots). Since the radiant is close to the pole the right ascension covers a wide range. Even the high threshold Ursid radiants span more than 10° in declination. The concentration of black dots below the Ursids is caused by early Quadrantids.

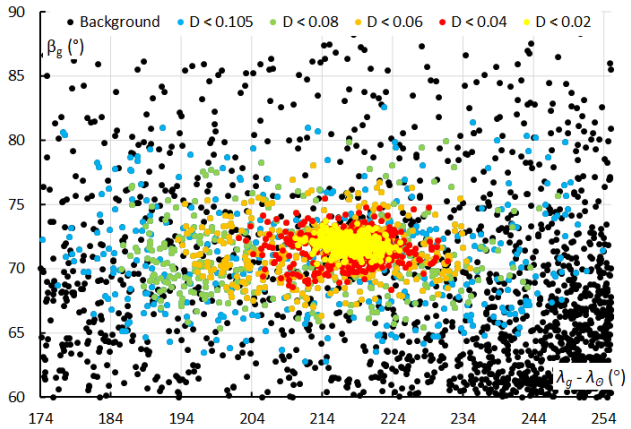

Figure 2 – The geocentric Ursid radiant in Sun-centered ecliptic coordinates.

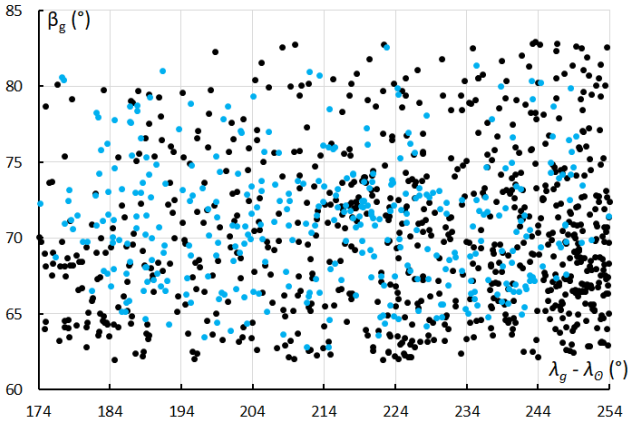

Figure 3 – The backround of Figure 2 with sporadics and dispersed low threshold Ursids which appears hidden by the high and very high threshold Ursid radiants in Figure 2.

Equatorial coordinates are not very suitable to compare meteor shower radiants because of the radiant drift caused by the movement of the Earth around the Sun. The Sun-centered ecliptic coordinates neutralizes this radiant drift by simply subtracting the solar longitude from the ecliptic longitude. *Figure 2* shows this plot. With the ecliptic latitude around 72°, close to the ecliptic pole the radiant appears rather elongated in longitude. Also, in these ecliptic coordinates the Ursids appear as a widely dispersed radiant with a very compact concentration of very similar orbits (red and yellow dots). *Figure 3* displays the same region with only the sporadic radiants and low threshold Ursids. Anyone using only radiant position and velocity to identify Ursids would count all these sporadics as Ursids while their orbits are very different from the Ursid orbit.

5 Ursid activity profiles based on orbits

The number of Ursid orbits collected gives us a glue about the activity level. Poor weather and the variable capture capacity will affect the number of sporadic orbits in the same way as the Ursid orbits. We count the number of sporadic orbits and the number of Ursid orbits in time bins of 0.25° in solar longitude shifted by 0.05 in solar longitude at each step and calculate the percentage of Ursid orbits relative to the number of sporadic orbits. As sporadic orbits we consider all orbits that could not be identified with any known meteoroid stream. The resulting activity curve is shown in *Figure 4*.

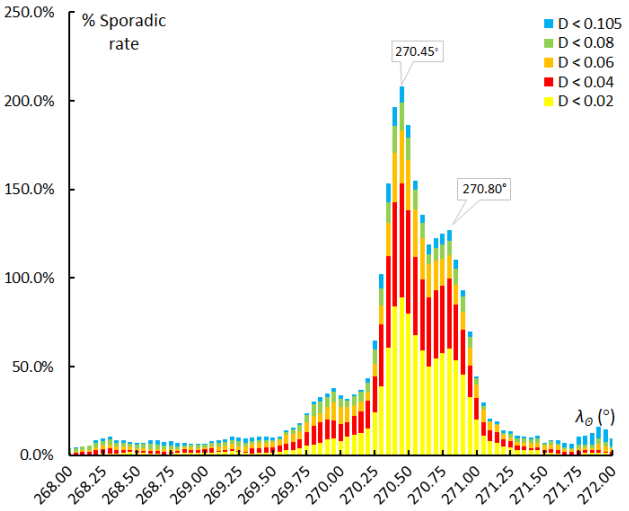

Figure 4 – The number of Ursid orbits in function of the solar longitude expressed as a percentage of the sporadic background counted in bins of 0.25° in solar longitude, shifted by 0.05°.

The most striking aspect is the shape of the profile with a peak that occurs about a little bit earlier than the outbursts observed in the past. The shoulder in the profile 0.35° later may indicate a secondary maximum. The low threshold, very dispersed Ursid orbits (blue and green) have very little effect on the activity profile. The trend is very well visible among the very compact group of Ursid orbits (red and yellow). The Ursids seem to be very variable in strength from year to year. Therefore, we compare the number of Ursid orbits collected year by year, not as percentages but raw numbers of Ursid orbits counted in 0.25° bins in solar

longitude, shifted by 0.05° for each step. No calibration was applied. For 2006 and 2007 too few orbits were recorded. In 2019 Ursids were almost absent or perhaps missed. SonotaCo covers the Japanese observing window, EDMOND covers mainly the European observing window while the CAMS network mainly covers the American observing and the European window. Thanks to the long winter nights there is a large overlap between the networks. With a circumpolar radiant active during the longest night of the northern hemisphere the three networks provide global coverage, if lucky with the weather. The number of available orbits by each network is mentioned for the interval $270.0° < \lambda_\odot < 271.5°$, to verify if the suspected period with a possible maximum activity has been covered by the networks or not.

2008: SonotaCo had 55 orbits of which 6 Ursids, EDMOND had 90 orbits with 47 Ursids. The highest number of orbits was recorded at $\lambda_\odot = 270.45°$ by EDMOND. Only the usual annual low Ursids activity was recorded without anything unusual.

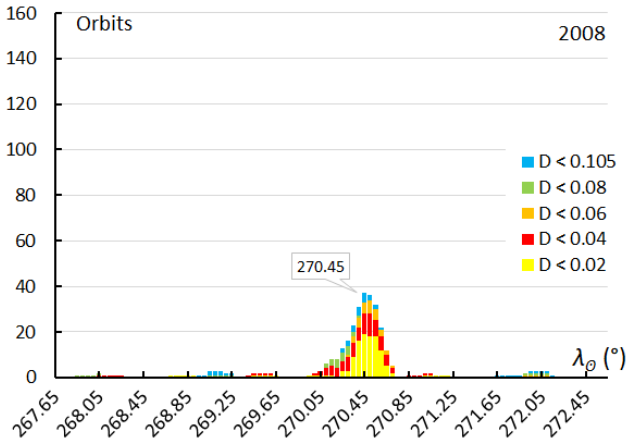

Figure 5 – The number of Ursid orbits counted in 2008 in bins of 0.25° in solar longitude shifted 0.05° at each step.

2009: SonotaCo had 272 orbits of which 32 Ursids, EDMOND had no orbits at all during the suspect interval. The highest number of orbits was recorded at $\lambda_\odot = 270.60°$.

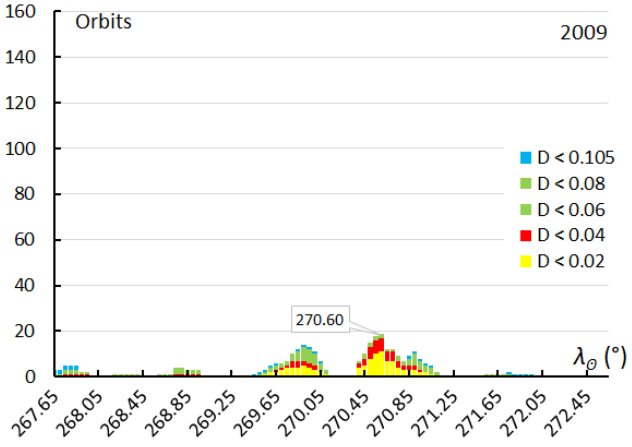

Figure 6 – The number of Ursid orbits counted in 2009 in bins of 0.25° in solar longitude shifted 0.05° at each step.

2010: SonotaCo had 211 orbits of which 50 Ursids, EDMOND had only 3 orbits but no Ursids, CAMS had no orbits in the suspect interval. The highest number of orbits was recorded at $\lambda_\odot = 270.50°$.

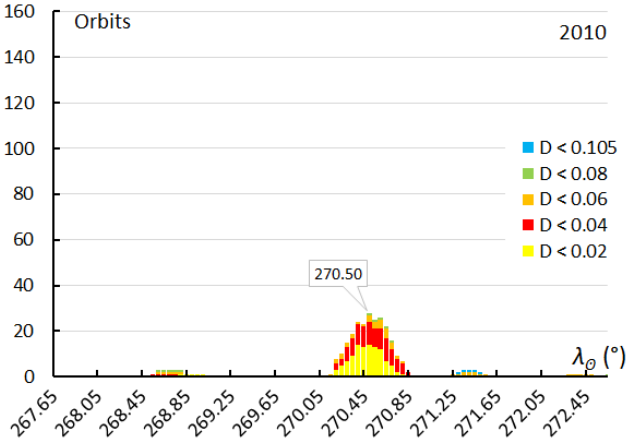

Figure 7 – The number of Ursid orbits counted in 2010 in bins of 0.25° in solar longitude shifted 0.05° at each step.

2011: SonotaCo had 376 orbits of which 89 Ursids, EDMOND had 293 orbits of which 105 Ursids, CAMS had 748 orbits of which 47 Ursids in the suspect interval. The highest number of orbits was recorded at $\lambda_\odot = 270.40°$.

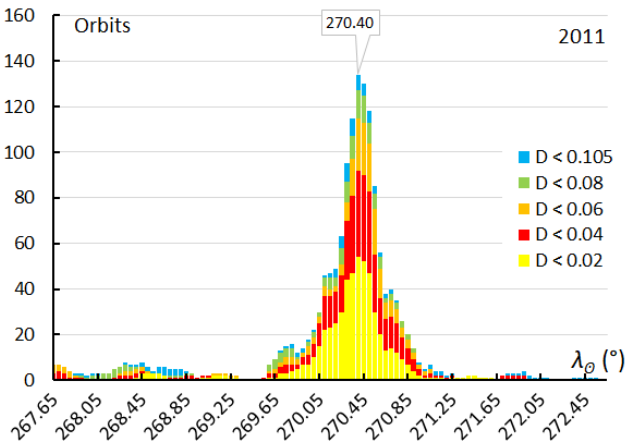

Figure 8 – The number of Ursid orbits counted in 2011 in bins of 0.25° in solar longitude shifted 0.05° at each step.

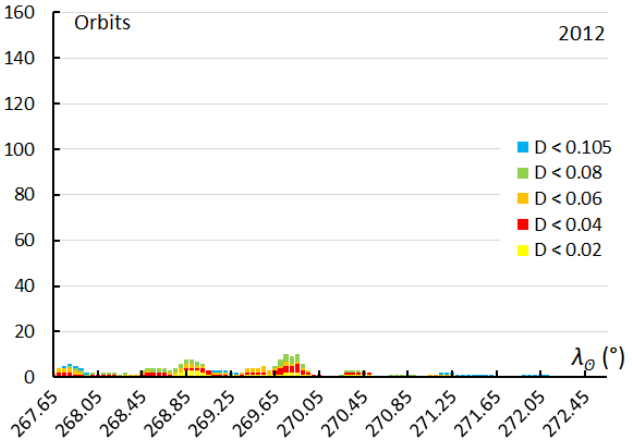

Figure 9 – The number of Ursid orbits counted in 2012 in bins of 0.25° in solar longitude shifted 0.05° at each step.

2012: SonotaCo had 34 orbits of which 3 Ursids, EDMOND had 39 orbits of which 3 Ursids, CAMS had no orbits in the suspect interval. During this year the suspected time interval with the possible Ursid maximum was missed.

2013: SonotaCo had 155 orbits of which 17 Ursids, EDMOND had 98 orbits of which 13 Ursids, CAMS had 544 orbits of which 66 Ursids in the suspect interval. The highest number of orbits was recorded at $\lambda_\odot = 270.60°$. The highest numbers of Ursid orbits recorded seem to be shifted few hours later than at $\lambda_\odot = 270.45°$. Most of these Ursids were recorded by CAMS in the USA. The number of orbits dropped suddenly as the next observing window obviously suffered poor observing conditions.

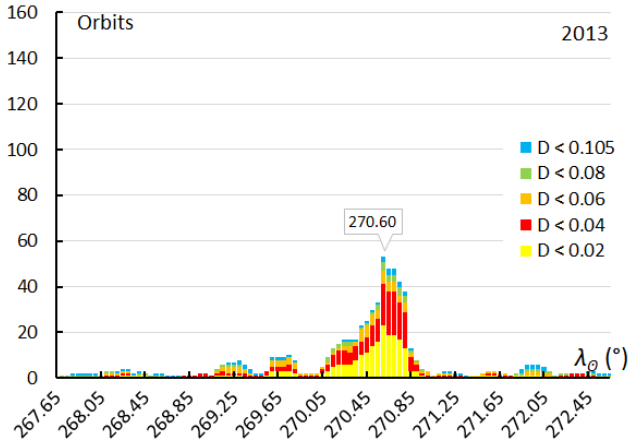

Figure 10 – The number of Ursid orbits counted in 2013 in bins of 0.25° in solar longitude shifted 0.05° at each step.

2014: SonotaCo had 170 orbits of which 23 Ursids, EDMOND had 108 orbits of which 48 Ursids, CAMS had 496 orbits of which 31 Ursids in the suspect interval. The highest number of orbits was recorded at $\lambda_\odot = 270.85°$. This year Esko Lyytinen predicted a possible encounter with a dust trail from 1405 at $\lambda_\odot = 270.838°$ (Jenniskens, 2006). This encounter was also confirmed by CMOR and by other video observing efforts. Although the peak level was rather modest this peak occurred about 0.4° in solar longitude later than the usual annual Ursid maximum.

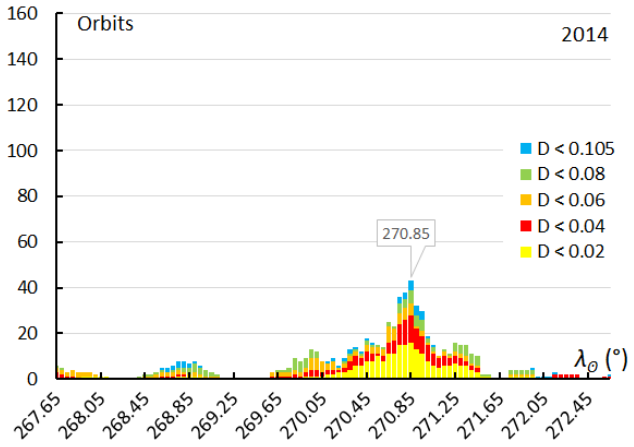

Figure 11 – The number of Ursid orbits counted in 2014 in bins of 0.25° in solar longitude shifted 0.05° at each step.

2015: SonotaCo had 45 orbits of which 3 Ursids, EDMOND had 166 orbits of which 43 Ursids, CAMS had 107 orbits of which 1 Ursid in the suspect interval. The highest number of orbits was recorded at $\lambda_\odot = 270.70°$.

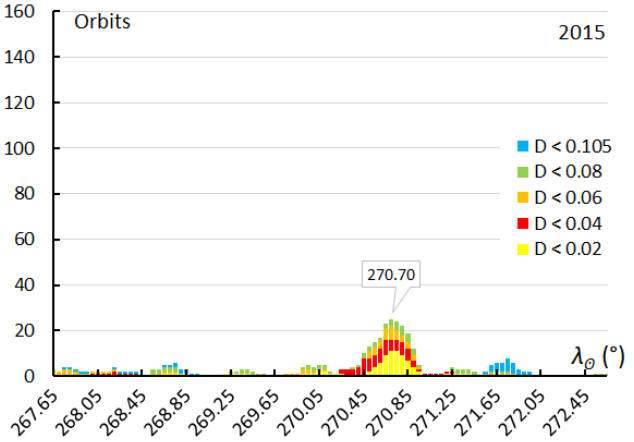

Figure 12 – The number of Ursid orbits counted in 2015 in bins of 0.25° in solar longitude shifted 0.05° at each step.

2016: SonotaCo had 109 orbits of which 12 Ursids, EDMOND had 654 orbits of which 148 Ursids, CAMS had 485 orbits of which 149 Ursid in the suspect interval. The highest number of orbits was recorded at $\lambda_\odot = 270.80°$. Also, this year Esko Lyytinen had predicted the possible encounter of a dust trail of 1076 at $\lambda_\odot = 270.76°$ (Jenniskens, 2006). The profile is interesting as the first maximum which is the annual Ursid peak was unusually strong and mainly covered by EDMOND, while the maximum due to the dust trail of 1076 was mainly covered by CAMS in the USA.

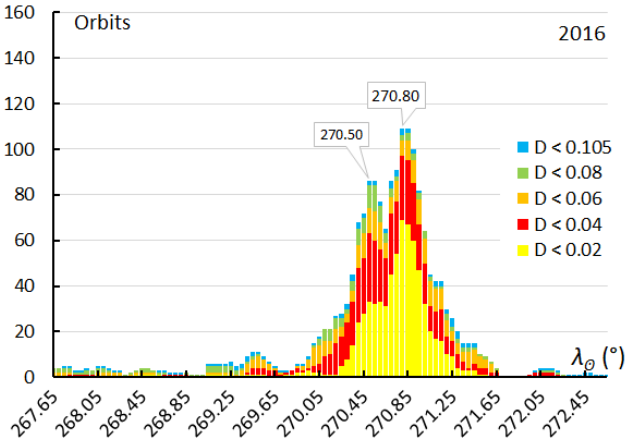

Figure 13 – The number of Ursid orbits counted in 2016 in bins of 0.25° in solar longitude shifted 0.05° at each step.

2017: After 2016 no more EDMOND orbit has been released while CAMS data from 2017 onwards is still kept under embargo. Only SonotaCo data is available and had 313 orbits of which 99 Ursids in the suspect interval. The highest number of orbits was recorded at $\lambda_\odot = 270.75°$.

The activity profile in *Figure 4* shows the annual Ursid maximum at $\lambda_\odot = 270.45°$ and a shoulder caused by dust trails encountered in some years at about $\lambda_\odot = 270.80°$.

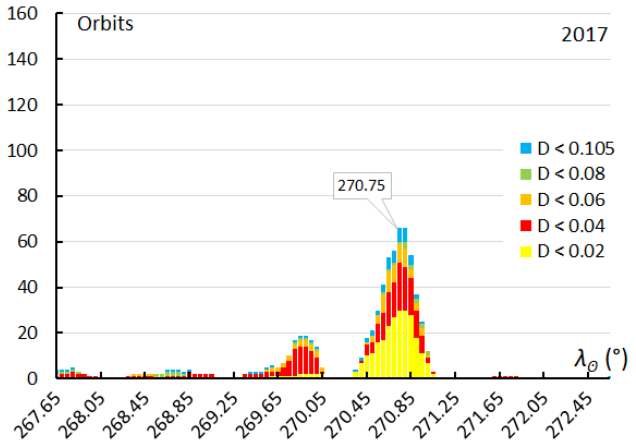

Figure 14 – The number of Ursid orbits counted in 2017 in bins of 0.25° in solar longitude shifted 0.05° at each step.

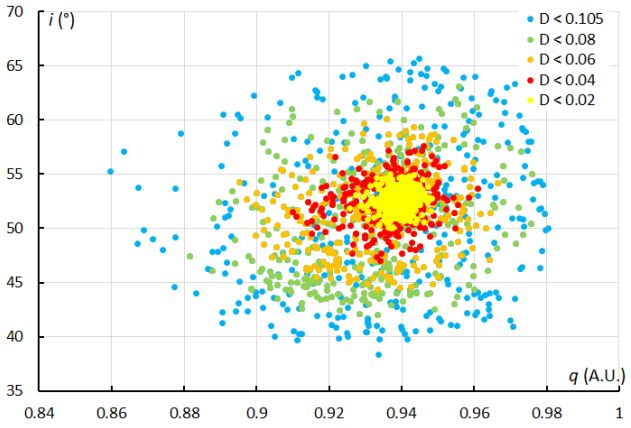

Figure 16 – The distribution of inclination *i* against the perihelion distance *q* for the Ursids for the different classes of dispersion.

6 The Ursid orbital elements

The Ursid parent comet 8P/Tuttle has its node far outside the orbit of the Earth so that dust released from the comet can only encounter the Earth when it gets far enough inside the comet's orbit. Esko Lyytinen and Peter Jenniskens solved this mystery (Jenniskens, 2006). After 45 revolutions the dust lags half an orbit behind the comet and intersects the Earth's orbit. This explains the outbursts when the comet was at its aphelion. Besides these outbursts the Ursids also display annual activity although comparable to typical minor shower activity except for some years when specific dust trails encounter the Earth.

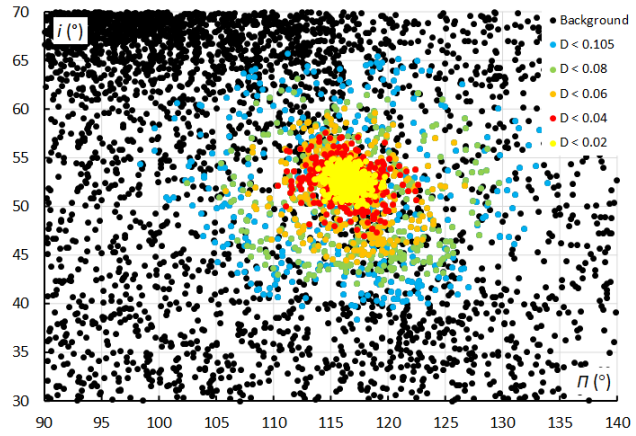

Figure 15 – The distribution of inclination *i* against the length of perihelion *Π* for non-Ursids and the Ursids for the different classes of dispersion.

Looking at the orbital elements of the Ursids, we see a large spread on the orbits which form a rather diffuse meteoroid stream with a distinct core of very similar orbits. The spread on Ursid orbits in *Figure 15* is larger than for most other meteoroid streams. The concentration in the upper left corner is caused by Quadrantid orbit. The distribution of the perihelion distance *q* against the inclination *i* shows a spread of more than 25° in inclination (*Figure 16*).

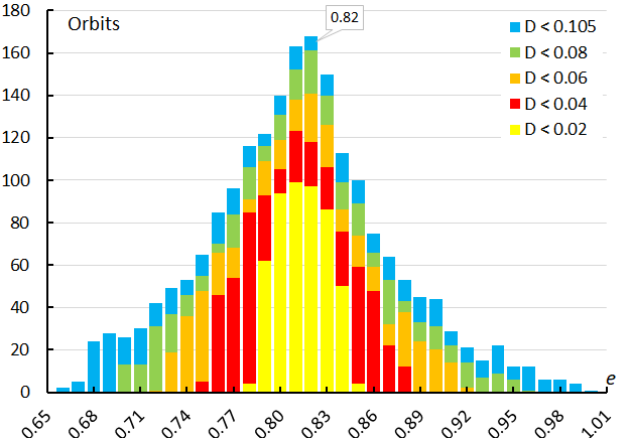

Figure 17 – Histogram with the distribution of the eccentricity *e* for the Ursid orbits with different colors for the shells in function of dispersion, from dispersed (blue, low similarity) to compact (yellow, very high similarity).

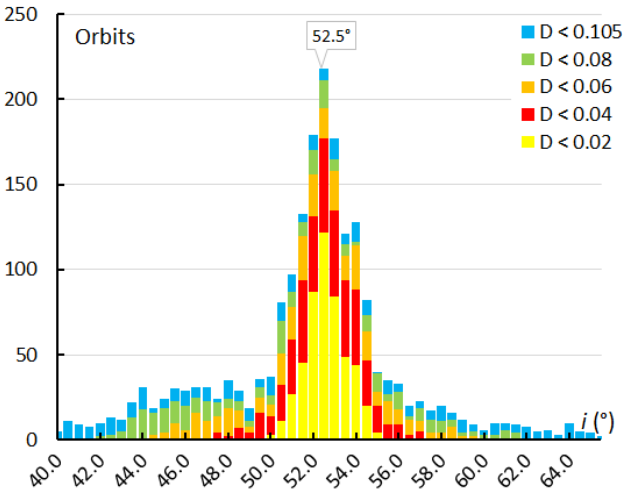

Figure 18 – Histogram with the distribution of the inclination *i* for the Ursid orbits with different colors for the shells in function of dispersion, from dispersed (blue, low similarity) to compact (yellow, very high similarity).

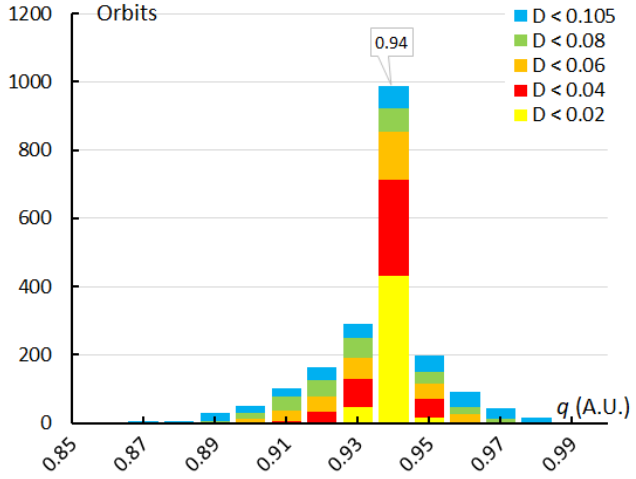

Figure 19 – Histogram with the distribution of the perihelion distance q for the Ursid orbits with different colors for the shells in function of dispersion, from dispersed (blue, low similarity) to compact (yellow, very high similarity).

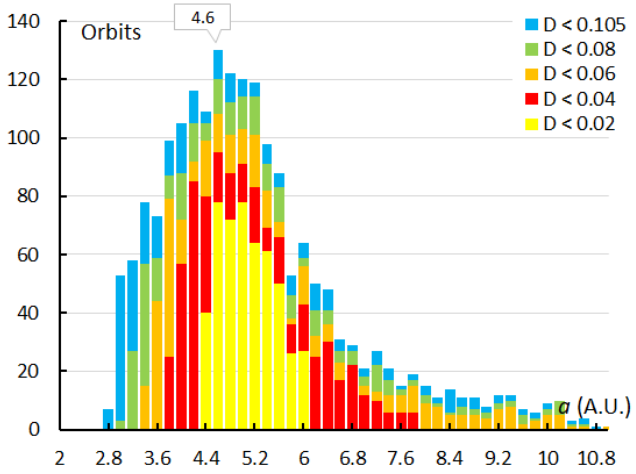

Figure 20 – Histogram with the distribution of the semi major axis a for the Ursid orbits with different colors for the shells in function of dispersion, from dispersed (blue, low similarity) to compact (yellow, very high similarity).

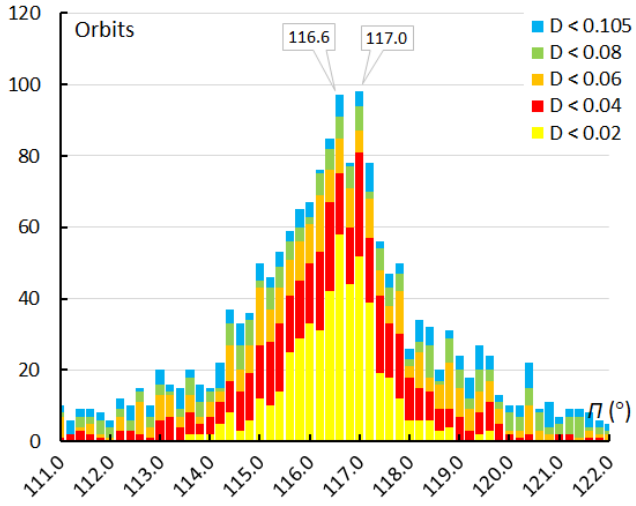

Figure 21 – Histogram with the distribution of the length of perihelion Π for the Ursid orbits with different colors for the shells in function of dispersion, from dispersed (blue, low similarity) to compact (yellow, very high similarity).

The histograms with the distribution of the different orbital elements are typical for a rather diffuse meteoroid stream (*Figures 17 to 21*). The more compact group of very similar orbits appear mainly during the annual maximum of the Ursids and during the maxima caused by specific dust trails, this is also visible in the activity profiles discussed in *Section 5*. Compact orbits are shown in yellow.

The length of perihelion Π is the only time related orbital element and displays a remarkable dip on the top, with two peaks separated by 0.4° in length of perihelion (*Figure 21*). This corresponds to the annual maximum visible in most activity profiles at $\lambda_\odot = 270.45°$ and the secondary peak at $\lambda_\odot = 270.80°$ to $270.85°$ caused by specific dust trails in some years like in 2016 (*Figure 13*) and which appears as a shoulder in the general activity profile (*Figure 4*). The difference corresponds to about 9 to 10 hours between the encounter of the Earth with the annual concentration in the Ursid stream and the occasionally present dust trails.

7 Velocity distribution of the Ursids

Every meteor shower is mainly defined by its radiant which indicates the direction from where it encounters the Earth and its velocity relative to the Earth which determines together with the radiant direction the orbit relative to the Sun in our solar system. Radiant size and velocity range determine how compact or how dispersed a meteoroid stream appears at its encounter with our planet. That is the reason why the measured velocities deserve proper attention just like the radiant characteristics.

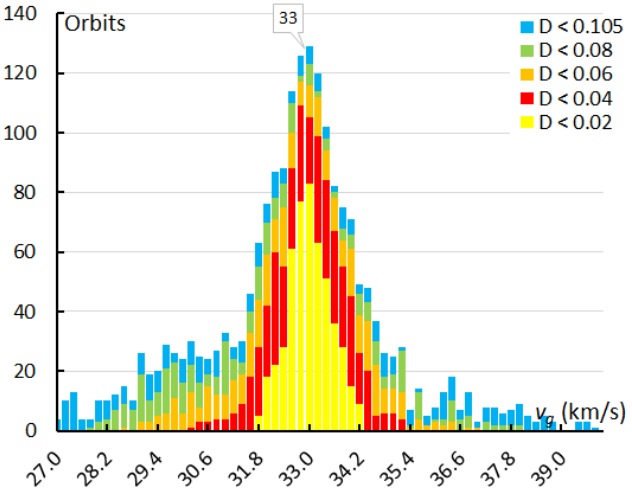

Figure 22 – Histogram with the distribution of the geocentric velocity v_g for the Ursid orbits with different colors for the different shells of dispersion, from dispersed (blue, low similarity) to compact (yellow, very high similarity).

In *Figure 22* we see the distribution of the measured geocentric velocities. 33 km/s is the most representative velocity for the Ursids, also listed in *Tables 1, 2 and 3*. The distribution appears skew with more slower velocities than faster velocities. When we look at the radiant distribution in Sun-centered ecliptic coordinates we see the fastest Ursids appear in the direction of the apex (bottom right in *Figure 23*) and slower Ursids away from the apex. The higher the inclination, the faster the Ursids. This appears in both the color code plot of the inclination against the perihelion

distance (*Figure 24*) and the plot of the inclination against the length of perihelion (*Figure 25*).

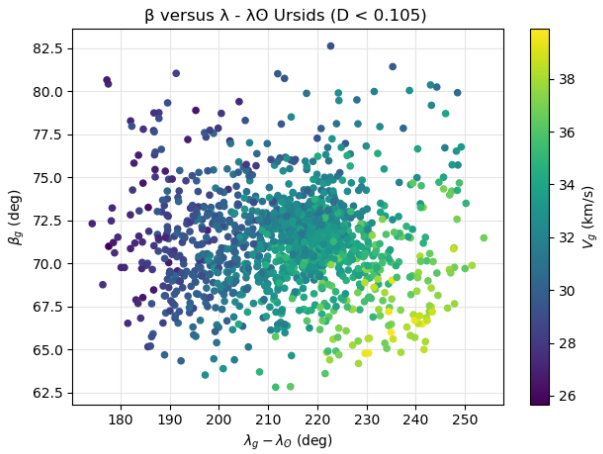

Figure 23 – The Ursid radiant in Sun-centered ecliptic coordinates color coded for the geocentric velocity.

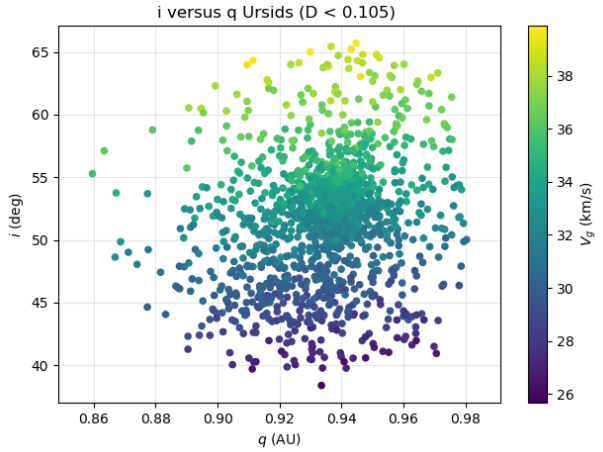

Figure 24 – The orbit distribution with the inclination *i* against the perihelion distance *q* color coded for the geocentric velocity.

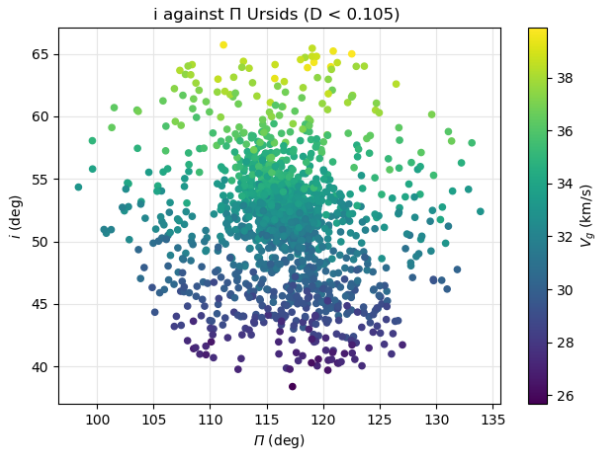

Figure 25 – The orbit distribution with the inclination *i* against the length of perihelion *Π* color coded for the geocentric velocity.

The relationship between the inclination and the velocity of the Ursids becomes very clear when we plot the velocity against the inclination. All orbits for all similarity classes appear close to the regression line which is the same for all degrees of dispersion (*Figure 26*).

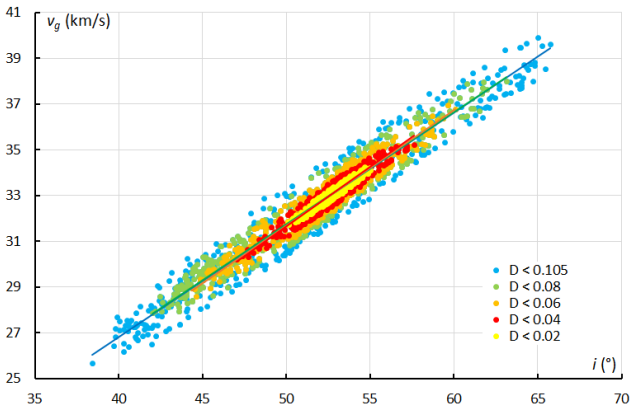

Figure 26 – The geocentric velocity v_g in function of the inclination.

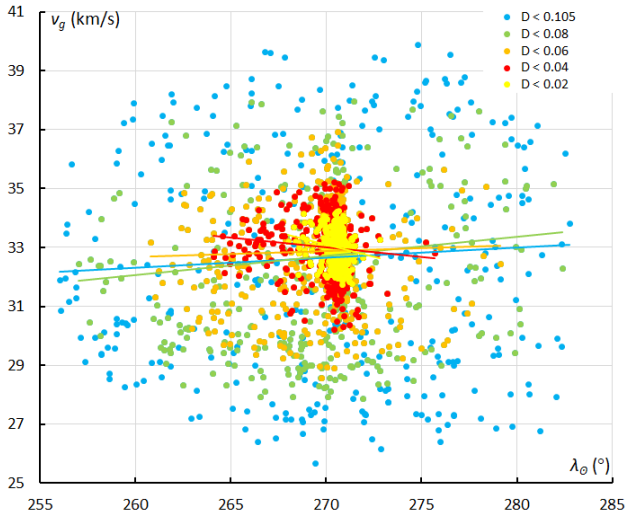

Figure 27 – The geocentric velocity v_g in function of time, solar longitude $\lambda_\odot$.

Looking at the variation of the geocentric velocity with time, no trend can be derived throughout the activity period of the Ursid shower. The velocity remains stable during the activity period (*Figure 27*). Note that the Ursid activity consists mainly of very dispersed orbits with a wide spread on the velocities beyond the nights around the maximum activity.

8 The Ursid luminosity

The absolute magnitudes were averaged in time bins of 0.5° in solar longitude shifted in steps of 0.05° (*Figure 28*). The Ursids appear to be fainter than the sporadic meteors! When I saw the graph, I double checked the source data. The sporadics are all meteors for which the orbit could not be identified with any known meteor shower. The strange pattern of the sporadic magnitudes is puzzling. CAMS has more fainter meteors than Edmond and SonotaCo, but the solar longitudes were collected for the three networks combined during 7 years, 2010 until 2016 included. The sporadics seem to get slightly brighter during the considered observing interval, another feature without an explanation.

Some bright ursids have been reported in the past during some outburst but overall, the main activity of the Ursids seems to consist of faint meteors, something rather unusual for shower meteors. It may be interesting to look at the

average magnitude per year to check if there are strong differences between years with only annual activity and years with outbursts.

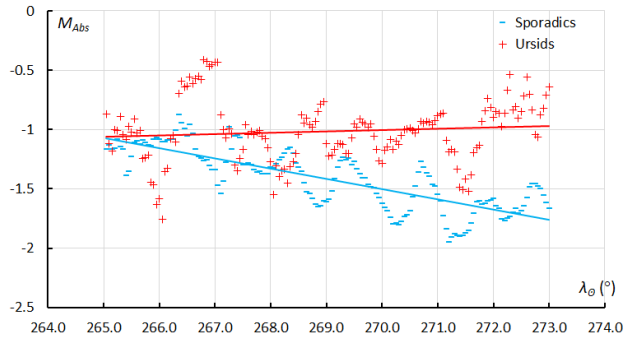

Figure 28 – The average absolute magnitude for the Ursids and for sporadic meteors in function of time.

9 Another outburst in 2020?

The two most recent years, 2014 and 2016, with a prediction by Esko Lyytinen and Peter Jenniskens for enhanced activity caused by a dust trail did materialize. In 2020 Earth may encounter a dust trail of 829 at $\lambda_\odot = 270.57°$, which is 2020 December 22 at 6^h10^m UT. There is also a chance to encounter a dust trail of 815 during the interval $270.44° < \lambda_\odot < 270.92°$ or 2020 December 22 between 3^h and 22^h UT. If one or both dust trails are encountered, each may produce enhanced activity during about one hour. Lyytinen and Jenniskens mention rather high hourly rates as a possibility. However, caution is required with this kind of predictions, nothing can be guaranteed and in the worst case the Ursids will just show their modest annual maximum without any outburst. For the next chance to encounter Ursid dust trails, we must wait until 2028 when the comet will be at its aphelion, a similar situation like with the 1945 and 1986 outbursts.

The last time that the Ursids parent comet 8P/Tuttle passed its perihelion was on 2008 January 27, the next perihelion passage will be 2021 August 27. The 2020 Ursid return is very similar to the 1993 return when very good Ursid rates were observed ahead of the perihelion passage later in 1994.

10 Conclusion

Considering the long-term history of meteor observations, the Ursids remain remarkably absent in 19th and early 20th century. The radiant could barely be detected with a typical minor shower behavior with too few meteors to be recognized as a meteor shower by visual observers. The unexpected outburst in 1945 got plenty of attention in literature and since then, the Ursids ranked on most shortlists as a major meteor shower. Apart from some very weak activity in the years after 1945, the shower remained again unnoticed until 1986 when another outburst was observed. Since then, the Ursids were better monitored but apart from some years with dust trail encounters the Ursid activity remained barely noticeable. The shower should be better qualified as a minor shower with variable activity and potential outbursts.

The Ursids appear to be a very dispersed meteor shower with a sharp annual peak at $\lambda_\odot = 270.45°$ with modest activity. Outbursts related to dust tails produced short lived sharp peaks slightly after the annual maximum.

11 Acknowledgment

The author thanks *Denis Vida* for providing the scripts to plot the velocity distribution with a color gradient and to compute the average orbit according to the method of Jopek et al. (2006). Thanks to the volunteers who maintain the IAU working list of meteor showers (Jopek and Kaňuchová, 2014, 2017; Jopek and Jenniskens, 2011).

We thank the SonotaCo Network members in Japan who have been observing every night for more than 10 years, making it possible to consult their orbits. We thank the camera operators of the CAMS[1] networks[2]. And we thank the contributors to EDMOND[3], including: BOAM (Base des Observateurs Amateurs de Meteores, France), CEMeNt (Central European Meteor Network, cross-border network of Czech and Slovak amateur observers), CMN (Croatian Meteor Network or HrvatskaMeteorskaMreza, Croatia), FMA (Fachgruppe Meteorastronomie, Switzerland), HMN (Hungarian Meteor Network or Magyar Hullocsillagok Egyesulet, Hungary), IMO VMN (IMO Video Meteor Network), MeteorsUA (Ukraine), IMTN (Italian amateur observers in Italian Meteor and TLE Network, Italy), NEMETODE (Network for Meteor Triangulation and Orbit Determination, United Kingdom), PFN (Polish Fireball Network or Pracownia Komet i Meteorow, PkiM, Poland), Stjerneskud (Danish all-sky fireball cameras network, Denmark), SVMN (Slovak Video Meteor Network, Slovakia), UKMON (UK Meteor Observation Network, United Kingdom).

References

Bečvář A. (1945). Circ. IAU No. 1026 (24 January 1946).

Bochníček Z., Vanýsek V. (1948). "The Meteoric Swarm of the Ursids". *Bull. Astron. Inst. Czech.*, **1**, 26–27.

Boschin W., Ganzini D., Candolini A., Candolini G. (2003). "Radio observations of the 2002 December Ursids". *WGN, Journal of the International Meteor Organization*, **31**, 29–30.

Brown P., Vaubaillon J., Jenniskens P., Yrjola I. (2015). "Ursid Meteors 2014". CBET 4041, January 2015.

Ceplecha Z. (1951). "Umids-Bečvář's Meteor Stream". *Bull. Astron. Inst. Czech.*, **2**, 156–160.

[1] http://cams.seti.org/
[2] http://cams.seti.org/FDL/
[3] https://fmph.uniba.sk/microsites/daa/daa/veda-a-vyskum/meteory/edmond/

Clegg J.A., Hughes V.A., Lovell A.C.B. (1948). "Bečvář's Meteor Stream". *Journal of the British Astronomical Association*, **58**, 134–139.

Denning W.F. (1916). "Méchain-Tuttle's Comet of 1790–1858 and a Meteoric Shower.". *Observatory*, **39**, 466–467.

Denning W.F. (1923). "Radiant Points of shooting Stars observed at Bristol chiefly from 1912 to 1922 inclusive". *Mon. Not. R. Astron. Soc*., **84**, 43–56.

Drummond J. D. (1981). "A test of comet and meteor shower associations". *Icarus*, **45**, 545–553.

Gajdoš Š., Tóth J., Kornoš L. (2015). "Ursid 2014 observations using the AMOS all-sky camera". In, Rault J.-L., Roggemans P., editors, *Proceedings of the International Meteor Conference*, Mistelbach, Austria, 27-30 August 2015. International Meteor Organization, pages 133–135.

Hillestad T.E. (1987). "The 1986 Ursid outburst in Norway". *WGN (Werkgroepnieuws)*, **15**, 59–60.

Imoto S., Hasegawa I. (1958). "Historical Records of Meteor Showers in China, Korea and Japan". *Smithsonian Contribution to Astrophysics*, **2**, 131–144.

Jenniskens P., Lyytinen E. (2000). "Possible Ursid Outburst on December 22, 2000". *WGN, Journal of the International Meteor Organization*, **28**, 221–226.

Jenniskens P., Lyytinen E. (2001). "2000 Ursid Outburst Confirmed". *WGN, Journal of the International Meteor Organization*, **29**, 41–45.

Jenniskens P., Lyytinen E., de Lignie M.C., Johannink C., Jobse K., Schievink R., Langbroek M., Koop M., Gural P., Wilson A.M., Yrjölä I., Suzukie K., Ogawa H., de Groote P. (2002). "Dust Trails of 8P/Tuttle and the Unusual Outbursts of the Ursid Shower". *Icarus*, **159**, 197–209.

Jenniskens P. (2006a). "Meteor showers and their parent comets". Cambridge, UK: Cambridge University Press. Pages 263–270.

Jenniskens P. (2006b). "Ursid meteors 2006". CBET 788, 2006 December 28.

Jenniskens P. (2010). "Ursids meteors 2009". CBET 2147, 2010 January 10.

Jenniskens P., Gural P. S., Grigsby B., Dynneson L., Koop M. and Holman D. (2011). "CAMS: Cameras for All-sky Meteor Surveillance to validate minor meteor showers". *Icarus*, **216**, 40–61.

Jenniskens P., Nénon Q., Albers J., Gural P. S., Haberman B., Holman D., Morales R., Grigsby B. J., Samuels D. and Johannink C. (2016). "The established meteor showers as observed by CAMS". *Icarus*, **266**, 331–354.

Jenniskens P. (2017). "Ursids meteors 2016". CBET 4363, 2017 February 20.

Jenniskens P. (2020). Personal communications.

Jopek T. J. (1993). "Remarks on the meteor orbital similarity D-criterion". *Icarus*, **106**, 603–607.

Jopek T. J., Rudawska R. and Pretka-Ziomek H. (2006). "Calculation of the mean orbit of a meteoroid stream". *Monthly Notices of the Royal Astronomical Society*, **371**, 1367–1372.

Jopek T. J., Jenniskens P. M. (2011). "The Working Group on Meteor Showers Nomenclature: A History, Current Status and a Call for Contributions". In, W.J. Cooke, D.E. Moser, B.F. Hardin, and D. Janches, editors, *Meteoroids: The Smallest Solar System Bodies, Proceedings of the Meteoroids Conference,* held in Breckenridge, Colorado, USA, May 24-28, 2010. Edited by, NASA/CP-2011-216469, pages 7–13.

Jopek T. J. and Kaňuchová Z. (2014). "Current status of the IAU MDC meteor showers database". In, Jopek T. J., Rietmeijer F. J. M., Watanabe J., and Williams I. P., editors, *Proceedings of the Meteoroids 2013 Conference*, Poznań, Poland, 26-30 August 2013. A.M. University Press, pages 353–364.

Jopek T. J. and Kaňuchová Z. (2017). "IAU Meteor Data Center-the shower database: A status report" *Planetary and Space Science*, **143**, 3–6.

Kornoš L., Matlovič P., Rudawska R., Tóth J., Hajduková M. Jr., Koukal J. and Piffl R. (2014). "Confirmation and characterization of IAU temporary meteor showers in EDMOND database". In Jopek T. J., Rietmeijer F. J. M., Watanabe J., Williams I. P., editors, *Proceedings of the Meteoroids 2013 Conference*, Poznań, Poland, Aug. 26-30, 2013. A.M. University, pages 225–233.

Koseki M. (2021). "Meteor shower activities scoped through SonotaCo net video observations 2007-18". *eMetN*, 6, 91–220, submitted.

Kronk G.W. (1988). "Meteor showers, A descriptive catalog". Enslow publishers, Inc., USA, UK.

Martin P. (2020a). "Winter and Ursids observations 2019". *eMetN*, **5**, 137–138.

McBeath A. (2005). "SPA Meteor Section results: an overview of the 2004 Ursids". *WGN, Journal of the International Meteor Organization*, **33**, 63–64.

Moreno-Ibáñez M., Trigo-Rodríguez J. M., Madiedo J. M., Vaubaillon J., Williams I.P., Gritsevich M., Morillas L. G., Blanch E., Pujols P., Colas F., Dupouy P.

(2017). “Multi-instrumental observations of the 2014 Ursid meteor outburst”. *Monthly Notices of the Royal Astronomical Society*, **468**, 2206–2213.

Ogawa H. (2017). “Radio meteor observations in the world: Monthly Report for December 2016”. *eMetN*, **2**, 19–20.

Ohtsuka K., Shioi H., Hidaka E. (1995). “Enhanced activity of the 1994 Ursids from Japan”. *WGN, Journal of the International Meteor Organization*, **22**, 69–72.

Prentice J.P.M. (1948). “Visual observations of Bečvář’s Meteor Stream”. *Journal of the British Astronomical Association*, **58**, 140.

Roggemans P., Steyaert C. (1987). “Again, on the Ursids”. *WGN (Werkgroepnieuws)*, **15**, 25–26.

Roggemans P. (1987). “On the Ursids, once more”. *WGN (Werkgroepnieuws)*, **15**, 50–51.

Roggemans P. (2017). “Variation in heights of CAMS meteor trajectories”. *eMetN*, **2**, 80–86.

Roggemans P., Johannink C. and Cambell-Burns P. (2019). “October Ursae Majorids (OCU#333)”. *eMetN*, **4**, 55–64.

Roggemans P. and Johannink C. (2020). “Ursids (URS#015) in 2019”. *eMetN*, **5**, 117–120.

Southworth R. R. and Hawkins G. S. (1963). “Statistics of meteor streams”. *Smithson. Contrib. Astrophys.*, **7**, 261–286.

Steyaert C. (1987). “A note on periodic streams and the Ursids in particular”. *WGN (Werkgroepnieuws)*, **15**, 53–55.

Vanýsek V. (1947). “Les météores de la comète Tuttle (1790 II)”. *Bull. Astron. Inst. Czech*., **1**, 10–11.

Global Meteor Network and the 2020 Ursid return

Paul Roggemans

Pijnboomstraat 25, 2800 Mechelen, Belgium
paul.roggemans@gmail.com

The Global Meteor Network successfully covered the predicted enhanced Ursid activity meanly by its RMS cameras in the USA while other parts of GMN had partial or complete overcast sky. As many as 253 Ursid orbits were recorded between solar longitude 269° and 272°. The raw uncalibrated activity profile based on numbers of orbits is in good agreement with radio meteor data. The Ursid orbits recorded during the 2020 maximum consist mainly of a very compact structure with very similar orbits and a compact radiant, apart from few outliers.

1 Introduction

In a recent case study on the Ursid meteor shower (Roggemans, 2021) the predictions made by Lyytinen and Jenniskens (Jenniskens, 2006) were recalled for another possible outburst or enhanced activity caused by some old dust trails. In previous years bad weather interfered at many northern hemisphere locations preventing most observers from getting a glimpse of possible Ursid activity. The year 2020 was no exception and most visual observers as well as many cameras faced a completely overcast sky.

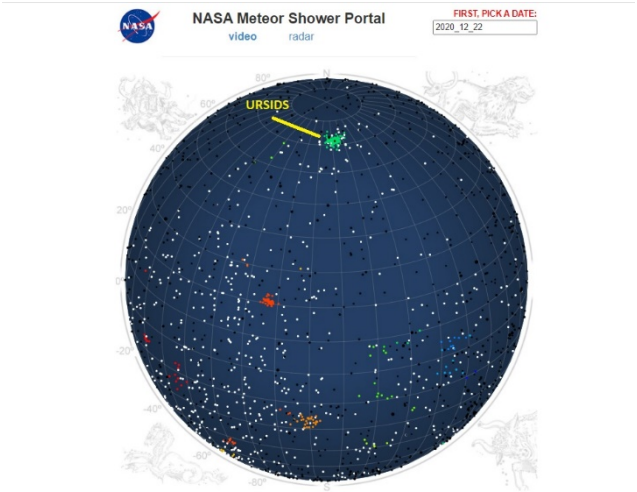

Figure 1 – The radiant plot for CAMS 2020 December 22 ($269.80° < \lambda_O < 270.82°$)[4].

Meanwhile we know from radio and radar observations that a distinct enhanced activity of the Ursids took place at the predicted time. The CAMS networks in the US and the United Arab Emirates recorded a nice number with 191 Ursid orbits during the interval $269.80° < \lambda_O < 270.82°$ (*Figure 1*). Unfortunately, the CAMS data is kept under embargo which is indeed not very helpful for anyone to know more about the 2020 Ursid return. Also, the CMOR radar map marks a distinct hot spot at the position of the Ursid radiant but no detailed data is available (*Figure 2*). Luckily the Global Meteor Network had clear sky during the crucial time span with possible enhanced activity.

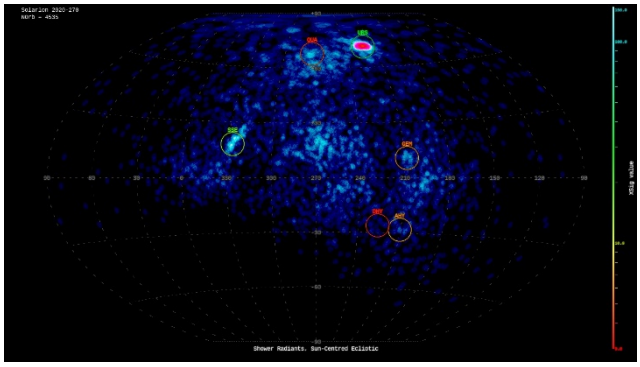

Figure 2 – The CMOR map during the 2020 Ursid activity.

2 Global Meteor Network Ursid data

The GMN currently consists of a number of regional networks, several of which are still in full expansion, spread over Canada, Europe, Israel and the US. Most parts of the GMN were badly affected by unfavorable weather most of the time. We limit the scope of this analysis to the time interval of 269. $0° < \lambda_O < 272.0°$ or 72 hours. During this time span GMN collected as many as 1492 orbits. 85% of these orbits were recorded by the RMS cameras installed in the US while the other 15% were obtained under less favorable circumstances by the RMS cameras installed in Belgium, Canada, Croatia, France, Germany, Ireland, Israel, Netherlands, Spain and the United Kingdom. It was very unfortunate that the large Russian RMS camera network remained overcast during this time interval.

3 The Ursid shower identifications

The online GMN data lists 265 multi-station meteors identified as Ursids during the 72 hours around the expected maximum. Applying the same method as used in the Ursid case study, the author identified 259 Ursid orbits based on the orbit similarity criteria explained in Roggemans et al. (2019). 12 of the 265 orbits identified as Ursids by the GMN algorithm were rejected for Ursid identification by the similarity criteria, mainly because of a deviant eccentricity, 8 being too low in eccentricity, 4 being hyperbolic. 6 of the 259 Ursid orbits identified by the similarity criteria were listed as sporadics by the GMN algorithm, all six with

[4] http://cams.seti.org/FDL/ (Select 2020 December 22 as date).

mainly a slightly deviant radiant position that was probably beyond the limits defined in GMN. All 18 possible Ursids are somehow outliers and therefore these are ignored for the further analysis which finally has 253 Ursid orbits collected by GMN.

4 The mean Ursid orbit based on GMN data

With a total of 253 Ursid orbits collected during 72 hours including the peak activity in a single year, the GMN made a major contribution to the global collection of known Ursid orbits (Roggemans, 2021). Determining a mean orbit (Jopek et al., 2006) for these GMN Ursid orbits using a iterative procedure based on the similarity criteria of Southworth and Hawkins (1963), Drummond (1981) and Jopek (1993) combined, allows to consider different classes of dispersion among the Ursid orbits. These should help to visualize the degree of dispersion and compactness within the meteoroid stream. The different classes of similarity are defined as follows:

- Low: $D_{SH} < 0.25$ & $D_D < 0.105$ & $D_H < 0.25$;
- Medium low: $D_{SH} < 0.2$ & $D_D < 0.08$ & $D_H < 0.2$;
- Medium high: $D_{SH} < 0.15$ & $D_D < 0.06$ & $D_H < 0.15$;
- High: $D_{SH} < 0.1$ & $D_D < 0.04$ & $D_H < 0.1$;
- Very high: $D_{SH} < 0.05$ & $D_D < 0.02$ & $D_H < 0.05$.

For each similarity class the mean orbit has been calculated and listed in *Table 1*. The mean orbits for each of the similarity classes are almost identical for the 2020 GMN data. Most orbits were registered during the peak of the shower activity which consists of very similar orbits. The general Ursids case study (see Roggemans, 2021) was based on combined CAMS, EDMOND and SonotaCo data for the period 2006–2019 covering the entire time span during which candidate Ursid orbits could be detected ($256° < \lambda_\odot < 283°$). Such a long activity period of 27 days with data accumulated from 14 years includes more dispersed particles separated from the main Ursid stream.

In *Table 2* the high threshold similarity orbits obtained by GMN in 2020 are compared with the same similarity class mean orbits obtained for CAMS, EDMOND and SonotaCo during previous years. These results agree very well.

5 The 2020 Ursid radiant

The compact nature of the 2020 Ursid return also appears very well in the radiant plot. *Figure 3* shows the radiant distribution in Sun-centered geocentric ecliptic coordinates to eliminate the radiant drift caused by the Earth moving on its own orbit around the Sun. Apart from few outliers, the very similar orbits form a very compact radiant area of about 3° in diameter. *Figure 4* shows the same map but with the velocity color coded. The compact radiant is formed by Ursids with almost identical geocentric velocity, while the few outliers at left have a lower velocity. A gradual increase in velocity in the direction of the Apex can be seen.

Table 1 – The mean orbits calculated for each similarity class according to the threshold of the D-criteria for the Ursids based on the shower identification described in Roggemans et al. (2019).

	Low	Medium Low	Medium High	High	Very high
$\lambda_\odot$ (°)	270.60	270.59	270.58	270.57	270.58
α_g (°)	218.9	218.9	218.9	218.7	218.8
δ_g (°)	+75.4	+75.4	+75.4	+75.4	+75.4
H_b (km)	103.1	103.1	103.1	103.2	104.1
H_e (km)	91.6	91.4	91.4	91.2	89.5
v_g (km/s)	33.1	33.1	33.2	33.2	33.2
λ-$\lambda_\odot$ (°)	218.6	218.6	218.6	218.7	218.6
β (°)	+71.9	+71.9	+71.9	+71.9	+71.9
a (AU)	4.99	4.99	4.99	4.99	4.99
q (AU)	0.9382	0.9382	0.9382	0.9382	0.9382
e	0.81215	0.81214	0.81215	0.81215	0.81215
ω (°)	206.1	206.1	206.1	206.1	206.1
Ω (°)	270.3	270.3	270.3	270.3	270.3
i (°)	52.4	52.4	52.4	52.4	52.4
Π (°)	116.4	116.4	116.4	116.4	116.4
Q (AU)	9.1	9.1	9.1	9.1	9.1
T_j	1.74	1.74	1.74	1.74	1.74
P (y)	11.2	11.2	11.2	11.2	11.2
N	253	243	229	194	126

Table 2 – The mean orbits calculated for each camera network separately for the Ursids that fulfill the high threshold criteria based on the shower identification by the author.

	GMN	CAMS	EDMOND	SonotaCo
$\lambda_\odot$ (°)	270.57	270.69	270.49	270.49
α_g (°)	218.7	219.4	219.1	218.8
δ_g (°)	+75.4	+75.7	+75.8	+75.6
H_b (km)	103.2	103.3	101.3	102.4
H_e (km)	91.2	92.8	88.1	89.2
v_g (km/s)	33.2	32.9	32.9	33.2
λ-$\lambda_\odot$ (°)	218.7	217.9	217.7	218.3
β (°)	+71.9	+72.1	+72.0	+71.9
a (AU)	4.99	4.99	4.92	5.05
q (AU)	0.9382	0.9382	0.9373	0.9376
e	0.812	0.812	0.810	0.814
ω (°)	206.1	206.1	206.3	206.2
Ω (°)	270.3	270.3	270.3	270.2
i (°)	52.4	52.4	52.5	52.8
Π (°)	116.4	116.4	116.6	116.3
Q (AU)	9.1	9.1	8.9	9.2
T_j	1.74	1.74	1.75	1.72
P (y)	11.2	11.2	10.9	11.3
N	194	300	334	318

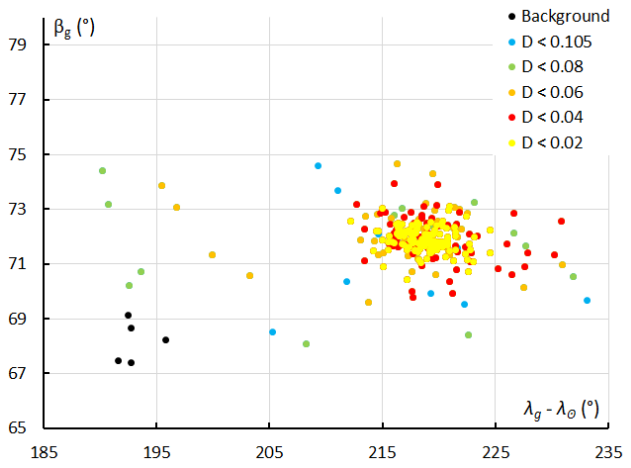

Figure 3 – The Ursid radiant in Sun-centered geocentric ecliptic coordinates, color coded according to the similarity classes.

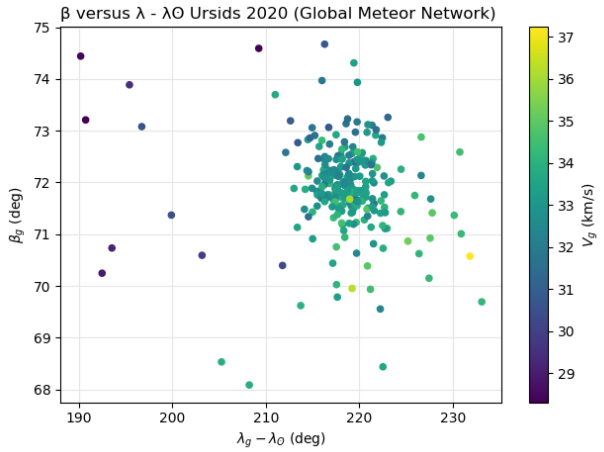

Figure 4 – The Ursid radiant in Sun-centered geocentric ecliptic coordinates color coded for the geocentric velocity.

6 The 2020 Ursid activity profile

Counting the number or Ursid orbits recorded in time bins of 0.15° in solar longitude (3.6 hours) shifted with steps of 0.05° in solar longitude (1.2 hours) results in *Figure 5*. The highest numbers of Ursid orbits appeared at solar longitude 270.80°, 270.55° and 270.45°.

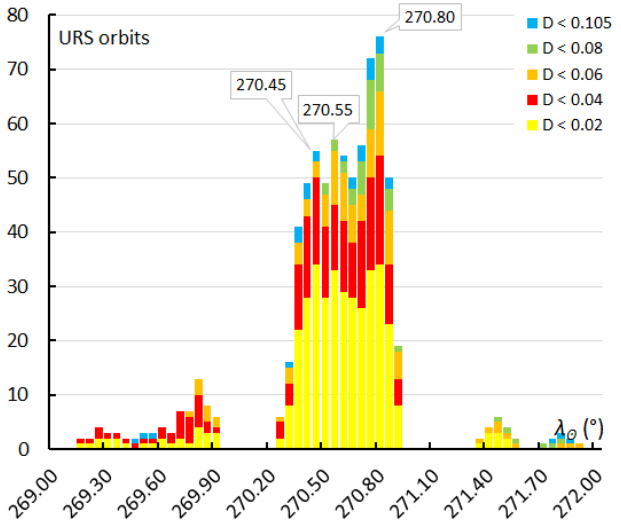

Figure 5 – The number of Ursid orbits counted in 2020 in bins of 0.15° in solar longitude shifted 0.05° at each step.

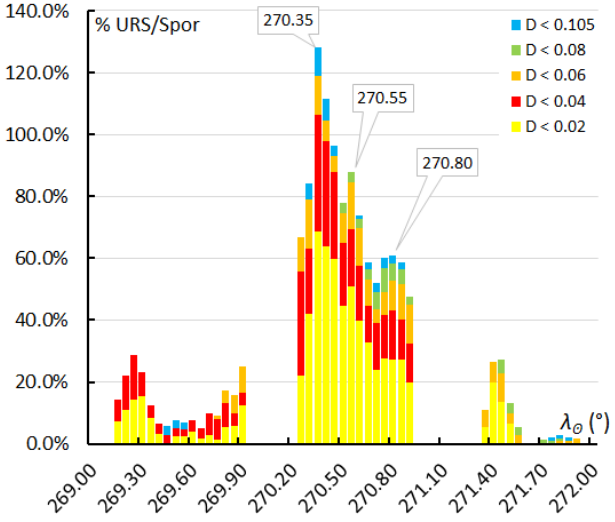

Figure 6 – The number of Ursid orbits expressed as a percentage of the sporadic background counted in bins of 0.15° in solar longitude, shifted by 0.05°.

Some of the time bins had too few orbits and were removed. With 85% of all the Ursid orbits collected at one region, there may be local observing circumstances as well as statistical fluctuations. The sky conditions will affect the sporadic background in the same way as it does for the number of Ursid orbits. Expressing the number of Ursid orbits as a percentage relative to the sporadic background results in *Figure 6*. The first peak appears earlier at $\lambda_\odot = 270.35°$, but this may be spurious due to statistical fluctuations with "only" 32 sporadic orbits recorded and 41 Ursids within this time bin. Around $\lambda_\odot = 270.80°$, 125 sporadic orbits were recorded and 76 Ursid orbits. The highest value seen in *Figure 5* is reduced to a shoulder on the profile in *Figure 6*. The more networks and the larger the number of cameras, the better statistical variations may be averaged out. In this case caution is required with activity profiles.

Global radio data (Ogawa and Sugimoto, 2021) saw the enhanced activity beginning at $\lambda_\odot = 270.29°$ and ending at $\lambda_\odot = 270.97°$, which is exactly the time span with the best numbers of Ursid orbits in *Figures 5 and 6*. The radio observers marked two peaks at $\lambda_\odot = 270.45°$ and $\lambda_\odot = 270.55°$, peaks which were confirmed by Japanese radio observers. No peak in the radio data at $\lambda_\odot = 270.80°$, but the activity profile for the ZHR equivalent for radio observations also shows a shoulder at this time. The radio data and the orbit data profiles indicate the same sub maxima at $\lambda_\odot = 270.45°$ and $\lambda_\odot = 270.55°$ as well as a shoulder in the activity profile at $\lambda_\odot = 270.80°$.

7 Ursid orbital elements

Some graphics can help to give insight in the structure of the meteoroid stream. The distribution of the inclination i against the length of perihelion Π (*Figure 7*) shows how a large majority of the Ursid orbits form a compact concentration with only a small number of outliers. The higher the inclination, the higher the geocentric velocity. The histogram for the length of perihelion Π (*Figure 8*)

seems to suggest that there are some groups of orbits with a slightly different length of perihelion *Π*. *Figure 9* shows the distribution of the inclination *i* against the perihelion distance *q*. The increase in velocity is very well visible.

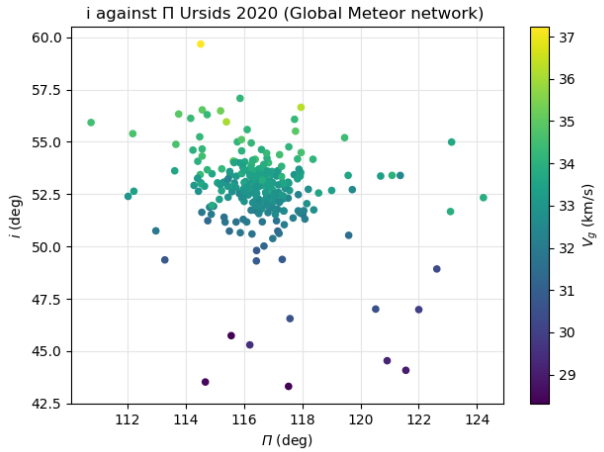

Figure 7 – The orbit distribution with the inclination *i* against the length of perihelion *Π* color coded for the geocentric velocity.

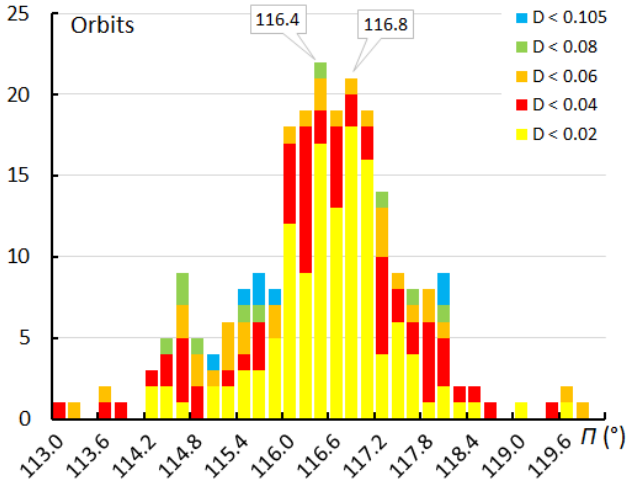

Figure 8 – Histogram with the distribution of the length of perihelion *Π* for the Ursid orbits with different colors for the shells in function of dispersion, from very dispersed (blue, low similarity) to compact (yellow, very high similarity).

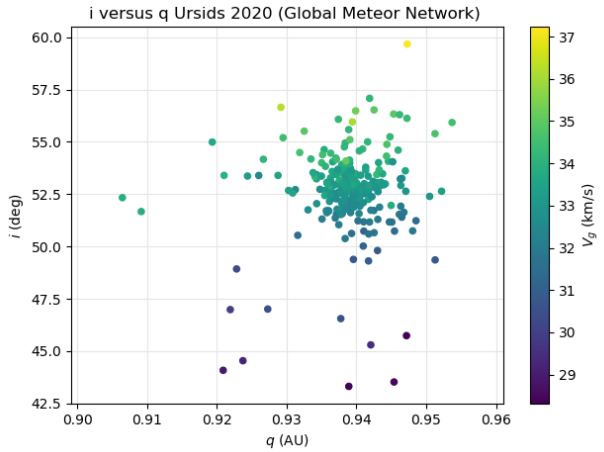

Figure 9 – The orbit distribution with the inclination *i* against the perihelion distance *q* color coded for the geocentric velocity.

From all these graphs it is obvious that the enhanced Ursid activity in 2020 was caused mainly by a compact component with very similar orbits combined with a more dispersed annual component.

8 Conclusion

Thanks to the efforts of the Global Meteor Network collaborators, a valuable dataset of Ursid orbits could be recorded although general bad weather conditions prevented most video camera networks on the northern hemisphere to record any glimpse of this shower. The multiple maxima indicate the presence of different dust trails combined with the annual activity.

Acknowledgment

We used the data of the Global Meteor Network[5] which is released under the CC BY 4.0 license[6]. The author thanks the camera operators of the global Meteor network and *Denis Vida* in particular for providing the scripts to plot the velocity distribution with a color gradient and to compute the average orbit according to the method of Jopek et al. (2006).

References

Drummond J. D. (1981). "A test of comet and meteor shower associations". *Icarus*, **45**, 545–553.

Jenniskens P. (2006a). "Meteor showers and their parent comets". Cambridge, UK: Cambridge University Press. Pages 263–270.

Jopek T. J. (1993). "Remarks on the meteor orbital similarity D-criterion". *Icarus*, **106**, 603–607.

Jopek T. J., Rudawska R. and Pretka-Ziomek H. (2006). "Calculation of the mean orbit of a meteoroid stream". *Monthly Notices of the Royal Astronomical Society*, **371**, 1367–1372.

Ogawa H., Sugimoto H. (2021). "Ursids 2020 with Worldwide Radio Meteor Observations". *eMetN*, **6**, 19–21.

Roggemans P., Johannink C. and Cambell-Burns P. (2019). "October Ursae Majorids (OCU#333)". *eMetN*, **4**, 55–64.

Roggemans P. (2021). "Ursids (URS#015) major or minor shower, and another outburst in 2020?". *eMetN*, **6**, 1–14.

Southworth R. R. and Hawkins G. S. (1963). "Statistics of meteor streams". *Smithson. Contrib. Astrophys.*, **7**, 261–286.

[5] https://globalmeteornetwork.org/data/

[6] https://creativecommons.org/licenses/by/4.0/

Ursids 2020 with Worldwide Radio Meteor Observations

Hiroshi Ogawa[1] and Hirofumi Sugimoto[2]
[1] h-ogawa@amro-net.jp

[2] **The Nippon Meteor Society**
hiro-sugimoto@kbf.biglobe.ne.jp

Worldwide Radio Meteor Observations recorded an Ursid outburst in 2020. The Ursid activity profile indicated the presence of two components. One was the annual activity; the other was an outburst activity. The outburst peak time occurred at $\lambda_\odot = 270.45°$ to $270.55°$ with an estimated ZHR of around 40. Besides, the detailed activity structure became clear by using Japanese observed data in time bins of 10 minutes.

1 Introduction

The Ursid meteoroid stream is one of the major showers at the end of the year in the month of December. For 2020, there were some dust trail encounters predicted based on the calculations by J. Vaubaillon, P. Jenniskens, E. Lyytinen and M. Sato for the period of December 22 03^h – 22^h(UT). (Rendtel, 2019).

Worldwide radio meteor observation data were provided by the Radio Meteor Observation Bulletin (RMOB)[7] (Steyaert, 1993) and by the radio meteor observations network in Japan (Ogawa et al., 2001). Radio meteor observations are possible even with bad weather and during daytime.

2 Method

For analyzing the worldwide radio meteor observation data, meteor activities are calculated by the "Activity Level" index (Ogawa et al., 2001). The activity profile was estimated by the Lorentz activity profile (Jenniskens, 2000). Besides of this analysis, also the Zenithal Hourly Rates were estimated (Sugimoto, 2017).

3 Results

3.1. Activity Level index

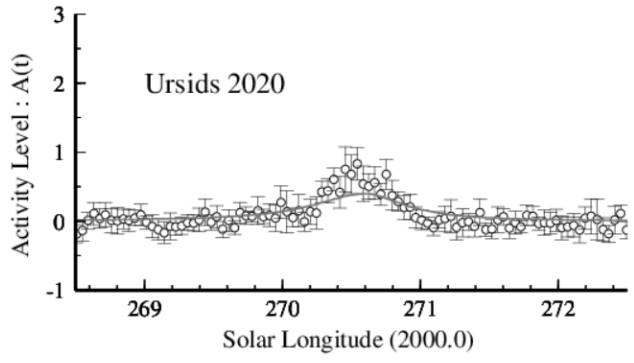

Figure 1 – Activity Level Index by radio meteor observations all over the world (the line is the average of the period for 2004–2019).

Figure 1 shows the result for the Ursids 2020 based on the calculations with the Activity Level Index. The line represents the average for the period for 2004–2019. The outburst was very distinct compared with past returns. The maximum activity level was estimated 0.8 ± 0.2 at $\lambda_\odot = 270.54°$ (December 22, 5^h UT). The enhanced activity began at 270.29° (December 21, 23^h UT) and ended at 270.97° (December 22, 15^h UT). *Table 1* shows the results around the peak value.

Table 1 – The Activity Level Index around the peak time.

Date (UT)	$\lambda_\odot$ (°)	Activity Level
Dec.21 21^h00^m–22^h00^m	270.204	0.1 ± 0.2
Dec.21 22^h00^m–23^h00^m	270.246	0.1 ± 0.2
Dec.21 23^h00^m–24^h00^m	270.288	0.4 ± 0.2
Dec.22 00^h00^m–01^h00^m	270.331	0.4 ± 0.2
Dec.22 01^h00^m–02^h00^m	270.373	0.6 ± 0.2
Dec.22 02^h00^m–03^h00^m	270.416	0.4 ± 0.2
Dec.22 03^h00^m–04^h00^m	270.458	0.8 ± 0.3
Dec.22 04^h00^m–05^h00^m	270.501	0.7 ± 0.3
Dec.22 05^h00^m–06^h00^m	270.543	0.8 ± 0.2
Dec.22 06^h00^m–07^h00^m	270.586	0.5 ± 0.3
Dec.22 07^h00^m–08^h00^m	270.628	0.5 ± 0.2
Dec.22 08^h00^m–09^h00^m	270.67	0.6 ± 0.2
Dec.22 09^h00^m–10^h00^m	270.713	0.4 ± 0.2
Dec.22 10^h00^m–11^h00^m	270.755	0.7 ± 0.2
Dec.22 11^h00^m–12^h00^m	270.798	0.4 ± 0.2
Dec.22 12^h00^m–13^h00^m	270.84	0.3 ± 0.1
Dec.22 13^h00^m–14^h00^m	270.883	0.2 ± 0.2
Dec.22 14^h00^m–15^h00^m	270.925	0.2 ± 0.2
Dec.22 15^h00^m–16^h00^m	270.967	0.1 ± 0.2
Dec.22 16^h00^m–17^h00^m	271.01	0.0 ± 0.1

Figure 2 shows the detailed Ursids 2020 activity structure with the two components separated using the Lorentz activity profile (Jenniskens, 2000). One component (Comp. 1) has its peak activity level as 0.5 at $\lambda_\odot = 270.67°$

[7] http://www.rmob.org/

(December 22, 8h UT) with full width half maximum (FWHM) –6.0 / +4.5 hours. The other component (Comp. 2) reached 0.5 activity level at $\lambda_\odot$ = 270.46° (December 22, 3h UT) with full width half maximum (FWHM) –2.5 / +2.0 hours (see *Table 2*). Comp. 1 is possibility the equivalent of the annual activity (average of the period for 2004–2019: activity level = 0.4 at $\lambda_\odot$ = 270.60° (Ogawa and Steyaert, 2017)). Comp. 2 may be the outburst component in 2020.

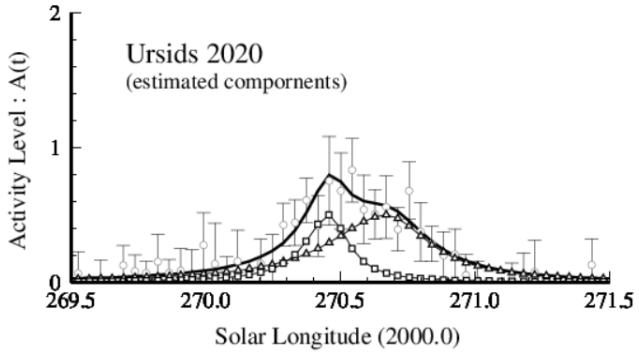

Figure 2 – Estimated components using the Lorentz profile. (the curve with triangles means Comp. 1, the curve with the circles is Comp. 2. The black line represents Comp. 1 and Comp. 2 combined. The circles with error margins are the Ursids observed in 2020).

Table 2 – The estimated components of the Ursids 2020.

Compo-nent	Max.	$\lambda_\odot$	Activity Level	FWHM (hours)
Comp. 1	Dec. 22nd 8h UT	270.67°	0.5	–6.0 / +4.5
Comp. 2	Dec. 22nd 3h UT	270.46°	0.5	–6.0 / +4.5

3.2. Estimated ZHR$_r$

Besides the activity level index analysis, also the Zenithal Hourly Rate (ZHR_r) was estimated by using the Radio Meteor Observations (*Figure 3*). Peak times occurred at December 22, 3h ($\lambda_\odot$ = 270.46°), 5h ($\lambda_\odot$ = 270.54°) and 7h to 8h ($\lambda_\odot$ = 270.63° to 270.67°) similar to the Activity Level Index results. The estimated ZHR_r were 37 ± 2, 39 ± 3 and 23 ± 3.

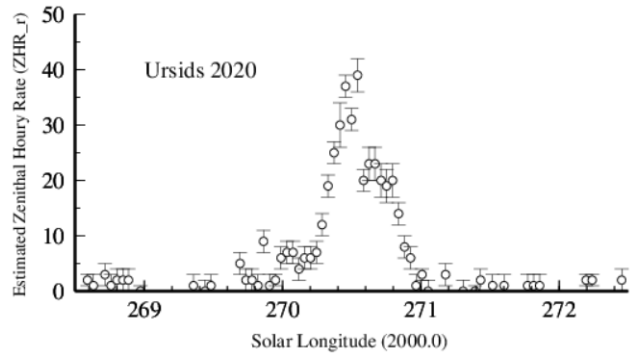

Figure 3 – The estimated ZHR_r obtained from the Woldwide radio meteor observations.

In order to visualize the detailed activity structure, we calculated the values in 10 minutes time bins by using the radio meteor observations from Japan only (*Figure 4*). This is because the Japanese observers record their data counted in 10 minutes time bins. The double outbursts were detected at $\lambda_\odot$ = 270.476° (December 22, 03h50m to 04h00m UT) and $\lambda_\odot$ = 270.561° (December 22, 05h50m to 06h00m UT). The ZHR_r values were estimated as 66 ± 15 and 66 ± 10.

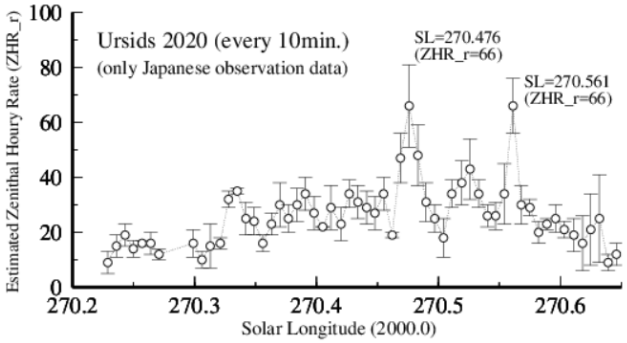

Figure 4 – Estimated ZHR_r every 10 minutes (using only Japanese observational data).

Acknowledgment

The Ursids 2020 data were provided by the following observers: *AAV Planetario_di_Venezia* (Italy), *Balogh Laszlo* (Hungary), *Bill Ward* (UK), *Chris Steyaert* (Belgium), *Daniel D SAT01_DD* (France), *Fabio Moschini _IN3GOO* (Italy), *Felix Verbelen* (Belgium), *GAML Osservatorio_Astronomico_Gorga* (Italy), *Hirofumi Sugimoto* (Japan), *Hironobu Shida* (Japan), *Hirotaka Otsuka* (Japan), *Ian Evans* (UK), *Istvan Tepliczky* (Hungary), *Jean Marie F5CMQ* (France), *Jochen Richert* (Switzerland), *Jose Carballada* (Spain), *Juan Zapata* (Mexico), *Karlovsky Hlohovec_Observatory* (Slovakia), *Kees Meteor* (Netherlands), *Kenji Fujito* (Japan), *Mario Bombardini* (Italy), *Masaki Kano* (Japan), *Masaki Tsuboi* (Japan), *Maurizio Morini _IU2JWG* (Italy), *Mike Otte* (USA), *Nobuo Katsura* (Japan), *Per DL0SHF* (Germany), *Philip Norton* (UK), *Philip Rourke* (UK), *Rafael Martinez* (Puerto Rico), *Rainer Ehlert* (Mexico), *Ronda Ronda* (Spain), *Salvador Aguirre* (Mexico), *Stan Nelson* (USA), *Tomohiro Nakamura* (Japan), *Tracey Snelus* (UK), *WHS Essen* (Germany).

The worldwide data were provided by the Radio Meteor Observation Bulletin (RMOB)[1].

References

Jenniskens P., Crawford C., Butow S. J., Nugent D., Koop M., Holman D., Houston J., Jobse K., Kronk G., and Beatty K. (2000). “Lorentz shaped comet dust trail cross section from new hybrid visual and video meteor counting technique implications for future Leonid storm encounters”. *Earth, Moon and Planets*, **82–83**, 191–208.

Ogawa H., Toyomasu S., Ohnishi K., and Maegawa K. (2001). “The Global Monitor of Meteor Streams by Radio Meteor Observation all over the world”. In, Warmbein Barbara, editor, *Proceeding of the Meteoroids 2001 Conference*, 6-10 August 2001,

Swedish Institute of Space Physics, Kiruna, Sweden. ESA Publications Division, European Space Agency, Noordwijk, The Netherlands, pages 189–191.

Ogawa H. and Steyaert C. (2017). “Major and Daytime Meteor Showers using Global Radio Meteor Observations covering the period 2001–2016”. *WGN, Journal of the International Meteor Organization*,**45**, 98–106.

Rendtel J. (2019). 2020 Meteor Shower Calendar. International Meteor Organization.

Sugimoto H. (2017). “The New Method of Estimating ZHR using Radio Meteor Observations”. *eMetN*, **2**, 109–110.

Return of Volantid meteor shower, expected to peak on New Year's Eve

P. Jenniskens

SETI Institute, 189 Bernardo Ave, Mountain View, CA 94043, USA
pjenniskens@seti.org

The Volantid meteor shower (VOL#758) was discovered on 2015 December 31 by the CAMS network in New Zealand and has been confirmed by VHF radar observations. No meteors from this shower were detected in later years until this year, 2020 December 27 and 28 when the CAMS networks in New Zealand, Australia, South Africa, Namibia and Chile recorded activity again. If the shower behaves this year in the same manner as in 2015, it is expected to grow in activity and peak on New Year's Eve Dec. 31. Southern hemisphere meteor observers are in a favorable geographic position for this shower which is too far south for observers in the northern hemisphere.

1 Introduction

The Volantids were first seen in 2015. *Figure 1* shows the group of meteors at –79° declination detected on the night of 2015 December 31, between 09^h12^m and 15^h45^m UT. Meteors were spread throughout the night with good rates around 10^h15^m UT ($\lambda_\odot = 279.18°$, J2000). Because of local daylight savings time, the new year started at 11^h00^m UT in New Zealand (Jenniskens et al. 2016). A New Year's Eve shower.

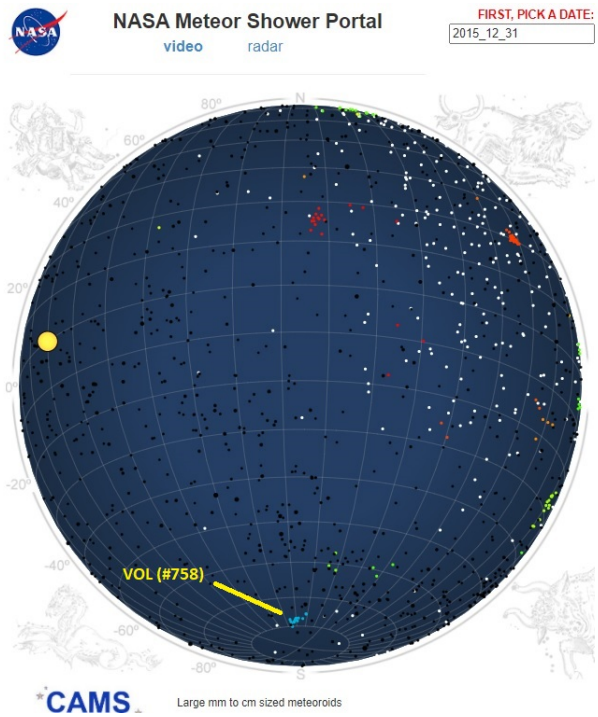

Figure 1 – The Volantid radiants on the CAMS radiant map of 2015 December 31.

The new shower was also detected using VHF meteor radars located in Australia and Antarctica. Analysis of this data showed activity from the Volantids for at least three days over the period 31 December 2015 – 2 January 2016, peaking with an apparent radiant at R.A. = 119.3 ± 3.7°, dec. = –74.5 ± 1.9° on January 1st. Measurements of the meteoroid velocity were made using the Fresnel transform technique, yielding a geocentric shower velocity $v_g = 28.1 \pm 1.8$ km/s (Younger et al., 2016).

The 2015 New Year's Eve shower inspired the illustration by Danielle Futselaar, shown in *Figure 2*. The shower has not returned since.

Figure 2 – Illustration created by D. Futselaar inspired by the discovery of the Volantids on December 31, 2015.

2 Return in 2020

As reported in a December 29 CBET telegram (Jenniskens, 2020), low-light video camera observations by CAMS New Zealand (*J. Baggaley*), CAMS Australia (*M. Towner*), CAMS South Africa (*T. Cooper*), CAMS Namibia (*T. Hanke*), and CAMS Chile (*S. Heathcote*, *E. Jehin*) have detected the Volantids, IAU shower number 758, in the night of 2020 Dec. 27 (5 meteors) and 28 (9 meteors)[8]. The radiant of the shower in the solar longitude period $\lambda_\odot = 275.8 – 276.7°$ (equinox J2000) was at high southern declination in the constellation Volans, the flying fish, with geocentric equatorial coordinates R.A. = 123.8 ± 2.5°,

[8] http://cams.seti.org/FDL/ for the date of 2020 Dec. 28.

Decl. = –69.2 ± 1.2°, and entry speed vg = 30.2 ± 1.0 km/s. The orbital elements measured are:

- q = 0.979 ± 0.003 AU
- a = 2.60 ± 0.50 AU
- e = 0.623 ± 0.070
- i = 50.7 ± 1.0°
- ω = 350.9 ± 2.8°
- Ω = 96.2 ± 0.3°

Last night, 2020 Dec 29, the shower continued to strengthen (*Figure 3*).

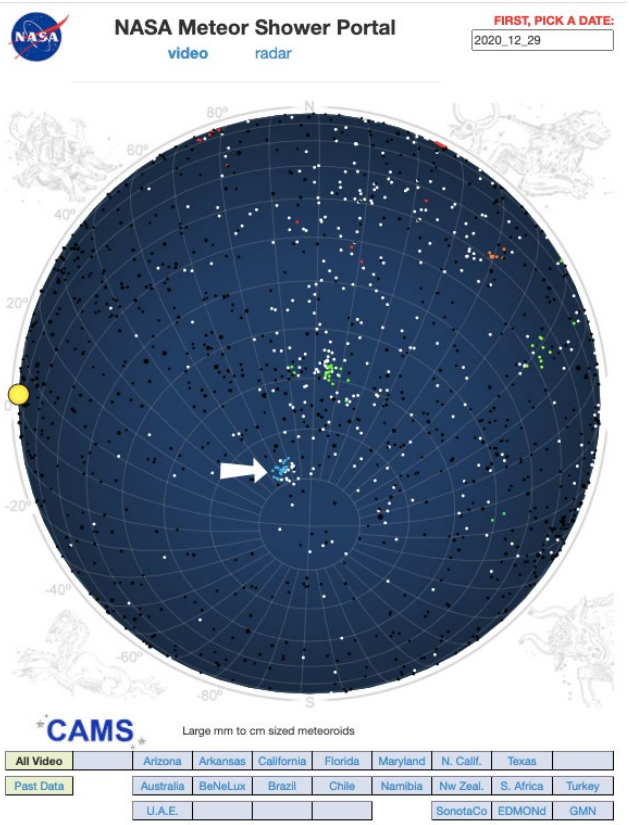

Figure 3 – The Volantid radiants on the CAMS radiant map of 2020 December 29.

If the shower behaves this year in the same manner as in 2015/2016, it is expected to grow in activity and peak on New Year's Eve Dec 31, 2020 in the western hemisphere, or the first day of the new year on January 1, 2021 on the eastern hemisphere.

The early sighting of the shower this year will enable targeted observations for the first time. The shower is expected to add to the New Year's Eve celebrations for observers in the southern hemisphere.

References

Jenniskens, P., Baggaley, J., Crumpton, I., Aldous, P., Gural, P. S., Samuels, D., Albers J., Soja R. (2016). "A surprise southern hemisphere meteor shower on New-Year's Eve 2015: the Volantids (IAU#758, VOL)". *WGN, Journal of the International Meteor Organization*, **44**, 35–41.

Jenniskens P. (2020). "Volantid meteors 2020". *CBET* 4901, 2020 December 29.

Younger J., Reid I., Murphy D. (2016). "Radar observations of the Volantids meteor shower". In, Roggemans A. and Roggemans P., editors, *Proceedings of the International Meteor Conference*, Egmond, the Netherlands, 2-5 June 2016. IMO, pages 352–357.

The very successful Lyrids 2020

Koen Miskotte

Dutch Meteor Society
k.miskotte@upcmail.nl

Many clear nights occurred over Europe during the period of April 15 to 30, 2020. As a result of the Corona pandemic, air traffic was halted and emissions on the ground had also been significantly reduced. This fact in combination with many high-pressure fields above Scandinavia resulted in many super clear nights for the BeNeLux. It was not only good to observe in the BeNeLux, it was also stable clear weather in other parts of Europe. In addition to data from Europe, there were also some small datasets from America, Asia and Australia. All in all, the Lyrid data could be well calculated. 55 observers reported 1472 Lyrids via the IMO site. In this article the results of the visual analysis of the Lyrids 2020 are presented and discussed.

1 Collecting data

As usual, the IMO site was first checked for available observations. The author also received observations from one observer who does not report to IMO. When the data was collected, a distinction was immediately made between the observations. The observations had to meet the following requirements:

- Only observations made with a limiting magnitude of 5.9 or higher were used.
- The coverage factor F may not exceed 1.10.

Table 1 – All observers who observed the Lyrids of 2020.

Observer	Obs.	T_{eff}	LYR	Loc.	Observer	Obs	T_{eff}	LYR	Loc.
Adam Tomasz	2	05^h30^m	8	PL	Kwinta Maciej	1	01^h00^m	7	PO
Amorim Alexandre	4	07^h02^m	5	BR	Lunsford Robert	6	14^h35^m	19	US
Bader Pierre	9	16^h57^m	54	DE	Maidik Alexandr	2	02^h00^m	5	UA
Bahmba Sachin	4	15^h00^m	23	IN	Marsh Adam	3	09^h19^m	19	AU
Baláž Martin	1	01^h36^m	7	ES	Martin Pierre	2	04^h49^m	16	CA
Brown Steve	1	02^h00^m	6	GB	Miskotte Koen	7	21^h54^m	97	NL
Casoli Marc	1	03^h15^m	10	FR	Novichonok Artyom	1	00^h30^m	3	RU
Cooper Tim	1	01^h00^m	0	ZA	Rendtel Ina	13	12^h00^m	146	DE
Csorgei Tibor	1	00^h30^m	3	SK	Rendtel Jurgen	14	12^h53^m	168	DE
Dygos Jaroslaw	3	08^h17^m	33	PL	Richter Janko	4	06^h49^m	11	DE
Edin Howard	1	01^h46^m	8	US	Ross Terrence	9	11^h54^m	42	US
Enno Sven-Erik	1	01^h30^m	19	LV	Sadiv Jan	2	02^h02^m	8	SL
Enzlein Frank	1	04^h15^m	31	DE	Schmeissner Stefan	2	03^h53^m	9	DE
Fekete János	1	01^h00^m	4	HU	Scholten Alex	1	01^h15^m	17	NL
Gaarder Kai	8	21^h56^m	44	NO	Schultze Kai	1	04^h42^m	25	DE
Gerber Christoph	2	04^h00^m	8	DE	Sperberg Ulrich	7	16^h19^m	88	DE
Govedič Mitja	1	01^h27^m	16	SI	Stone Wesley	1	02^h00^m	26	US
Growe Matthias	4	03^h09^m	4	DE	Stumpf Stephen	1	00^h55^m	7	US
Hickel Gabriel	3	03^h54^m	17	BR	Upaddhyay Shivam	1	05^h30^m	14	IN
Hughes Glenn	3	04^h14^m	5	AU	Vaclavikova Marcela	1	02^h15^m	12	CZ
Imrich Dominik	1	01^h15^m	3	SI	Vandeputte Michel	1	06^h00^m	50	BE
Johannink Carl	2	04^h01^m	26	DE	van Leuteren Peter	1	02^h39^m	22	NL
Jónás Károly	1	06^h00^m	34	HU	Weiland Thomas	5	17^h43^m	78	AT
Knöfel André	1	03^h19^m	30	DE	Winkler Roland	3	05^h34^m	14	DE
Konecny Jiri	1	02^h15^m	14	CZ	Wullaert Patrick	1	01^h13^m	13	FR
Koschack Ralf	3	07^h30^m	65	DE	Wächter Frank	1	01^h12^m	5	DE
Kostenko Roman	3	05^h28^m	28	PO	Wächter Sabine	8	10^h43^m	29	DE
Kozich Pete	1	01^h20^m	6	US	Zeller Paul	1	03^h00^m	11	US

Table 2 – Population index *r* for the Lyrids in April 2020.

Date (2020)	$\lambda_\odot$ (°)	$r_{[1;5]}$	±	$r_{[0;5]}$	±	$r_{[-1;5]}$	±	$r_{[-2;5]}$	±
14–15–16	25.70151	2.89	0.38	3.47	0.39	–	–	–	–
16–17	27.16914	3.9	0.48	3.15	0.51	–	–	–	–
17–18	28.14698	3.88	0.51		–	–	–	–	–
18–19	29.12434	3.15	0.45	2.96	0.47	–	–	–	–
19–20	30.10123	4.27	0.39	3.36	0.41	–	–	–	–
20–21	31.07762	2.88	0.26	2.84	0.25	2.5	0.24	2.47	0.24
21–22	32.05351	3.1	0.09	2.74	0.08	2.5	0.08	2.39	0.08
22–23	33.02889	2.88	0.17	2.55	0.16	2.55	0.15	2.43	0.15
23–24	34.00373	3.43	0.56		–	–	–	–	–
24–25–26	35.46499	3.56	0.46	2.94	0.43	–	–	–	–
26–27–28	37.41136	3.88	0.47	3.82	0.32	–	–	–	–

In total, 56 observers conducted 166 observation sessions, resulting in 1472 Lyrids. See also *Table 1*.

2 Population index *r*

To determine the population index r, all supplied magnitude distributions were checked on the following rule. The average magnitude of the observed meteors should not differ by more than 4 magnitudes from the observed limiting magnitude. After this check, of the 1019 Lyrids, 838 remained. These 838 Lyrids were used to determine the *r* value (Steyaert, 1981).

The results are shown in *Table 2* and *Figures 1 and 2*. Most results, as expected, were obtained with $r_{[1;5]}$. The disadvantage is that you exclude the Lyrids of 0, –1 and –2, which usually appear around the maximum and this gives a distorted picture for that period. In that regard, $r_{[0;5]}$ gives a better result and you can clearly see that more bright meteors are observed around the Lyrid maximum. Logically, the uncertainty in the nights around the maximum is also much lower. For 20–21, 21–22 and 22–23 April 87, 506 and 180 Lyrids respectively were used to determine the population index *r*.

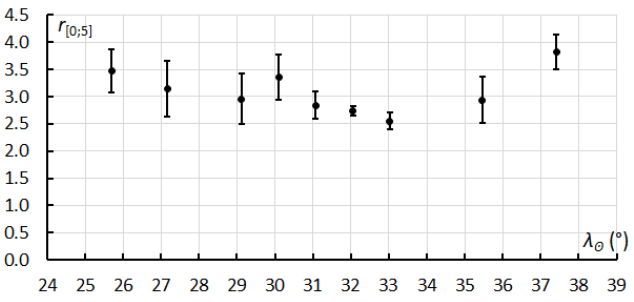

Figure 1 – Population index $r_{[0;5]}$ of the Lyrids in the period April 14–28, 2020.

The *r* values from $r_{[0;5]}$ were ultimately used for the final ZHR calculations. For the maximum the *r* value could also be determined over periods of one hour, in steps of half an hour. These results are shown in *Table 2* and *Figure 2*.

According to Rendtel (2019) the Lyrid maximum should occur on April 22, 2020 around 06^h40^m UT ($\lambda_\odot = 32.32°$), but the maximum time will vary from year to year between $\lambda_\odot = 32.00°$ and 32.45°. This is between April 21, 2020 22^h38^m UT and April 22, 2020 09^h42^m UT. It is known that more bright meteors appear quite soon after the maximum, the population index *r* then decreases quickly. If we look at *Figure 2*, we see a steady decrease in the population index *r* after $\lambda_\odot = 32.09°$. This could indicate that the maximum occurred just before this period. We will discuss this further in the next Section.3.

Table 3 – Population index *r* for the Lyrids during the night 21–22 April 2020.

Date+UT	$\lambda_\odot$ (°)	$r_{[-2;5]}$	±	$r_{[-1;5]}$	±
21–04–2020 21^h30^m	31.959	–	–	2.47	0.40
21–04–2020 22^h30^m	31.993	–	–	2.82	0.33
21–04–2020 23^h00^m	32.013	2.53	0.30	2.74	0.31
21–04–2020 23^h30^m	32.033	2.58	0.30	2.67	0.31
22–04–2020 00^h00^m	32.054	–	–	2.74	0.30
22–04–2020 00^h30^m	32.074	2.51	0.18	2.77	0.18
22–04–2020 01^h00^m	32.094	2.34	0.20	2.66	0.21
22–04–2020 01^h30^m	32.114	2.20	0.19	2.34	0.19
22–04–2020 02^h00^m	32.135	2.04	0.20	2.17	0.20

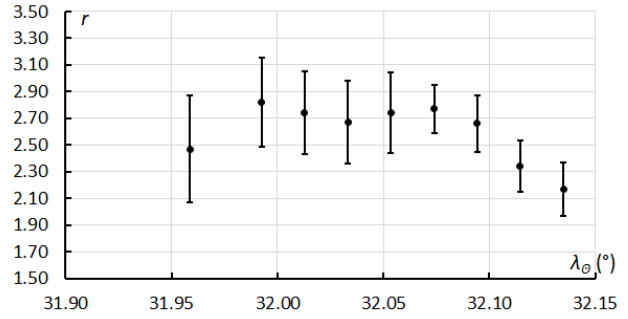

Figure 3 – Population index *r* of the Lyrids during the night 21–22 April 2020.

3 Zenithal Hourly Rates

After all Lyrid data was entered in the ZHR spreadsheet, the data was selected again on the following criteria.

- Radiant heights, minimum radiant height must be 25 degrees or higher.
- In case of too short observation periods, if possible, several short consecutive counting periods were added into longer periods.
- Extreme ZHR outliers were removed.

Among the 1472 Lyrids reported to the IMO and the author, 1083 remained after the first selection process from Section 1. After the second selection process described above, 1046 Lyrids were ultimately left. *Table 4* and *Figure 4* are the result of the calculations.

From *Figure 3* it is clearly visible that the ZHR is between 2 and 4 between $\lambda_\odot = 24°$ and 30°. After that, the activity increases to a maximum ZHR of 18. Only after $\lambda_\odot = 34°$ to 35° the ZHR drops below 5 again.

When did the maximum occur? We now zoom in on the maximum. A nice tool to get an idea when the (possible) maximum has fallen is the graph by Hirofumi Sugimoto. See *Figure 4* and also online[9].

Figure 4 shows that according to the radio ZHR method (Sugimoto, 2017), the maximum occurred exactly at $\lambda_\odot = 32.3°$. As the author already wrote in this article about the population index *r*, it seems that based on the population index *r* calculations the maximum has taken place around $\lambda_\odot = 32.09°$.

The night 21–22 April 2020 was then examined in detail. The ZHR values in *Table 5* and *Figure 5* were calculated on the basis of 25- to 60-minute counts. These were then averaged according to the "weighted average" method.

From *Figure 5* it seems that, based on visual observations, the maximum of the Lyrids has taken place over Europe, around $\lambda_\odot = 32.074°$. This is April 22, 2020 around 00^h27^m UT. Indeed, we also see the population index *r* decrease after this maximum. With a ZHR of only 14.6 ± 1.2, this is a weak Lyrid year. In the Meteor Shower Calendar 2020 (Rendtel, 2019) it is stated that when the peak is ideal, i.e. at $\lambda_\odot = 32.32°$, the ZHR is usually around 23. The further away from the 32.32° maximum the peak is, the lower the maximum ZHR is, with a minimum ZHR of 14. We now found a peak at $\lambda_\odot = 32.074°$ with a ZHR of 14.6 ± 1.2. That is roughly 6 hours earlier than the ideal time and thus seems to support the statement from the Meteor Shower Calendar 2020 of IMO. But there is still a 'problem'.

It is very unfortunate that the "ideal" maximum was expected on April 22, 2020 at 06^h40^m UT. The Sun is already above the horizon in Europe, while the radiant from America is still relatively low (except in the north east). Only 4 observers were active around this time. Unfortunately, their data could not be used due to too low limiting magnitudes or too high cloud percentages. A quick calculation of all these data with limiting magnitudes of 4.0, 5.0 and 5.1, and with one observer who had low radiant heights and cloud factors with F = 1.04, 1.85 and 1.66 resulted in ZHR values between 10 and 200! It should be clear why the author prefers not to use observing data with too low limiting magnitudes.

Table 4 – Lyrids 2020 ZHR based on 1046 Lyrids.

Day	UT	$\lambda_\odot$ (°)	ZHR	±
13	22.42	24.168	1.4	1.4
14	23.22	25.180	2.8	2.8
16	0.32	26.204	2.9	0.5
16	9.98	26.598	1.7	1.0
17	0.19	27.177	4.0	0.8
18	0.44	28.165	3.2	0.6
18	23.72	29.113	3.4	0.6
20	0.30	30.114	3.0	0.5
20	7.41	30.403	8.5	3.5
20	23.88	31.045	4.9	0.9
21	0.90	31.114	7.3	0.9
21	21.50	31.952	11.2	2.7
21	22.44	31.990	9.6	1.8
21	23.49	32.033	11.2	1.2
22	0.49	32.074	14.8	1.2
22	1.49	32.114	13.3	1.1
22	2.28	32.146	11.2	1.7
22	9.92	32.457	9.8	1.6
22	17.38	32.760	7.4	3.0
22	22.43	32.965	10.5	2.1
22	23.50	33.008	10.6	1.5
23	0.54	33.051	9.7	1.6
23	1.49	33.090	9.9	1.9
23	2.45	33.128	5.3	2.7
23	9.34	33.408	5.4	1.3
23	23.55	33.985	5.2	2.0
24	0.52	34.025	4.7	1.3
24	1.56	34.067	5.1	1.6
24	9.37	34.384	2.6	1.1
24	22.06	34.899	5.8	1.7
25	9.76	35.374	2.8	1.1
26	1.43	36.010	2.2	0.9
26	9.76	36.348	1.8	0.8
27	0.24	36.935	2.8	0.6
28	0.84	37.932	3.0	0.9
29	8.32	39.206	2.9	1.7
30	0.58	39.865	2.2	2.2
30	10.38	40.261	0.9	0.9

[9] http://www5f.biglobe.ne.jp/~hro/Flash/2020/LYR/index.html

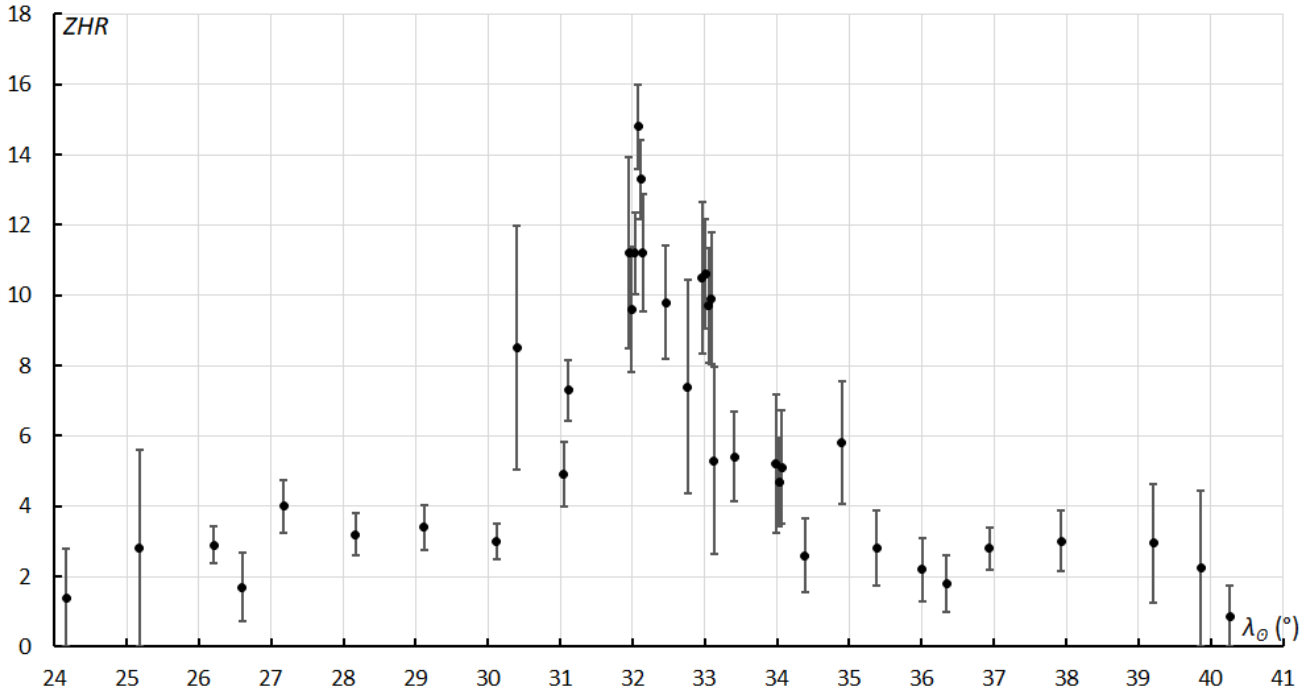

Figure 3 – The Lyrids ZHR curve based on Table 3. The solar longitude shown represents the period April 13–30, 2020.

Table 5 – ZHR of the Lyrids between April 21, 2020 21^h00^m UT and April 22, 2020 12^h00^m UT.

Day	UT	$\lambda_\odot$ (°)	Periods	LYR	ZHR	±	$r_{[-2;5]}$	OBS
21	21.50	31.952	4	17	11.3	2.7	2.47	4
21	21.96	31.971	5	18	10.6	2.5	2.68	5
21	22.47	31.991	8	29	11.8	2.2	2.82	8
21	23.04	32.015	15	71	11.4	1.4	2.66	12
21	23.49	32.033	19	94	11.2	1.2	2.58	14
22	0.05	32.055	21	116	11.7	1.1	2.54	16
22	0.49	32.074	22	154	14.6	1.2	2.51	16
22	1.02	32.095	20	140	13.0	1.1	2.36	13
22	1.49	32.114	20	140	12.1	1.0	2.2	16
22	1.95	32.133	17	122	13.1	1.2	2.13	13
22	2.25	32.148	5	42	12.9	2.0	2.04	6
22	8.62	32.404	1	8	19.4	6.8	2.04	1
22	9.15	32.425	1	9	17.6	5.9	2.04	2
22	9.63	32.445	1	5	9.4	4.2	2.04	2
22	10.13	32.465	1	4	7.7	3.8	2.04	1
22	10.63	32.486	1	3	3.9	2.2	2.04	1
22	11.63	32.526	1	1	1.2	1.2	2.04	1

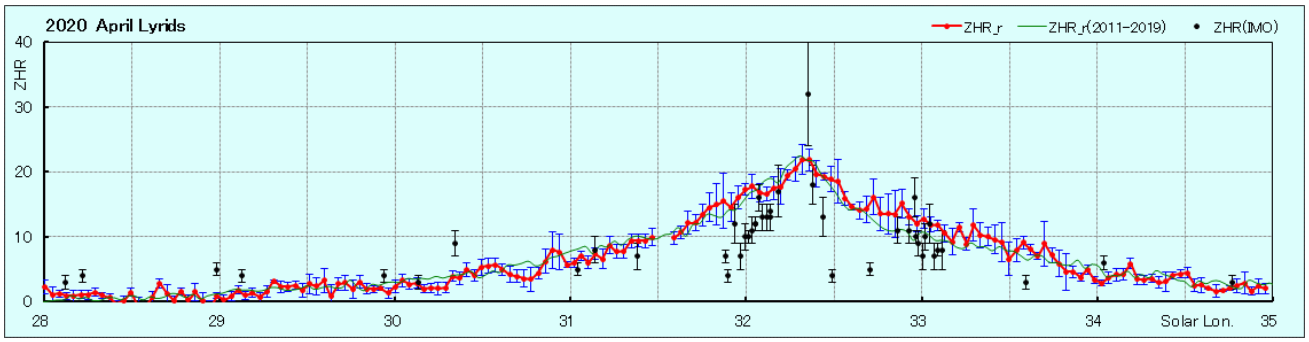

Figure 4 – The radio ZHR curve of the Lyrids 2020 by H. Sugimoto.

If we then look at American data that meet the requirements described earlier in this article, the observations of two observers remain: Bob Lunsford and Wesley Stone. These were added to the graph in *Figure 5*. The result of this we find in *Figure 6*. We must keep in mind that on the one hand it is data from just two observers of which two counting periods coincides, and on the other hand, the overlapping period is very close in terms of ZHR and both are experienced observers who have been active for many years. This indicates that these observations are reliable.

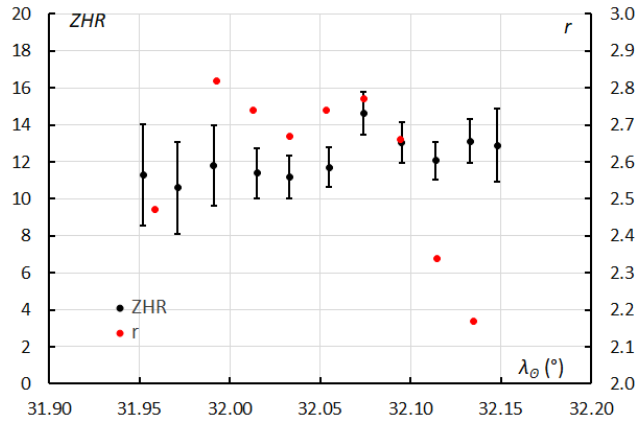

Figure 5 – ZHR and population index *r* of the Lyrids during the night April 21–22 together in one graph. Only European data.

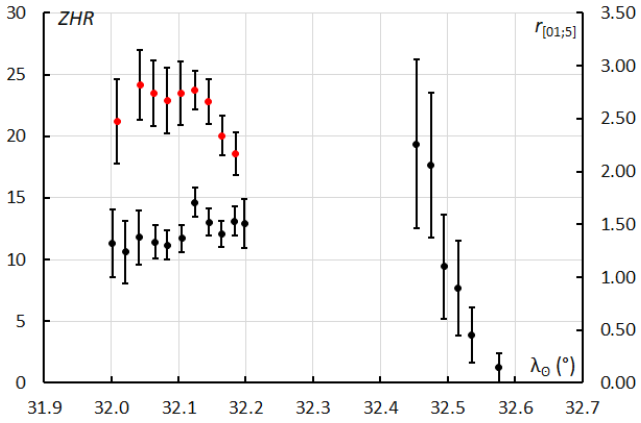

Figure 6 – Detailed graph of the Lyrids at night 21–22 April 2020 between 21^h00^m and 12^h00^m UT.

Figure 6 therefore shows the problem of the Lyrids anno 2020: at first sight a maximum above Europe around $\lambda_\odot = 32.074°$. The ZHR is correct, the population index *r* trend is also what you would expect. However, the good US data immediately indicates higher ZHR values than found in Europe, albeit with larger uncertainties and by only two observers, with immediately a decrease in the ZHR values. This is also what you would expect at a maximum around 32.32° (April 22, 2020 6^h40^m UT). But unfortunately, there is no good observational data available from around that period.

According to the radio method, a maximum (ZHR 22) is found at the "correct" $\lambda_\odot = 32.32°$. A sub-peak is visible when the European "maximum" was found. The way Sugimoto converts the radio observations to a ZHR curve is described in (Sugimoto, 2017).

4 Conclusion

All in all, based on the visual data, it seems difficult to determine when the "real" maximum took place. However, if we look at all observations in comparison with the radio ZHR data, you could cautiously state that the Lyrid maximum probably took place at $\lambda_\odot = 32.3°$.

It is very unfortunate that there are no more observers active in Asia and America, people who observe meteors on a regular basis. Please, try to observe some nights outside the annual meteor shower maxima. Data from the end of July and August is particularly welcome, so the author can make reliable C_p calculations for the observers.

Acknowledgments

A very big thank you goes to all observers who have observed the Lyrids. Without their efforts this analysis was not possible! Their names are all listed in *Table 1*. In addition, a word of thanks to Carl Johannink and Michel Vandeputte for reading this article critically and giving advice for this article. And last but not least a thank you to Paul Roggemans for checking my English!

References

Rendtel J. (2019). Meteor Shower Calendar 2020, IMO.

Steyeart C. (1981). "Populatie indexbepaling : methode en nauwkeurigheid". Technische Nota nr. 5 VVS Werkgroep Meteoren.

Sugimoto H. (2017). "The new method of estimating the ZHR using radio meteor observations". *eMetN*, **2**, 109–110.

Perseids 2020 revisited

Koen Miskotte

Dutch Meteor Society
k.miskotte@upcmail.nl

Additional visual observational data from the Canadian meteor observer, Pierre Martin, brought more evidence for a secondary peak at solar longitude 141° in the ZHR profile of the Perseid meteor shower.

1 Introduction

A few weeks after the publication of (Miskotte 2020a; 2020c), another set of observations had become available online on the IMO website of the experienced meteor observer Pierre Martin from Canada. An extensive description of these observations with many beautiful photos can be found on MeteorNews[10] (Martin, 2020).

It is clear that there was something special going on. His observations describe well the experiences of Paul Jones, who observed from Florida (USA) at the same time. Unfortunately, Paul Jones was unable to produce an observational report for analysis due to widely varying weather circumstances (Miskotte 2020a; 2020c).

2 Pierre Martin's observations: population index *r* and *ZHR*

Pierre Martin's observations can be found on the IMO site[11].

Pierre wrote about his observations: "*What a great night with a lot of action! As soon as my cameras were up and running, I started visual observing soon after 10:00pm (EDT) and I continued until 5:00am the next morning, for a total of 6 hours of observing (excluding breaks). In that time, I counted 296 meteors (252 Perseids, 7 South delta Aquariids, 4 Anthelions, 4 North delta Aquariids, 2 kappa Cygnids, 1 eta Eridanid and 26 sporadics). PER hourly rates were: 35, 30, 54, 45, 51 and 37 (the final count was a little less than an hour in brightening twilight). These rates were better than I expected especially due to the fact that the traditional peak was expected to occur nearly a day earlier. There was a mix of both bright and faint Perseids. The brightest Perseid was a –5 fireball seen at 12:51am that had a terminal flash and a 12 seconds train*".

During 5.48 hours effective observing time he counted 296 meteors, 251 of which were Perseids. This under decreasing circumstances due to the rising Waning Crescent Moon from Lm 6.8 to 5.5. He mentioned a striking number of faint and bright Perseids.

The population index *r* was first calculated from the observational data. Overlapping periods have been calculated. The outcome is somewhat surprising. Although Pierre speaks of many faint and bright Perseids, the population index *r* has an interesting trend. This runs steadily from low (= many bright meteors) to high (= many faint meteors). See *Figure 1* for the result.

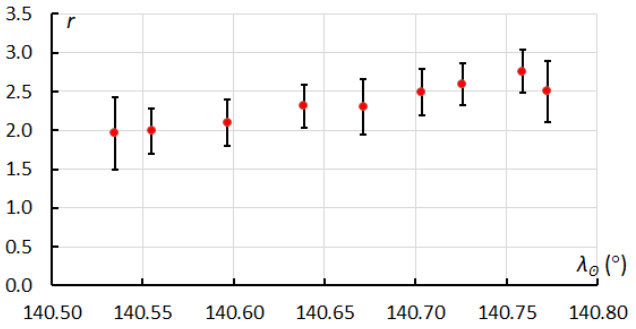

Figure 1 – Population index *r* [–2;+5] calculated from the observational data of Pierre Martin. The timescale shown is roughly August 13, 2020 between 2^h00^m and 9^h00^m UT.

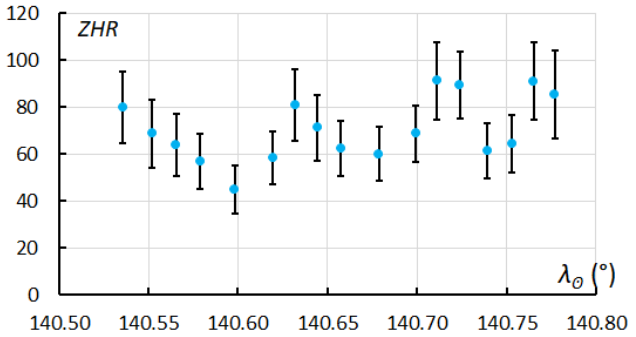

Figure 2 – ZHR Perseids calculated from Pierre Martin's observational data. The period runs from August 13 between 02^h00^m and 09^h00^m UT.

For the ZHR, periods of 0.500 to 0.666 effective hours have been calculated, a single period is slightly longer and, as with the population index *r*, overlapping periods were used. Three peaks appear to be visible; the result is shown in *Figure 2*.

First, we see a decreasing activity, perhaps decreasing annual activity. A first peak occurs around $\lambda_\odot = 140.63°$ (ZHR 80), then a slightly stronger peak $\lambda_\odot = 140.72°$ (ZHR 90) and the third peak appears at $\lambda_\odot = 140.77°$ (also ZHR 90). During the last peak, a –8 or brighter Perseid appeared, not directly visually but a 20 second luminous trail was seen

[10] https://www.meteornews.net/2020/10/23/observations-august-11-12-and-12-13-2020/

[11] https://www.imo.net/members/imo_vmdb/view?session_id=81140

just next to the Moon! In *Figure 3* the *r* value and the *ZHR* are combined.

It is clearly noticeable here that the lowest *r* values coincided with the decreasing ZHR after the annual peak. This also seems to fit a bit into the picture with the 2019 outburst. In the run-up to $\lambda_\odot = 141°$, an increase of bright Perseids was noticeable over western Europe towards dawn. Due to the increasing twilight, it is not clear whether the *r* value subsequently increased during the course of the 2019 peak (Miskotte, 2020b).

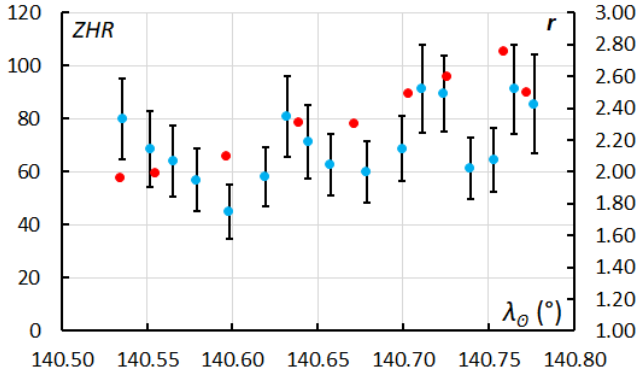

Figure 3 – ZHR and population index *r* based on data from Pierre Martin.

Then we also looked at the radio ZHR. Pierre Martin's ZHR curves are combined with Hirofumi Sugimoto's radio ZHR curve. A reasonably similar picture, see *Figure 4*.

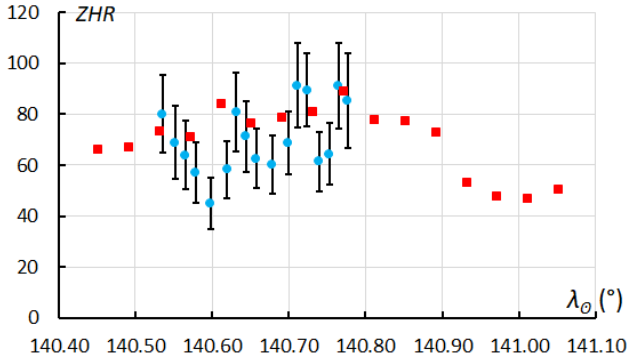

Figure 4 – The radio ZHR curve combined with the visual ZHR curve.

Pierre Martin's observational data is a nice visual confirmation of the peak of activity observed in the radio ZHR curve. It is unfortunate that the data from Florida observer Paul Jones could not be used in this analysis (Miskotte 2020a, 2020c). The 2020 peak fell as much as 0.17 degrees (4 hours) earlier in solar longitude than the 2018 peak (Miskotte, 20219) and even 0.25 degrees (6 hours) earlier in solar longitude than the 2019 radio ZHR peak (Miskotte, 2020b).

This is interesting: in 2019, in the run-up to the (radio) peak, many bright Perseids were observed from Western Europe. The peak was not observed visually itself, or only under very poor conditions. Also, in 2020 in the run-up to the peaks also some more bright Perseids occurred, weakening during the peaks.

The question is also whether this is the same structure we see, because of the considerable spread of the maximum. It remains to be seen whether we see a peak in activity again in 2021. So, observing is the motto!

References

Miskotte K. (2019). "The Perseids in 2018: Analysis of the visual data". *eMetN*, **4**, 135–142.

Martin P. (2020). "Visual observations August, 2020". *eMetN*, **5**, 430–434.

Miskotte K. (2020a). "Perseïden 2020: voor de derde keer een uitbarsting rond zonslengte 141 graden?". Radiant, 42, 87–89.

Miskotte K. (2020b). "Perseids 2019: another peak in activity around solar longitude 141.0°?". *eMetN*, **5**, 25–29.

Miskotte K. (2020c). "Perseids 2020: again, enhanced Perseid activity around solar longitude 141°?". *eMetN*, **5**, 395–397.

The proper name for AUD (#197) is ZDR

Masahiro Koseki

NMS (The Nippon Meteor Society), 4-3-5 Annaka Annaka-shi, Gunma-ken, 379-0116 Japan
geh04301@nifty.ne.jp

The AUD (#197) entry in the IAUMDC working list of meteor showers is confusing. The first reference orbit listed for AUD, AUD0, is a Harvard radar observation but very weak, slightly above the detection level. The second entry, AUD1, is a CAMS video observation and a conglomerate of two meteor shower activities; one should be named as ZDR that had been properly suggested by former researchers and the second one could be named AXD (August ξ-Draconids, preliminary name). ZDR (#73) in the IAUMDC list cannot be confirmed by other video observations. ZDR (#73) and AUD (#197) should be removed from the IAUMDC list or renamed by other more suitable names.

1 Introduction

The August Draconids (AUD#197) shower has been first found by Sekanina in the Harvard radar observations, but it may be another different stream activity than the later 'AUD' records. The IAUMDC lists two other AUD observations though these are possibly misled by the activity of the CDC (Cygnid-Draconid Complex, see Koseki, 2014b), especially by the AXD and ZDR showers (see *Section 4* in detail).

ZDR in the IAUMDC list seems to be false. The author pointed out that ZDR is badly treated in the IAUMDC working list; the name of ZDR is not correctly used by Jenniskens (2006, page 721)[12]. He also commented that the ZDR shower is equal to the θ-Herculids. The first line of his ZDR entry suggests it is based on the source 'BA' but 'BA' is not listed in his book. Meanwhile, Koseki (2014b) pointed out that one of the members of the Cygnid-Draconid Complex coincides with the ZDR proposed by Terentjeva (1966) and Lindblad (1971).

It is necessary to clear out what is active during the activity period and in the area of 'AUD'. We use the 2018 January 13 $20^h35^m17^s$ version of the IAUMDC meteor shower database. Meanwhile, the shower list has been changed suddenly without written explanations.

2 AUD (#197) in the Harvard radar observations

The first orbit reference for the AUD (#197) in the IAUMDC shower list is the Harvard radar observation in 1968–69 (Sekanina, 1976, see *Table 1*). Sekanina reported other series of radar observations in 1961–65 (Sekanina, 1973) and we refer to these simply as 61–65 and 68-69 observations hereafter. We had better checked the observations in detail at first. *Figure 1* shows the radar radiant distribution with the reference meteor showers.

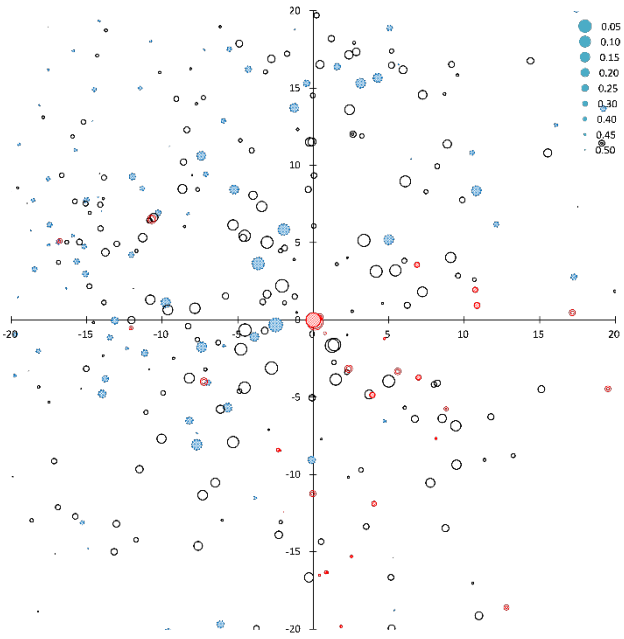

Figure 1 – Harvard radar radiant distributions in an azimuthal equidistant projection in ecliptic coordinates centered at $(\lambda-\lambda_\odot, \beta) = (164.2°, 88.2°)$ during $\lambda_\odot = 132°\sim152°$. The line $\lambda-\lambda_\odot = 164.2$ is the y-axis, the units are degrees. Symbols; shaded blue circles: 61–65 observations, black circles: 68–69 observations, red circles: are meteor showers listed in the IAUMDC (shaded) and the other important list (double), (Koseki, 2009). Radii are in accordance with *D(M,N)* values.

Table 1 – The summary data of AUD (#197) entries. 0197AUD02 is omitted because it is similar to 0197AUD01.

Code	$\lambda_\odot$	α	δ	$\lambda-\lambda_\odot$	β	v_g	e	q	i	ω	Ω
	(°)	(°)	(°)	(°)	(°)	(km/s)		A.U.	(°)	(°)	(°)
0197AUD00	142	272.5	65.1	164.2	88.2	17.3	0.335	1.007	30.4	185.6	141.9
0197AUD01	143	271.7	58.9	133.6	82.3	21.1	0.644	1.008	33.8	188.7	142.6

[12] http://www.astro.sk/~ne/IAUMDC/STREAMLIST/meteoroidstreamworkinglist.pdf

Larger circles, which are closer to the core of the stream, seem to be concentrated on the center, but it is an apparent effect. It is necessary to check whether this concentration means a real shower activity by the *D(M,N)* distribution; D_{SH} values (Southworth and Hawkins, 1963) calculated between the mean orbit *M* and the individual orbits *N*. We calculate D_{SH} values between the AUD0 (#197) orbit and all the Harvard radar meteors and show the result in *Figure 2*. The shape is very different from video data; major showers are buried in a monotonous profile contrary to the complex profiles with sharp peaks (see Koseki, 2020a). Meteor showers observed by radar look different compared to video ones. Radar showers cannot be detected by video and vice versa (Koseki, 2014a). We should exclude the prejudice that a meteor shower can be observed by all observational techniques.

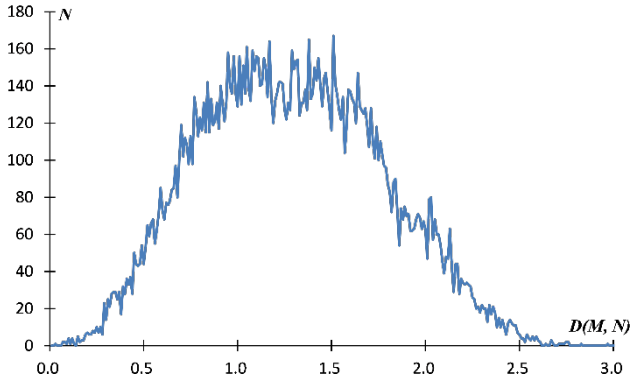

Figure 2 – Distribution of *D(M,N)* values of 68–69 Harvard radar meteors for AUD0.

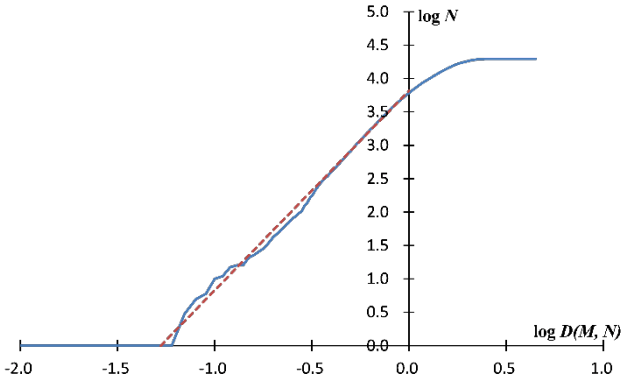

Figure 3 – Logarithmic cumulative distribution of *D(M,N)* values for 68–69 Harvard radar meteors; the supposed calculated sporadic distribution *D(M,N)* = 0.4~1.0 is shown by a dashed line.

Figure 3 shows the distribution on a logarithmic scale with the supposed sporadic distribution (dashed line). We should not consider all the meteors below the D_{SH} limit, such as $D_{SH} < 0.2$, as belonging to the meteor shower. There are even sporadic meteors with $D_{SH} < 0.1$ naturally, because sporadic meteors are distributed randomly. We can estimate the real number of AUD meteors by the difference between the straight line and the dashed line in *Figure 3*. The numbers of supposed AUD are slightly above 0 within the range of D_{SH} smaller than 0.2. Its activity may be very weak (*Figure 4*). Though Sekanina reported AUD by 68–69 observations (Sekanina, 1976), it is interesting whether AUD can be detected in the 61–65 observations. *Figure 5* is the result of the 61–65 observations after processing the data in the same way as the 68–69 data and the AUD shower activity cannot be not certified from this 61–65 dataset.

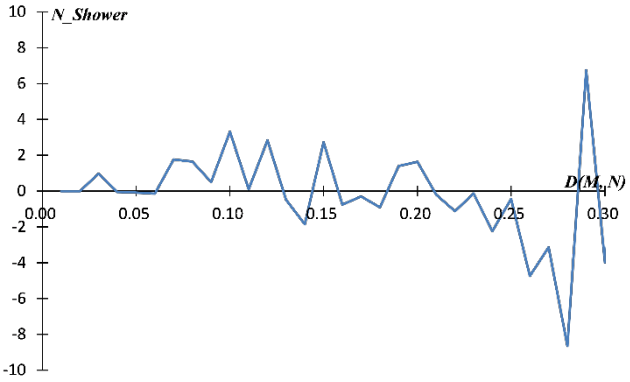

Figure 4 – The estimated AUD meteors in 1968–69 with *D(M,N)*; the difference of the real distribution in Figure 3 minus the supposed sporadics.

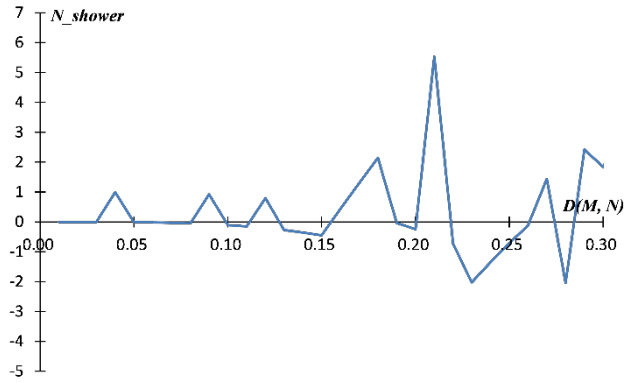

Figure 5 – The estimated AUD meteors in 1961–65, with *D(M,N)*; the difference of the real distribution in Figure 3 minus the supposed sporadics.

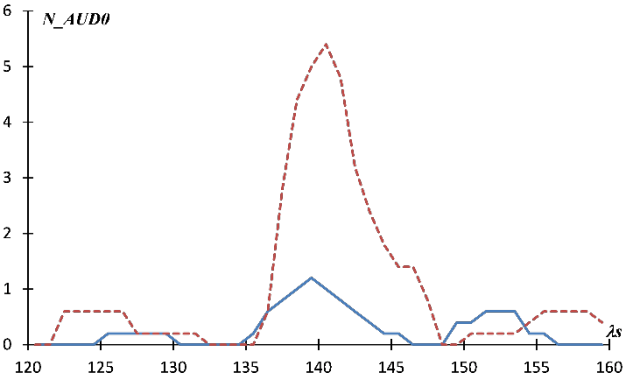

Figure 6 – The distribution of *D(M,N)* < 0.2 meteors in function of $\lambda_{\odot}$, blue line for 61–65 data, red dashed line for 68–69 data.

We can find several possible AUD radiants with *D(M,N)* < 0.2, and their distribution along with $\lambda_{\odot}$ seems interesting (*Figure 6*). These meteors make clear peaks around $\lambda_{\odot} = 140°$ both in the 61–65 and the 68–69 observations. The 68–69 peak is much higher than that of 61–65. But these peaks are false; Harvard radar observations were intermittent (*Figure 7*). Both observation series intended to observe the Perseids and the observations were operated around the Perseid maximum. It is natural that the larger the total number of observations, the more *D(M,N)* < 0.2 meteors. It is unfortunate for us that there are no or very few observations between $\lambda_{\odot} = 145$~150 when the ZDR (not the IAUMDC's ZDR, see

following sections) reaches its maximum. We cannot confirm the AUD nor the ZDR activity in the Harvard radar observation series; we will continue the study of the AUD and the ZDR in the following sections.

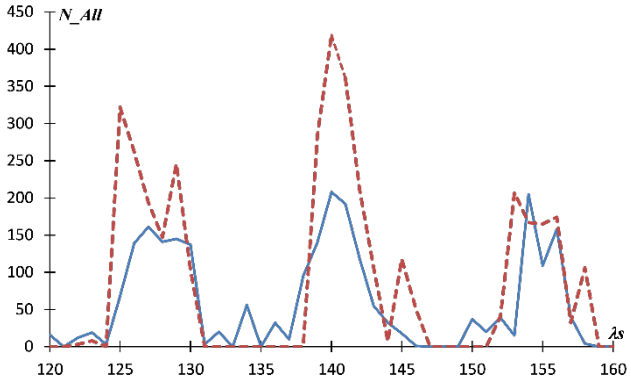

Figure 7 – The sum of all radar meteors in 1 degree $\lambda_\odot$ bins; radar operations were interrupted several times.

3 AUD (#197) in CAMS

The second entry of the AUD shower in the IAUMDC list is from CAMS, AUD1 (*Table 1*). But, AUD1 seems different from AUD0. *Figure 8* gives the radiant distribution around AUD0 based on CAMS data; the plotting method is the same as in *Figure 1*. There are more $D(M,N) < 0.2$ radiants than in *Figure 1*. It is obvious that video meteors, which are brighter, are numerous in this field. This does not mean that the AUD0 activity is confirmed by CAMS observations. Many $D(M,N) < 0.2$ radiants belong to other showers (*Figure 9* and *Table 2*). *Figure 10* shows that CAMS did not catch the AUD0 activity. The number of $D(M,N) < 0.2$ meteors is obviously below the supposed sporadic distribution (dashed line). The geocentric velocity of AUD1 is some 4 km/s higher than AUD0. AUD1 is not equal or equivalent to AUD0; AUD1 seems to be another shower with brighter video meteors.

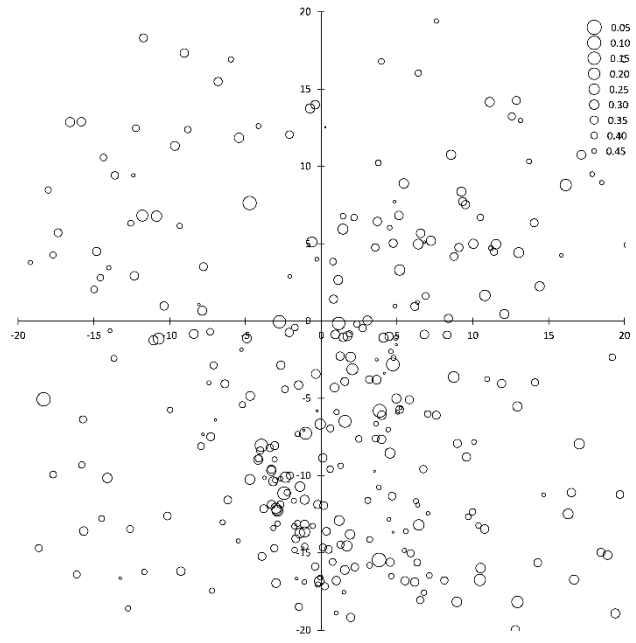

Figure 8 – CAMS radiant distribution around AUD0; centered at $(\lambda - \lambda_\odot, \beta) = (164.2°, 88.2°)$. The center position, the period and the radii of circles are done in the same way as in Figure 1.

Table 2 – The IAUMDC showers that appear in Figure 9, (x, y) represents the position in Figure 9.

Code	$\lambda_\odot$ (°)	$\lambda - \lambda_\odot$ (°)	β (°)	v_g km/s	x	y
0012KCG10	135.8	161.2	71.9	23	0.9	–16.3
0012KCG08	136.9	159.3	68.3	22.5	1.8	–19.8
0012KCG05	137	155.7	72.7	22	2.5	–15.3
0855ATD00	138.3	276.7	78.1	33.1	-11	6.3
0012KCG04	140.7	161.5	71.9	21.9	0.8	–16.3
0012KCG09	140.9	162.9	71.7	23	0.4	–16.5
0012KCG07	141	147.7	75.8	20.9	4	–11.9
0197AUD00	142	164.2	88.2	17.3	0	0
0197AUD01	143	133.6	82.3	21.1	3.9	–4.8
0470AMD01	144.4	78.5	79.1	18.98	10.8	0.9
0012KCG02	145	176.4	79.5	24.8	-2.2	–8.4
0012KCG00	145.2	177	79.6	24.8	-2.3	–8.4
0012KCG01	145.2	158.1	74.5	24	1.6	–13.6
0470AMD00	145.4	73.2	79.3	19.5	10.7	1.9
0197AUD02	146.5	112.4	81.1	21.1	7	–3.7
0012KCG03	147.6	172	75.7	24.9	-2	–12.4
0470AMD02	149	59.5	82.9	21.3	6.9	3.6
0012KCG06	150	106.5	84.4	23.1	4.7	–1.2

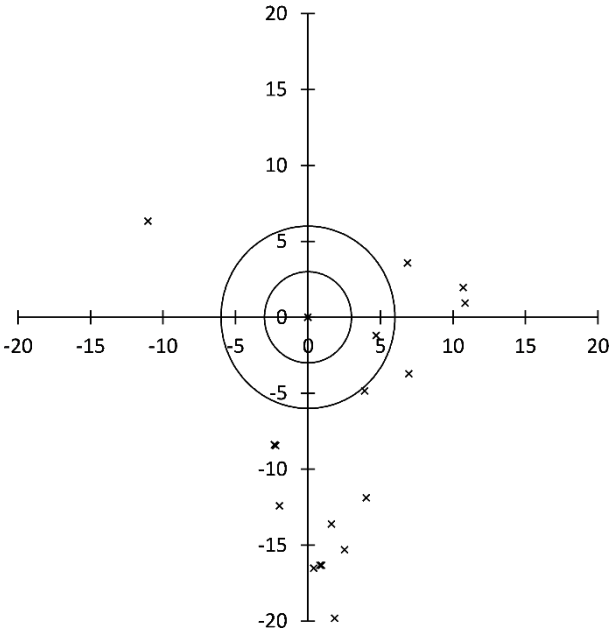

Figure 9 – The IAUMDC showers radiant distribution around AUD0. The center position and the period are the same as in Figures 1 and 8. The showers plotted in this figure are listed in Table 2.

Figure 11 shows all AUD1 meteors classified in the CAMS catalogue and we can see that the distribution curiously bends. *Figure 12* reveals the cause for this unnaturalness. KCG is below left of the center and its distribution is elongated but not bent. CAMS' AUD spreads from the center to right upward and left downward suggesting two elongated extents. *Figure 13* strengthens the supposition that AUD1 consists of two shower activities; one reaching

its maximum at $\lambda_\odot = 140°$ and another around $\lambda_\odot = 150°$. We try to confirm these two components in the next section.

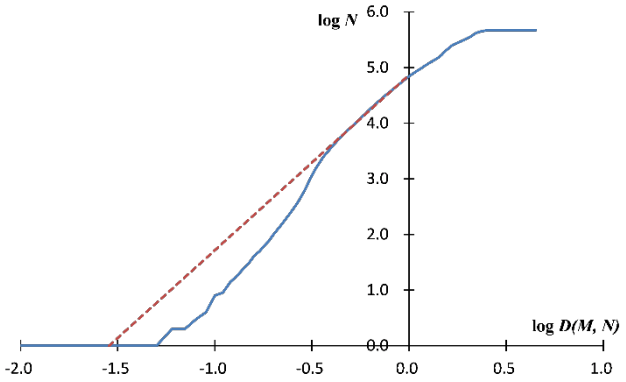

Figure 10 – Logarithmic cumulative distribution of *D(M,N)* values for CAMS meteors for AUD0; supposed calculated sporadic distribution *D(M,N)* = 0.4~1.0 is shown by a dashed line.

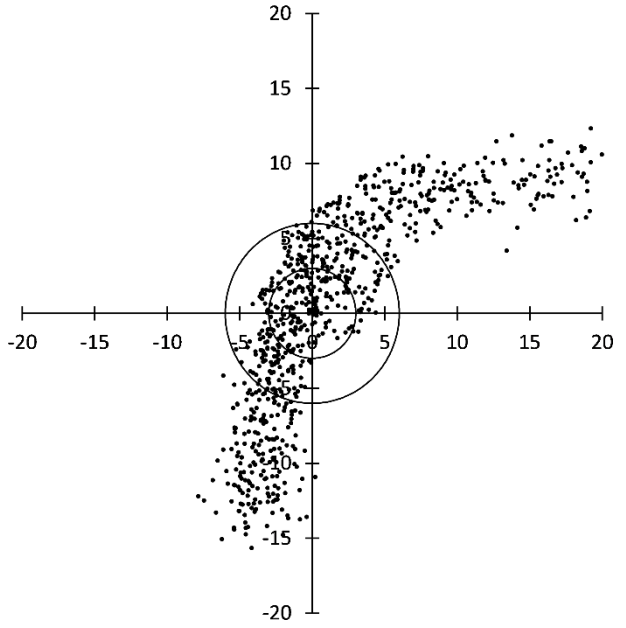

Figure 11 – The radiant distribution of AUD1 meteors classified in the CAMS catalogue centered at $(\lambda - \lambda_\odot, \beta) = (133.6°, 82.3°)$.

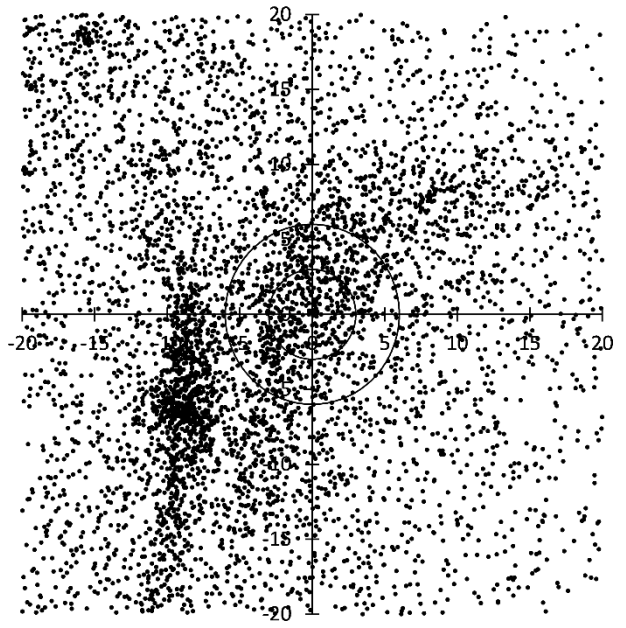

Figure 12 – The radiant distribution of CAMS meteors during $\lambda_\odot = 120$~160 centered at $(\lambda - \lambda_\odot, \beta) = (133.6°, 82.3°)$.

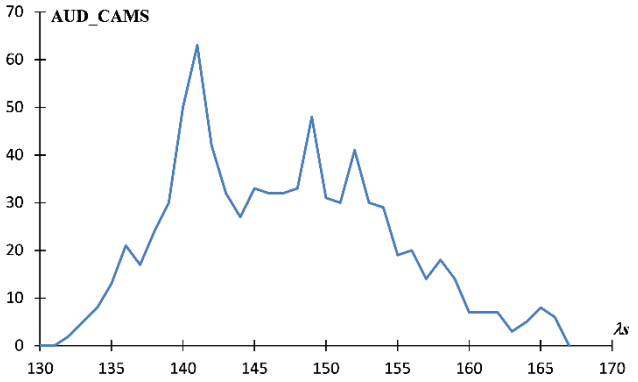

Figure 13 – AUD1 meteors classified according to the CAMS catalogue in 1 degree $\lambda_\odot$ bins.

4 Recent observations on the CDC (Cygnid-Draconid Complex)

The author suggested at least four independent meteor shower activities in the Cygnus-Draco area in August (Koseki, 2014b) and confirmed these by three more recent video data sets; SonotaCo net, EDMOND and CAMS (Koseki, 2020b). These four shower activities have mistaken observers by their complexity. GDR (#184) crosses the KCG (#012) radiant path, the AXD (August ξ Draconids, preliminary name) runs parallel to the KCG and the early ZDR (#073) (not AUD (#197), see next section) activity overlaps with late AXD activity (*Figure 14*).

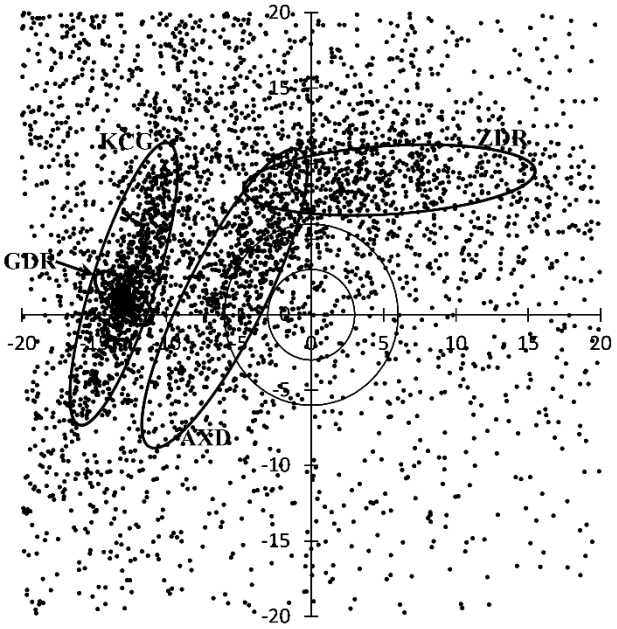

Figure 14 – Four meteor shower activities represented by EDMOND observations during $\lambda_\odot = 120°$~$160°$ centered at $(\lambda - \lambda_\odot, \beta) = (116°, 68°)$.

AXD was named KCG3 in the first paper (Koseki, 2014b) and marked as a steady shower activity and more active than the KCG in regular years (*Table 3*). AXD is located about 5 degrees west of the KCG and, therefore, not only visual observers but also video observers tend to misidentify AXD meteors as KCG.

Table 3 – The numbers of shower meteors classified in the SonotaCo net observations (Koseki, 2020b).

Year	2007	2008	2009	2010	2011	2012	2013	2014	2015	2016	2017	2018	Total
GDR	11	11	5	8	0	2	0	18	6	5	1	7	74
KCG	135	2	5	8	2	7	20	93	4	5	0	2	283
AXD	21	2	7	7	7	9	8	2	6	7	3	9	88
ZDR	2	1	11	14	3	15	7	1	1	2	7	5	69

Table 4 – The comparison between four CDC shower activities from earlier results (Koseki, 2014). The upper lines are the earlier results, the lower lines are the result for this study.

Code	$\lambda_\odot$ (°)	$\lambda-\lambda_\odot$ (°)	β (°)	α (°)	δ (°)	vg km/s	e	q A.U.	i (°)	ω (°)	Ω (°)
GDR	125.3	168.1	73.5	280.3	50.9	27.2	0.947	0.978	40.2	202.3	125.3
	125	167.1	73.1	279.9	50.4	26.8	0.931	0.978	39.5	202.7	125
KCG	141.4	164.4	70.9	287	49.6	22.3	0.703	0.968	33.8	206.5	141.4
	140	163	71.7	285.4	50	22.1	0.698	0.973	33.7	205.4	140
AXD	145	139	81.7	272.9	58.2	21.3	0.642	1.004	33.7	190.1	145
	146	145.1	81.8	275.7	58.8	21.3	0.629	1.005	34.1	191.2	146
ZDR	151.3	47.8	82.5	255.1	62.4	21.3	0.641	1.006	33.8	174.5	151.3
	156	42.7	80.7	250.8	62.2	20.6	0.627	1.006	32.6	171.9	156

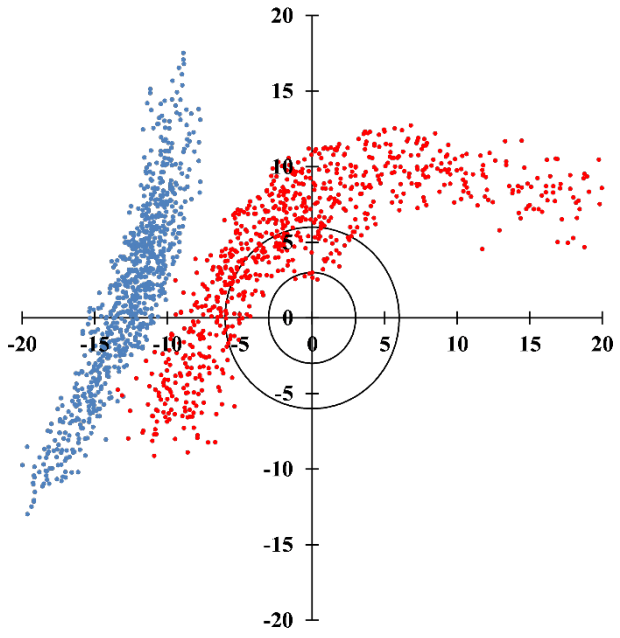

Figure 15 – The radiant distributions of the KCG and AUD by CAMS according to its own shower definition. Blue circles (left) are the KCG and red circles (right) are the AUD.

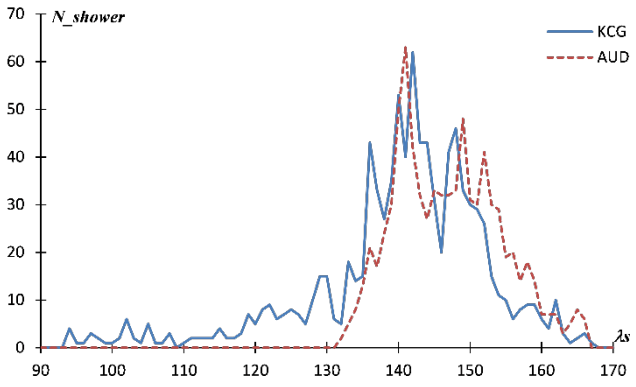

Figure 16 – Activity profiles for the KCG and the AUD by CAMS according to its own shower definition.

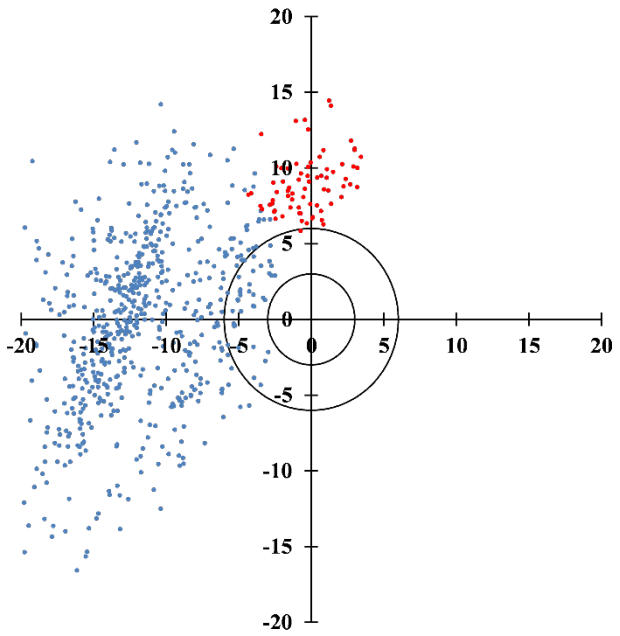

Figure 17 – Radiant distributions of the KCG and the AUD by SonotaCo net according to its own shower definition. Blue circles (left and center) are KCG and red circles (above the center) AUD.

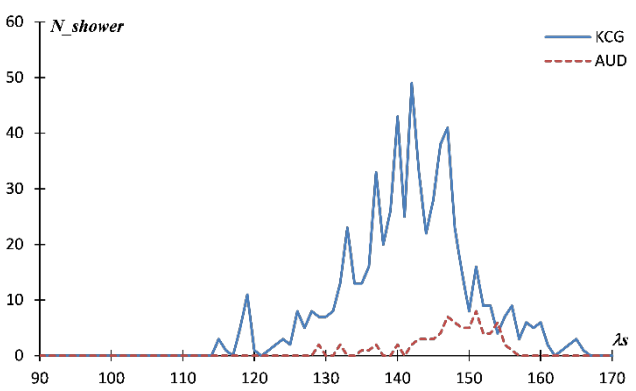

Figure 18 – Activity profiles of KCG and AUD by SonotaCo net according to its own shower definition.

It is worthy to note the difference in the shower classification between the three video datasets; we can visualize the difference by comparing the activity profiles and the radiant distributions according to their own classification. *Figure 15* represents the radiant distributions of the KCG and the AUD by CAMS. Compared with *Figure 14* it is obvious that CAMS classified AXD meteors as AUD and clearly distinguished AXD from KCG. *Figure 16* shows that CAMS extended the KCG activity to early July ($\lambda_\odot < 95°$) and the KCG in CAMS overflow *Figure 15* leftwards below. SonotaCo net included AXD meteors as KCG but separated them from AUD (*Figure 17*). KCG seems strikingly more active than AUD in SonotaCo net (*Figure 18*) but this is caused because CAMS missed enhanced KCG activity while SonotaCo net had it twice. EDMOND inherits the definition of SonotaCo net and the results are similar to it (*Figure 19 and 20*); the sharp peak at $\lambda_\odot = 126°$ is clearly due to the GDR activity.

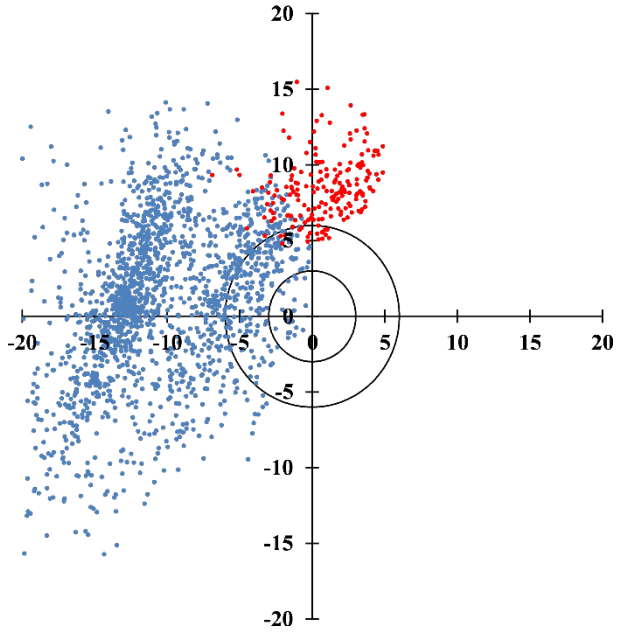

Figure 19 – Radiant distributions of the KCG and the AUD by EDMOND according to its own shower definition. Blue circles (left and center) are KCG and red circles (above the center) AUD.

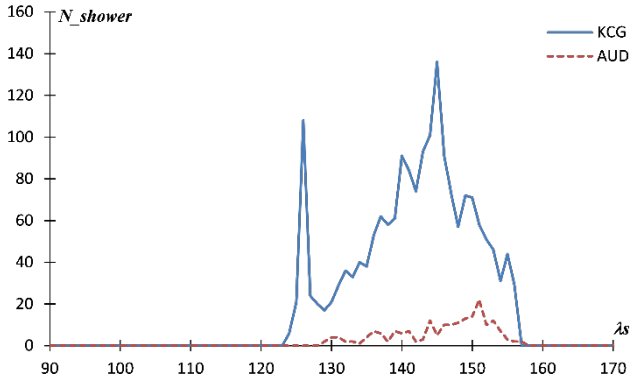

Figure 20 – Activity profiles of the KCG and the AUD by EDMOND according to its own shower definition.

It would have been better to search for the shower identification in the usual way rather than to use the classifications done by the networks in their own way. The author investigated the above mentioned four CDC shower activities (Koseki, 2020b) using his first study as the starting points (Koseki, 2014b). We use the mean radiant points and collect shower meteors by several iterations taking the radiant drift into consideration. The search periods are limited in time in order to exclude duplications in the shower identification (see *Figure 14*): GDR $119.6° < \lambda_\odot < 129.6°$, KCG $130° < \lambda_\odot < 154°$, AXD $135° < \lambda_\odot < 145°$, ZDR $150° < \lambda_\odot < 160°$. The summaries of the results are given in *Table 4* and *Figure 21*. Both investigations are based on different methods but they are in good agreements. It is necessary to be careful that the activity profiles are limited according to the above-mentioned search periods. The hump in the profile of the GDR around $\lambda_\odot = 140°$ is caused by another meteor shower activity, such as the AXD, which occurs on the path of the estimated radiant drift.

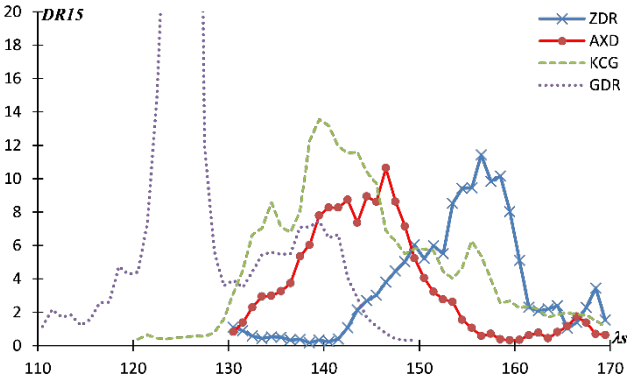

Figure 21 – Activity profiles by counting meteors taking the estimated radiant drift into account.

5 ζ-Draconids in photographic meteors

The name of ζ-Draconids owes to Denning (1899) and was reminded to us by Terentjeva (1966) and Lindblad (1971). Lindblad reexamined it later (Lindblad, 1995). *Figure 22*

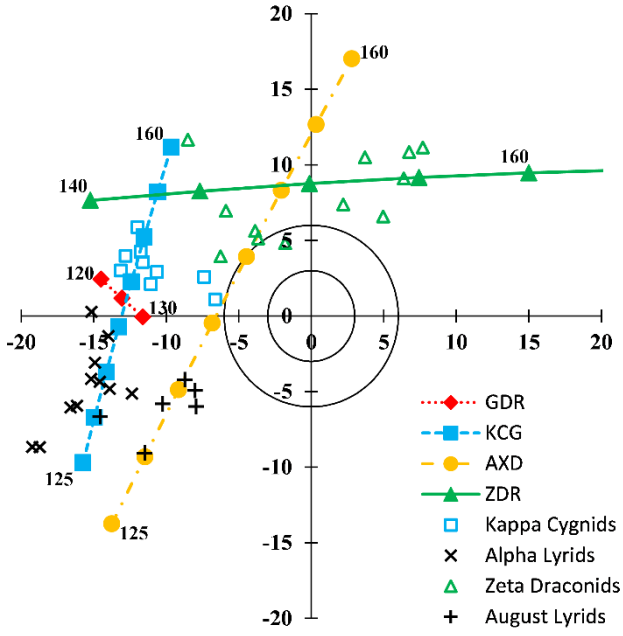

Figure 22 – Four meteor shower activities found by Lindblad (1995) with the radiant drift estimated from EDMOND observations. The paths of the radiant drift with their markers are extended both side from the examined periods (see text Section 4).

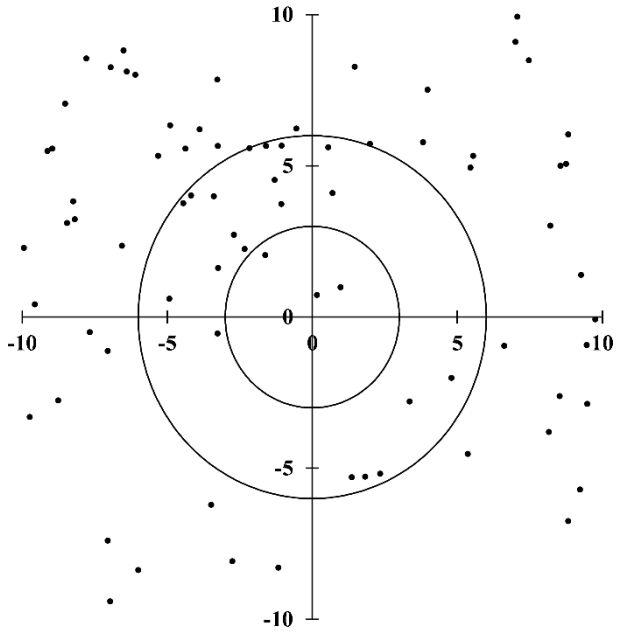

Figure 23 – The radiant distribution by SonotaCo net for the ZDR (#073). 112° < $\lambda_\odot$ < 132°, centered at ($\lambda - \lambda_\odot$, β) = (33.2°,86.6°).

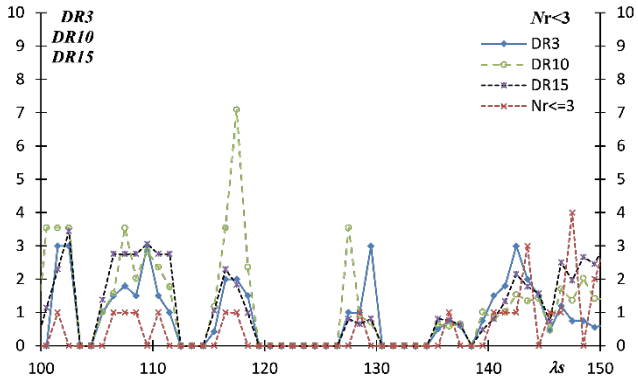

Figure 24 – Meteor shower activities in Figure 23 around ZDR(#073) by SonotaCo net.

shows his four shower activities with the radiant drift estimated from EDMOND observations. It is clear their ζ-Draconids coincide with our ZDR. This is why we call this activity not AUD but ZDR.

We notice that the AXD shower activity is not mentioned by Lindblad (1995). 3 zeta Draconid meteors, 2 kappa Cygnids and 5 August Lyrids in *Figure 22* might represent the AXD shower. It is very interesting that the KCG are divided into two activities: alpha Lyrids and kappa Cygnids. Lindblad studied shower activities by using a computerized discrimination criterion with $D_{SH} < 0.10$. This level is obviously too small though it is suitable for short lived shower activities and for high precision meteors. Three out of the four activities, KCG, AXD and ZDR, are more than twenty days active (*Figure 21*) and the radiant areas are elongated even if we take the radiant drift into consideration. Many *D*-criteria assume that the position of the perihelion axis does not move and data are distributed spherically in the *D* space. In *Figure 22* we can visually see the elongated radiant distribution and the radiant drift, but in case of an analysis on the basis of *D*-criteria we cannot handle such nature. When we use only one of the search methods, *D*-criteria or radiant distribution, we would obtain apparent and false results.

The entry for ZDR (#073) in the IAUMDC working list of meteor showers is problematic, because it was connected with θ-Herculids in the first IAU list (Jenniskens, 2006) and later this initial ZDR has been replaced by recent video data. The present ZDR in the IAUMDC list is quite different from the first one and from the θ-Herculids, and, moreover, we cannot find any trace of it (*Figure 23 and 24*). It is only based on single station video meteors.

6 Conclusion

This study confirms the author's former results; we can confirm two meteor shower activities in the neighborhood of the KCG: ZDR and AXD (*Table 4*). AUD in CAMS consists of two shower activities, AXD and ZDR, and does not relate to AUD0. AUD in the IAUMDC list should be classified as 'working'. The present ZDR in the IAUMDC list should be removed or renamed, because the ZDR stream has been known as a different meteor shower activity by several observers and researchers, Denning, Terentjeva and Lindblad, before the present ZDR were included in the IAUMDC list.

Acknowledgment

The author thanks the network coordinators and camera operators of SonotaCo net[13], CAMS[14] and EDMOND[15] for the availability of the orbit data used in this investigation.

References

Denning W. F. (1899). "General catalogue of the radiant points of meteoric showers and of fireballs and shooting stars observed at more than one station". *Mem. Roy. Astron. Soc*., **53**, 203–292.

Jenniskens P. (2006). "Meteor Showers and their parent comets", Cambridge, Table 7, 'Working list of cometary meteor showers', 691–746.

Jenniskens P., Nénon Q., Albers J., Gural P. S., Haberman B., Holman D., Morales R., Grigsby B. J., Samuels D. and Johannink C. (2016). "The established meteor showers as observed by CAMS". *Icarus*, **266**, 331–354.

Kornoš L., Koukal J., Piffl R., and Tóth J. (2014a). "EDMOND Meteor Database". In, Gyssens M., Roggemans P., Zoladek, P., editors, *Proceedings of the International Meteor Conference*, Poznań, Poland, Aug. 22-25, 2013. International Meteor Organization, pages 23–25.

[13] http://sonotaco.jp/doc/SNM/
[14] http://cams.seti.org/CAMS-v3-2010to2016.xlsx
[15] https://fmph.uniba.sk/en/microsites/daa/division-of-astronomy-and-strophysics/research/meteors/edmond/

Kornoš L., Matlovič P., Rudawska R., Tóth J., Hajduková M. Jr., Koukal J., and Piffl R. (2014b). "Confirmation and characterization of IAU temporary meteor showers in EDMOND database". In, Jopek T.J., Rietmeijer F.J.M., Watanabe J., Williams I.P., editors, *Proceedings of the Meteoroids 2013 Conference*, A.M. University, Poznań, Poland, Aug. 26-30, 2013. Pages 225–233.

Koseki M. (2009). "Meteor Shower Records: A Reference Table of Observations from Previous Centuries". *WGN, Journal of the IMO*, **37**, 139–160.

Koseki M. (2014a). "Various meteor scenes I: The perception and the conception of a 'meteor shower'". *WGN, Journal of the IMO*, **42**, 170–180.

Koseki M. (2014b). "Various meteor scenes II: Cygnid-Draconid Complex (κ-Cygnids)". *WGN, Journal of the IMO*, **42**, 181–197.

Koseki M. (2020a). "Problems in searching for meteor showers". *WGN, Journal of the IMO*, **48**, 99–107.

Koseki M. (2020b). "Cygnid-Draconid Complex (κ-Cygnids) II - Call for Observations κ-Cygnids 2021". *WGN, Journal of the IMO*, **48**, 129–136.

Lindblad B. A. (1971). "A Computerized Stream Search among 2401 Photographic Meteor Orbits". *Smithsonian Contributions to Astrophysics*, **12**, 14–24.

Lindblad B. A. (1995). "The orbit of the kappa Cygnids and related meteor streams". *Earth, Moon, and Planets*, **68**, 397–404.

Sekanina Z. (1973). "Statistical Model of Meteor Streams. III. Stream search Among 19903 Radio Meteors". *Icarus*, **18**, 253–284.

Sekanina Z. (1976). "Statistical model of meteor streams. IV-A study of radio streams from the synoptic year". *Icarus*, **27**, 265–321.

Southworth R. B. and Hawkins G. S. (1963). "Statistics of meteor streams". *Smithsonian Contributions to Astrophysics*, **7**, 261–285.

Terentjeva A. K. (1966). "Minor meteor streams". In Collection of works 'Meteor Investigation', no. 1, from series 'Investigation Results According to International Geophysical Projects', Moscow. Nauka, pages 62–132. (In Russian).

Comparison of two meteor trajectory solvers on the 2020 Perseid shower

Eugene J. Mroz[1], **Denis Vida**[2], **Paul Roggemans**[3]

[1] **New Mexico Meteor Array, Santa Fe, NM, USA**
genemroz@gmail.com

[2] **Department of Earth Sciences and Department of Physics and Astronomy, University of Western Ontario, London, Ontario N6A 3K7, Canada**
dvida@uwo.ca

[3] **Pijnboomstraat 25, 2800 Mechelen, Belgium**
paul.roggemans@gmail.com

The Global Meteor Network trajectory solver obtains higher initial and geocentric velocities for identical Perseid meteors than the UFO solver of SonotaCo. Also, the average velocity for the GMN is slightly but statistically significant higher than for the UFO solver. The higher velocity explains a higher eccentricity for the orbits obtained by GMN. In spite of the lower velocity for the UFO solver, it has statistically significant higher beginning heights for these meteors while the ending heights are comparable. The length of the trajectories seems longer for the UFO solver than for the GMN while the durations are comparable. The differences between both solvers cannot be explained unless insight is provided in the computation method of the UFO solver.

1 Introduction

The Perseid meteor shower of August 2020 provided an opportunity to compare the results of two different meteor trajectory solvers and demonstrate anew that the frequency of meteor occurrence is an independent process that follows a Poisson distribution. The two trajectory solvers are UFO Orbit (v2.62) which is product of SonotaCo[16] and the Monte Carlo solver (Vida et al. 2020) used by the GMN[17] solver. The trajectory variables selected for comparison are velocity, eccentricity, beginning and ending heights, trajectory length and duration.

2 Trajectory Solvers

Each of these trajectory solvers, hereafter referred to as UFO and GMN, uses different methods for computing meteor velocities.

The GMN solver is an open-source trajectory solver based on the lines of sight approach by Borovička (1990), but includes meteor dynamics as an additional constraint, as suggested by Gural (2012). In contrast to Gural (2012), the method does not impose an empirical velocity model to the trajectory.

The UFO solver is a copyrighted and proprietary product of SonotaCo[1]. The user manual (available on the website) states that the algorithms used in UFO Orbit are mostly based on the document by Hasegawa and Koseikaku (1983). An internet search for this document was unsuccessful.

3 Data Source

The data for this study are taken from Perseid meteor observations made by the New Mexico Meteor Array during August 2020. The New Mexico Meteor Array is part of the Global Meteor Network (GMN)[2]. It consists of 23 stations that record the night skies above an area of about 40000 sq. km centered on Albuquerque, NM. A station consists of a Raspberry Pi single board computer, a low light level video camera and the RPi Meteor Station (RMS) software package for meteor detection. This system records and analyzes the video and extracts video clips of detected meteors that are archived and uploaded to the GMN server. The GMN server finds meteors which were observed by more than one station, computes the trajectories and calculates the orbits. In addition, the RMS software produces a data record of each meteor observation suitable for analysis by the freely available SonotaCo UFO Orbit (v2.62) software package.

From the August 2020 observations, 1031 Perseid meteor trajectories as computed by both GMN and UFO were deemed to be of the same event. This was done by selecting Perseid meteor trajectories from each methodology with trajectory start times within 1 second and a radiant separation angle of less than 5 degrees. After removing 29 pairs as outliers (more than 3 standard deviations from the mean velocity, height, length and duration), 1002 trajectory pairs were retained for statistical analysis using SAS University Edition software package Version 3.8 (Basic Edition).

[16] http://sonotaco.com/e_index.html

[17] https://globalmeteornetwork.org/

4 Approach

To compare the results of the GMN and UFO algorithms on the same set of 1002 meteor observations, we use a statistical procedure called a paired sample *t*-test. In this test, each subject (in this case, each meteor observation) is measured twice (a trajectory is calculated by GMN and UFO), resulting in pairs of observations (pairs of trajectory solutions). The paired sample *t*-test determines whether the mean difference between the two sets of observations (two sets of trajectory solutions) is zero. The null hypothesis assumes that the true mean difference is zero and the *t*-test tests whether observed departures from zero are statistically significant. A test statistic (*t*-statistic) is calculated from the mean and standard deviation of the data which is then compared to a theoretical distribution of the *t*-statistic derived from a normal distribution. The probability of obtaining the *t*-statistic under the null hypothesis at a specified degree of confidence is then calculated which is used to judge whether the results provide sufficient evidence to reject the null hypothesis. For this study we chose to use an *alpha* of 0.001 which corresponds to a 0.1% chance (or less) that the obtained result (that is, the mean difference of the two variables being compared) could happen by chance if the null hypothesis was true. By choosing a low value of *alpha*, we are setting a high bar so that there is a low probability that the measured difference happened by chance.

5 Velocity

Geocentric velocity is the velocity a meteor would have in the absence of the Earth's gravitational attraction. It is a function of the Earth's escape velocity and the initial velocity and altitude of the meteor when observed.

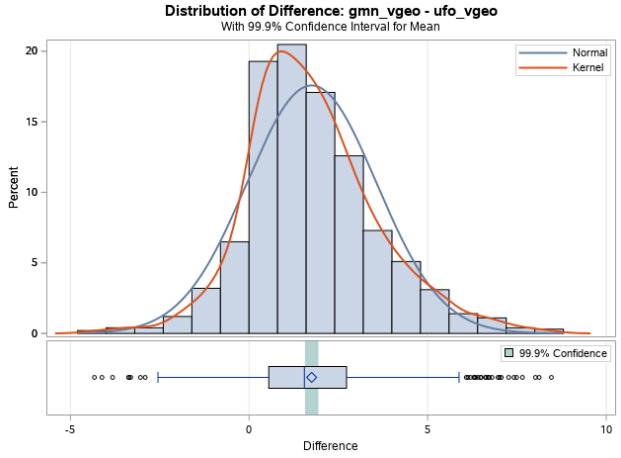

Figure 1 – Distribution of the differences in geocentric velocity v_g of Perseid meteors as computed by GMN and UFO.

GMN found the mean geocentric velocity v_g to be 58.6 km/sec compared with 56.8 km/sec by UFO. The 99.9% confidence limits of both means are ±0.2 km/s. These are both significantly lower than the accepted value of 59.1 km/sec (Jenniskens et al., 2016).

Figure 1 shows the distribution of the differences between the geocentric meteor velocities as computed by GMN and UFO on the same set of Perseid meteors. A paired *t*-test shows that GMN calculates the mean geocentric velocity to be 1.75 km/s faster than calculated by UFO (*Table 1*, $\Delta\ GMN_{Vg} - UFO_{Vg}$).

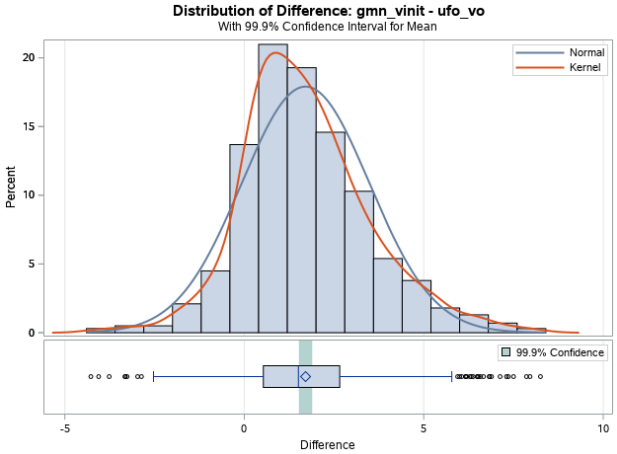

Figure 2 – Distribution of the differences in initial velocity of Perseid meteors as computed by GMN and UFO.

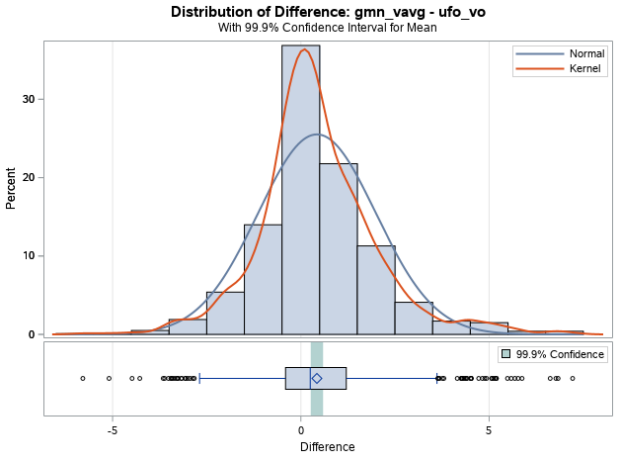

Figure 3 – Distribution of the differences in average velocity of Perseid meteors as computed by GMN and UFO.

As expected, this difference mirrors a difference of similar magnitude for the initial velocity used by each method. *Figure 2* shows the distribution of the differences in initial meteor velocities as computed by GMN and UFO. A paired *t*-test shows that the initial velocity as calculated by GMN is 1.71 km/s faster than the initial velocity used by UFO (*Table 1*, $\Delta\ GMN_{Vinit} - UFO_{Vo}$).

We believe this difference is the result of a difference in how initial velocity is determined. The GMN solver uses the first 40% of the data points along the trajectory to estimate the initial velocity and includes a deceleration term (Vida et al., 2020). Whereas UFO uses the average velocity over the entire track of the meteor. GMN also computes the average velocity so it is interesting to compare this to the average velocity computed by UFO. *Figure 3* shows the paired *t*-test for the average velocity as calculated by GMN is 0.43 km/s faster than that calculated by UFO (*Table 1*, $\Delta\ GMN_{Vavg} - UFO_{Vo}$). The reason for this difference is unclear.

Table 1 – Summary statistics from paired *t*-tests for 1001 meteor trajectories solved by GMN and UFO. Mean, is the average of the variable. Std. Dev. is the standard deviation of the variable. Std. Err. is the estimate standard deviation of the sample mean. Min., is the minimum value. Max., is the maximum value. LCL/UCL Mean, are the Lower and Upper 99.9% confidence limits of the mean. LCL/UCL Std. Dev. are the Lower and Upper 99.9% confidence limits of the standard deviation. *t*-value, or the *t*-statistic, this is the ratio of the mean of the difference in means to the standard error of the difference. Pr > |*t*|, here the *p*-value is the two-tailed probability computed using the *t*-distribution. If the *p*-value is less than the specified *alpha* level (0.001), then the difference is significantly different from zero.

Difference (Δ)	Mean	Std. Dev.	Std. Err.	Min.	Max.	LCL Mean	UCL Mean	LCL Std. Dev.	UCL Std. Dev.	*t*-Value	Pr > |*t*|
Δ GMN_{Vinit} – UFO_{Vo} (km/s)	1.71	1.78	0.06	–4.27	8.25	1.52	1.89	1.66	1.92	30.29	<0.0001
Δ GMN_{Vg} – UFO_{Vg} (km/s)	1.75	1.82	0.06	–4.33	8.47	1.56	1.94	1.69	1.96	30.55	<0.0001
Δ GMN_{Vavg} – UFO_{Vo} (km/s)	0.43	1.56	0.05	–5.79	7.22	0.26	0.59	1.46	1.69	8.63	<0.0001
Δ GMN_{ecc} – UFO_{ecc}	0.13	0.14	0.00	–0.35	0.64	0.11	0.14	0.13	0.15	29.61	<0.0001
Δ GMN_{Hb} – UFO_{Hb} (km)	–0.64	1.88	0.06	–9.88	13.14	–0.84	–0.45	1.75	2.03	–10.81	<0.0001
Δ GMN_{He} - UFO_{He} (km)	0.08	1.20	0.04	–7.42	9.60	–0.04	0.21	1.11	1.29	2.23	0.026
Δ GMN_{Len} – UFO_{Len} (km)	–1.18	3.07	0.10	–13.93	11.92	–1.50	–0.86	2.86	3.31	–12.18	<0.0001
Δ GMN_{dur} – UFO_{dur} (sec)	0.004	0.045	0.001	–0.189	0.203	–0.001	0.009	0.041	0.048	2.9	0.0038

6 Eccentricity

Eccentricity is a measure of how much an elliptical orbit deviates from a perfect circle and varies between 0 (circle) and 1 (parabola). Eccentricity values greater than 1 are indicative of hyperbolic trajectories. The Perseid meteors have a high eccentricity of 0.95 (Jenniskens et al., 2016) and it is of interest to compare the eccentricity as computed by both methods.

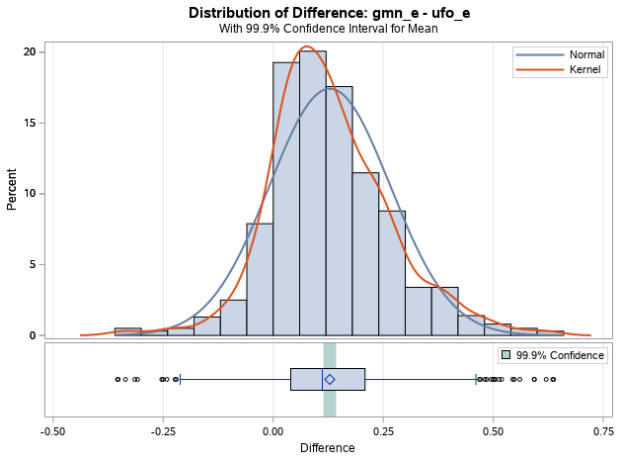

Figure 4 – Distribution of the *Δs* in eccentricity of Perseid meteors as computed by GMN and UFO.

For the GMN solver, the average eccentricity was 0.92 and 19.7% of the 1001 jointly computed trajectories had computed eccentricities of greater than 1. Whereas, the UFO solver had only 5.0% such trajectories but with a much lower average eccentricity of 0.79. *Figure 4* shows the distribution of the eccentricity *Δs*. A paired *t*-test shows the eccentricity as calculated by GMN is 0.13 higher than that calculated by UFO (*Table 1,* Δ GMN_{ecc} – UFO_{ecc}).

Obtaining accurate velocity measurement is important for meteors like the Perseids that have highly eccentric orbits. For the GMN solver, fast meteors such as the Perseids present a challenge because they result in fewer data points along the trajectory path from which to make an accurate velocity estimate. So, whereas the GMN solver tends to generate more accurate and faster initial velocities, this can easily result in a higher percentage of computed trajectories with an apparent (but false) hyperbolic trajectory. For the UFO solver, the lower average eccentricity and lower percentage of hyperbolic trajectory solutions are both probably a consequence of the lower velocity that results from using the average velocity over the entire meteor track.

7 Altitude

Both methods also solve for beginning and ending altitude of the observed meteor track. For the beginning altitude, the GMN solver is –0.64 km lower than the UFO solver (*Table 1*, Δ GMN_{Hb} – UFO_{Hb}). *Figure 5* shows the distribution of the Δs for beginning altitude.

For ending altitude, the GMN and UFO solvers give essentially the same result as can be seen *Table 1* (Δ GMN_{He} – UFO_{He}) where the mean value is 0.08 km but the probability of it being zero is 0.026 which is higher than our specified *alpha* of 0.001. Thus, the lower and upper 99.9% confidence limits for the mean (–0.04 to 0.21 km) encompass zero. *Figure 6* shows the distribution of the *Δs* for ending altitude.

The altitudes of the highest and lowest stations in the network are 2247m and 1485m, respectively; a difference of 762m. Perhaps the observed Δ reflects differences in how the two solvers handle the task of computing trajectories from sites with disparate altitudes.

It's not clear why the two solvers should produce a larger Δ and larger spread of values for the beginning altitude than for the ending altitude.

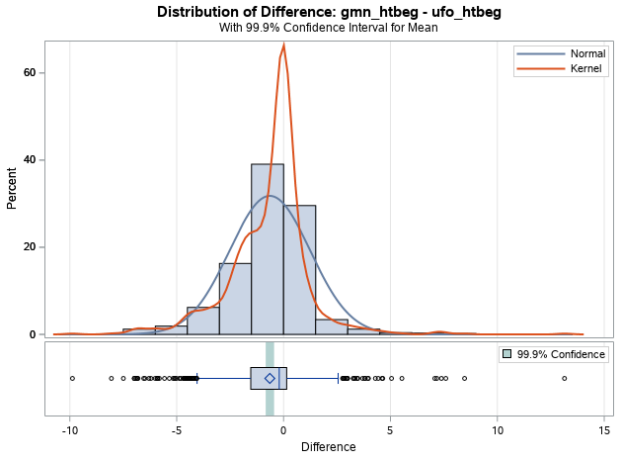

Figure 5 – Distribution of the Δs in beginning height of Perseid meteors as computed by GMN and UFO.

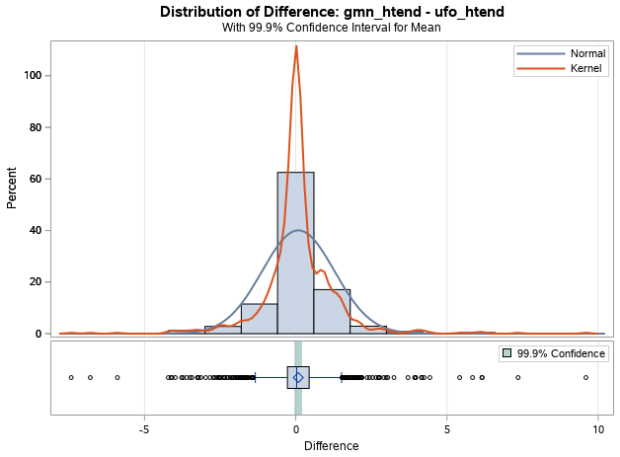

Figure 6 – Distribution of the Δs in ending height of Perseid meteors as computed by GMN and UFO.

8 Meteor track length

Comparing the solutions of the two solvers for meteor track length also reveals Δs. Track length is calculated as part of the output from the UFO solver but is not directly available from the GMN solver output. However, it can be estimated from the latitude, longitude and height of the track beginning and end points. This calculation was performed using the SAS function GEODIST which calculates the geodetic distance between the two coordinates and accounts for the curvature of the Earth (Vincenty, 1975). To account for vertical as well as horizontal distance traveled by the meteor, the Pythagorean theorem was employed together with the SAS GEODIST function to calculate the length of the meteor track between the beginning and ending latitude, longitude and altitude.

The results (*Table 1*, Δ GMN_{Len} – UFO_{Len}) show the GMN average track length to be about 1.18 km shorter than calculated by UFO. There seems to be a considerable number of observations skewed to the negative side of the distribution of the Δs (*Figure 7*). It is perhaps noteworthy that the camera system records 25 frames per second which is 0.04 seconds per frame. At a nominal velocity of 59 km/sec, a Perseid meteor travels 2.4 km within a 0.04 second (single frame) interval. So, the apparent Δ in trajectory length between the two methods is equivalent to about half of the exposure time of a single frame (0.02 seconds) which is below the temporal resolution capability of the meteor detection system. This may be a situation where the statistically significant Δ does not necessarily accurately signify a significant difference in the performance of the two solvers.

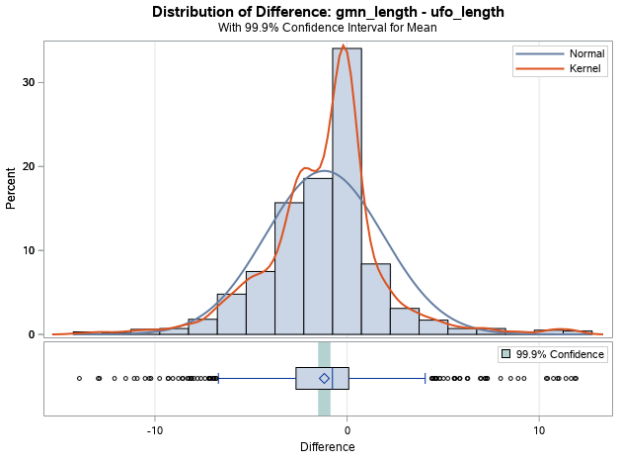

Figure 7 – Distribution of the Δs in track length of Perseid meteors as computed by GMN and UFO.

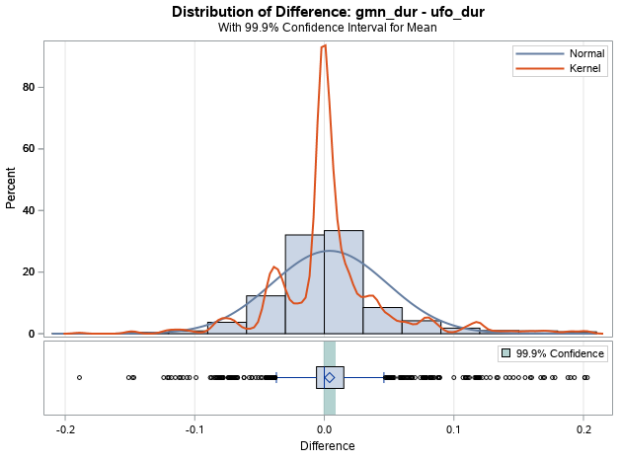

Figure 8 – Distribution of the Δs in duration of Perseid meteors as computed by GMN and UFO.

9 Meteor track duration

The two solvers are in much better agreement when it comes to the duration of the meteor track. The mean Δ is 0.004 seconds but the 99.9% confidence limits for the mean and the *p*-value shows that this is statistically indistinguishable from zero (*Table 1*, Δ GMN_{dur} – UFO_{dur}). *Figure 8* shows the distribution of the Δs.

10 Poisson distribution of Perseid meteors

Over suitably short time intervals, meteor events are independent and the arrival rate is constant. Therefore, the distribution of meteor events within this interval is expected to follow a Poisson distribution. We tested for this distribution using the observations of Perseid meteors from the entire GMN network. We chose the two-hour interval of peak intensity (21^h00^m – 23^h00^m, 12 August 2020 UTC) during which 277 Perseid meteors were observed throughout the network. These observations were then tabulated at 1-minute intervals. *Figure 9* shows the histogram of the number of Perseids observed per minute plotted as a fraction of the total (277) Perseids counted over two hours. Overlaying the data is a plot of the Poisson probability mass function (PMF) fit to the data. The goodness-of-fit can be judged by the chi-squared test which gives a result of $p = 0.48$ indicating that the data distribution is, as expected, statistically indistinguishable from a Poisson distribution.

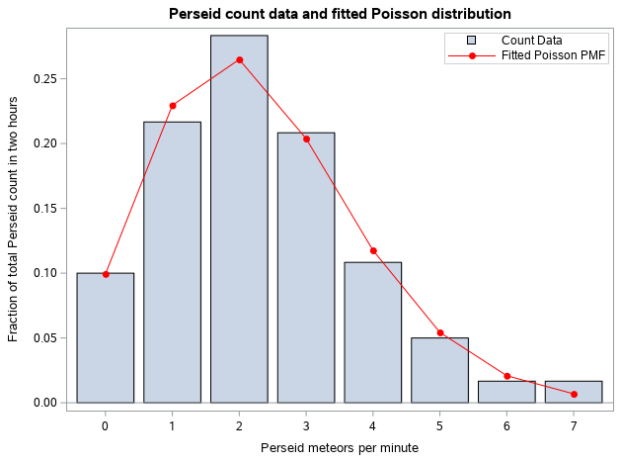

Figure 9 – Poisson distribution of Perseid meteors.

11 Discussion

The most significant differences between the two solvers appears to be how they compute meteor velocity and eccentricity. Unsurprisingly, the difference in how the initial velocity is estimated manifests itself as a difference in the apparent geocentric velocity and also affects the computed eccentricity of the orbit. For the other trajectory characteristics, although the differences between the two approaches are generally small, they appear to be statistically significant. How these relate to differences in the two trajectory solving algorithms is not clear. It would be immensely helpful to have better documentation of the algorithms used by UFO Orbit to better understand the similarities and differences in approach taken by these two methodologies.

Acknowledgments

This report would not have been possible without the generous commitment of personal time, effort and resources of the owner/operators of the stations that comprise the New Mexico Meteor Array: *Pete Eschman* (Coordinator), *John Briggs*, *Ollie Eisman*, *Jim Fordice*, *Bob Greschke*, *Tim Havens*, *Bob Hufnagel*, *Ron James*, *Steve Kaufman*, *Bob Massey*, *Alex McConahay*, *Gene Mroz*, *Jim Seargeant*, *Eric Toops*, *Bill Wallace* and *Steve Welch*.

We used the data of the Global Meteor Network[18] which is released under the CC BY 4.0 license[19].

References

Borovička J. (1990). "The comparison of two methods of determining meteor trajectories from photographs". *Bulletin of the Astronomical Institutes of Czechoslovakia*, **41**, 391–396.

Gural P. S. (2012). "A new method of meteor trajectory determination applied to multiple unsynchronized video cameras". *Meteoritics & Planetary Science*, **47**, 1405–1418.

Hasegawa I., Koseikaku K. (1983). "Tentai Kidou Ron (Determination of Orbits)". ISBN 4-7699-0572-6 C 3044.

Jenniskens P., Nénon Q., Albers J., Gural P. S., Haberman B., Holman D., Morales R., Grigsby B. J., Samuels D. and Johannink C. (2016). "The established meteor showers as observed by CAMS". *Icarus*, **266**, 331–354.

Vida D., Gural P., Brown P. G., Campbell-Brown M., Wiegert P. (2020). "Estimating trajectories of meteors: an observational Monte Carlo approach–I. Theory". *Monthly Notices of the Royal Astronomical Society*, **491**, 2688–2705.

Vincenty T. (1975). "Direct, and Inverse Solutions of Geodesics on the Ellipsoid with Application of Nested Equations". *Survey Review*, **22**, 88–93.

[18] https://globalmeteornetwork.org/data/

[19] https://creativecommons.org/licenses/by/4.0/

Global Meteor Network status report

Paul Roggemans

Pijnboomstraat 25, 2800 Mechelen, Belgium
paul.roggemans@gmail.com

A status update is presented for the GMN. In less than two years, 144950 orbits were collected, 391 different meteor showers have been detected among these orbits. By October 2020, 140 operational cameras were involved.

1 Introduction

Amateur video meteor observations started about 25 years ago and became the most popular meteor observing technique in the past ten years. Video camera observations were cheaper than traditional photography and easier to reduce the data. Compared to visual observers, video cameras did not suffer fatigue or physiologic effects like human observers. Forward scatter only provides the number of radio echoes recorded without any indication for position or shower association while the video data offers a wealth of detailed information. In the early years meteor video cameras were mainly used for single station meteor paths to locate radiants in a statistical way.

Video meteor observing became much more interesting as soon as amateurs created networks for multiple station video meteor observations. One of the pioneers in this field was Damir Segon with the Croatian Meteor Network in co-operation with Pete Gural (Gural and Šegon). In 2007 the SonotaCo Network started in Japan. Soon several national and regional video camera networks got started across Europe, all using the UFO Capture software developed by SonotaCo (SonotaCo, 2009). Few years later the European networks merged into EDMOND (Kornoš et al., 2014). The CAMS capture and detection software was developed by Pete Gural, and became operational in October 2010 (Jenniskens et al., 2011). Several other networks were started across the world, but CAMS, EDMOND and SonotaCo became the major providers of publicly available orbit meteor data.

2 GMN as new provider of orbit data

In 2014 Croatian amateurs had the idea to use the cheap Raspberry Pis for meteor work. Already in 2015 the idea of a large network of cheap video meteor cameras was discussed at a conference in Austria (Zubović et al., 2015), but it took a couple of years more of testing and developing before the first Raspberry Pi Meteor System could be offered for sale. In October 2018 Denis Vida informed the author that the RMS cameras were offered for sale and I ordered one, I received my first RMS camera in November 2018 and got it installed right in time for Geminids 2018. I was impressed by the first results.

Thanks to the efforts of Denis Vida, the RMS cameras produce CAMS compatible output which can be easily used for CAMS with an app provided by Pete Gural. So far eight RMS cameras contribute to the CAMS BeNeLux network (Roggemans, 2020). Meanwhile, the Global Meteor Network became the fastest expanding video camera network with currently 140 RMS cameras contributing worldwide. The number of collected orbits is very impressive. *Table 1* lists the scores for each month. With a total of 50263 orbits obtained in 2019, this score will be easily doubled in 2020 as the counter until end October was at 94190 orbits with still two meteor rich months to come.

Table 1 – Number of orbits collected by GMN per month.

Month	Number of orbits
2018-12	497
2019-01	564
2019-02	1284
2019-03	537
2019-04	876
2019-05	1242
2019-06	1523
2019-07	1961
2019-08	5387
2019-09	6058
2019-10	11978
2019-11	7710
2019-12	11143
2020-01	7539
2020-02	5330
2020-03	5101
2020-04	7248
2020-05	5698
2020-06	5738
2020-07	10973
2020-08	19422
2020-09	14252
2020-10	12889
Total	144950

Table 2 – The number of meteor shower orbits collected by GMN, shower identification according to the IAU MDC[20] Working list of meteor showers.

Shower	Orbits	Shower	Orbits	Shower	Orbits	Shower	Orbits	Shower	Orbits
Sporadics	86282	SSC#161	14	LBO#322	6	AED#450	29	PTA#556	29
CAP#1	932	NZC#164	748	XCB#323	26	CAM#451	5	SFD#557	189
STA#2	2400	SZC#165	140	EPR#324	14	MPS#456	216	MCB#559	10
SIA#3	78	JBO#170	5	EPG#326	75	JEC#458	51	SSX#561	11
GEM#4	2871	ARI#171	25	SSE#330	2	JEO#459	57	DOU#563	43
SDA#5	1910	JPE#175	297	AHY#331	83	AXC#465	38	SUM#564	14
LYR#6	779	PHE#176	3	OCU#333	123	AOC#466	15	OHY#569	64
PER#7	10424	OCY#182	20	DAD#334	276	LAQ#473	50	FBH#570	25
ORI#8	5838	PAU#183	64	XVI#335	70	ICE#476	49	TSB#571	12
DRA#9	7	GDR#184	150	DKD#336	130	TCA#480	270	SAU#575	7
QUA#10	963	EUM#186	13	NUE#337	1102	NZP#486	11	CHA#580	69
EVI#11	107	PCA#187	56	OER#338	298	NSU#488	13	NHE#581	115
KCG#12	288	XRI#188	1	PSU#339	45	DEL#494	39	JBC#582	23
LEO#13	439	BPE#190	63	TPY#340	54	DAB#497	4	GCE#584	78
URS#15	139	ERI#191	320	XUM#341	28	FPL#501	32	THY#585	10
HYD#16	581	UCE#194	160	HVI#343	209	DRV#502	61	FNC#587	24
NTA#17	1574	BIN#195	1	FHE#345	33	AIC#505	255	FCA#589	13
AND#18	62	AUD#197	640	XHE#346	56	FEV#506	141	VCT#590	6
MON#19	196	AUR#206	210	BPG#347	1	UAN#507	146	ZBO#591	33
COM#20	503	SPE#208	622	ARC#348	107	JRC#510	20	PON#592	12
AVB#21	171	BAU#210	359	LLY#349	4	RPU#512	20	TOL#593	20
LMI#22	235	KLE#212	6	JMC#362	47	OMC#514	18	RSE#594	3
EGE#23	358	NPI#215	192	PPS#372	683	OLE#515	80	POS#599	104
NOA#25	315	SPI#216	69	ALN#376	15	FMV#516	87	ICT#601	9
NDA#26	890	NDR#220	163	OLP#384	39	ALO#517	6	KCR#602	5
KSE#27	20	DSX#221	11	OBC#386	82	AHE#518	14	FAR#608	18
SOA#28	504	SOR#225	185	CTA#388	216	BAQ#519	21	TLY#613	24
ETA#31	872	XDR#242	46	THA#390	54	MBC#520	28	THD#618	1
NIA#33	296	ZCN#243	2	NDD#391	2	AGC#523	125	XCS#623	156
ZCY#40	394	NHD#245	13	NID#392	49	LUM#524	28	XAR#624	544
DLI#47	106	AMO#246	25	ACA#394	36	SLD#526	18	LTA#625	43
GDE#65	7	NOO#250	397	GCM#395	51	EHY#529	96	LCT#626	215
SSG#69	118	ALY#252	3	GUM#404	35	ECV#530	51	NPS#627	116
SLY#81	114	CMI#253	68	DPI#410	15	GAQ#531	54	STS#628	182
ODR#88	24	ORN#256	189	CAN#411	253	JXA#533	76	ATS#629	126
PVI#89	42	ORS#257	283	SIC#416	51	THC#535	4	TAR#630	183
NCC#96	183	OCT#281	38	SOL#424	132	FSO#536	2	DAT#631	248
SCC#97	238	FTA#286	51	FED#427	8	TTB#543	11	NET#632	54
PIH#101	280	DSA#288	73	DSV#428	166	JNH#544	28	PTS#633	77
AAN#110	29	DNA#289	20	ACB#429	34	XCA#545	8	TAT#634	150
ELY#145	74	TPU#307	1	JIP#431	20	FTC#546	103	ATU#635	67
NOP#149	32	PIP#308	41	ZCS#444	227	KAP#547	460	MTA#636	59
SOP#150	25	MVE#318	15	KUM#445	30	FAN#549	80	FTR#637	71
EAU#151	86	JLE#319	7	DPC#446	24	PSO#552	245	DZT#638	12
NOC#152	6	OSE#320	1	AAL#448	13	OCP#555	55	AOA#640	536

[20] https://www.ta3.sk/IAUC22DB/MDC2007/

Table 2 – The number of meteor shower orbits collected by GMN, shower identification according to the IAU MDC Working list of meteor showers, continued.

Shower	Orbits	Shower	Orbits	Shower	Orbits	Shower	Orbits	Shower	Orbits
DRG#641	1	ZPI#706	87	SED#796	28	SZE#849	16	SCV#888	2
JLL#644	41	BPX#707	1	ADS#802	16	MBA#850	2	YOP#889	1
BCO#647	71	RLM#708	2	LSA#803	16	PCY#854	31	ESU#890	4
TAL#648	206	FDC#712	19	FLO#807	111	ATD#855	3	FSL#891	36
OAV#651	92	CCR#713	14	XCD#810	47	EMO#856	18	EOP#893	21
OSP#652	22	RPI#714	177	NAA#812	6	FPB#858	42	JMD#894	22
RLY#653	70	ACL#715	518	CVD#814	12	MTB#859	10	OTA#896	30
APC#655	3	OCH#716	99	UMS#815	11	PAN#860	4	OUR#897	10
GSG#657	7	NGB#720	8	CVT#816	17	JXS#861	10	SGP#898	17
EDR#658	30	DAS#721	12	OAG#818	20	SSR#862	13	EMC#899	1
EPS#660	24	FLE#722	16	NUT#822	4	TLR#863	5	BBO#900	30
OTH#661	18	DEG#726	18	FCE#823	48	JSG#864	1	TLC#901	6
MUC#665	33	ISR#727	6	DEX#824	2	JES#865	9	DCT#902	29
JMP#668	22	PGE#728	10	XIE#825	21	ECB#866	9	OAT#903	21
MCY#671	5	DCO#729	3	ILI#826	61	FPE#867	11	OCO#904	6
HNJ#672	7	ATV#730	12	NPE#827	18	PSQ#868	5	MXD#905	4
MUA#679	29	FGV#732	21	TPG#828	1	UCA#869	16	ETD#906	30
JEA#680	17	MOC#734	15	JSP#829	25	JPG#870	12	MCE#907	8
OAQ#681	23	XIP#736	8	SCY#830	43	DCD#871	6	SEC#909	1
JTS#683	8	FNP#737	9	GPG#831	13	ETR#872	11	BTC#910	36
JPS#685	14	RER#738	12	LEP#832	9	OMI#873	10	TVU#911	21
JRD#686	4	LAR#739	15	KOR#833	12	PXS#874	45	BCY#912	30
KDP#687	8	OSD#745	64	ACU#834	2	TEI#875	23	OVI#917	2
TAC#689	81	EVE#746	19	ABH#836	2	ROR#876	20	TAG#918	11
ZCE#691	3	JKL#747	52	CAE#837	2	OHD#877	15	ICN#919	1
EQA#692	197	JTL#748	38	ODS#838	2	OEA#878	7	XSC#920	15
ANP#693	78	NMV#749	97	PSR#839	10	ATI#879	14	JLC#921	24
OMG#694	191	SMV#750	142	TER#840	5	YDR#880	38	PPE#922	3
APA#695	22	KCE#751	126	DHE#841	8	TLE#881	4	FBO#923	1
OAU#696	38	MID#755	5	DMD#843	13	PLE#882	3	SAN#924	4
AET#698	44	CCY#757	534	DTP#844	17	NMD#883	1	EAN#925	7
BCE#701	12	SCO#771	1	OEV#845	1	DEV#885	10		
ASP#702	10	SXP#786	3	BEL#847	4	ACV#886	11		
OAN#704	245	KCA#793	8	OPE#848	7	DZB#887	13		

One of the advantages of the Global Meteor Network is that it has cameras in Europe as well as the American continent. So far, only CAMS has more camera networks.

With almost 150000 orbits collected in less than two years, GMN is a most promising provider for meteor orbits. The EDMOND database contains 317830 orbits recorded since 2006 until 2016, unfortunately no new data has been included after 2016 and EDMOND data only spans the observing window for Europe. SonotaCo has 312511 orbits for the period 2007 to 2019, covering the observing window for Japan. CAMS made its orbit data public for the period 2010 to 2016, with in total 471582 orbits. Because of the embargo on the data, datasets with CAMS orbits were released only twice, once until 2013 and last time until 2016. Data about recent years is not available for analysis.

Looking at the number of orbits obtained for the showers of the IAU MDC Working list of meteor showers in *Table 2*, we see that GMN already collected a fair number of orbit data for 391 different meteoroid streams, including more orbit data than what was used for the major analysis of CAMS data on October 2010– March 2013 published in 2016 (Jenniskens et al., 2016).

For anyone interested in orbit data analysis, the Global Meteor Network looks very promising and deserves full support.

3 Global Meteor Network status

I plotted the current (31 October 2020) camera coverage of the network, hoping to convince new participants to join the project. I plotted the cameras for Europe for different areas because the multiple overlapping fields somehow mask where better coverage is required. The current coverage of the GMN cameras makes it most rewarding for new participants to join and help to cover as much of the atmosphere as possible to achieve a 7/7 and 24/24 global coverage.

Some regions of Europe already have good coverage and offer good possibilities to amateurs in neighboring countries to point cameras towards existing camera fields, or to expand the volume of atmosphere guarded by GMN. For existing camera networks, it is useful to know that the RMS software also produces a UFOCapture format csv file with all detections. A dense camera network with an optimal geographical spreading is ideal to cope with nights with very variable weather.

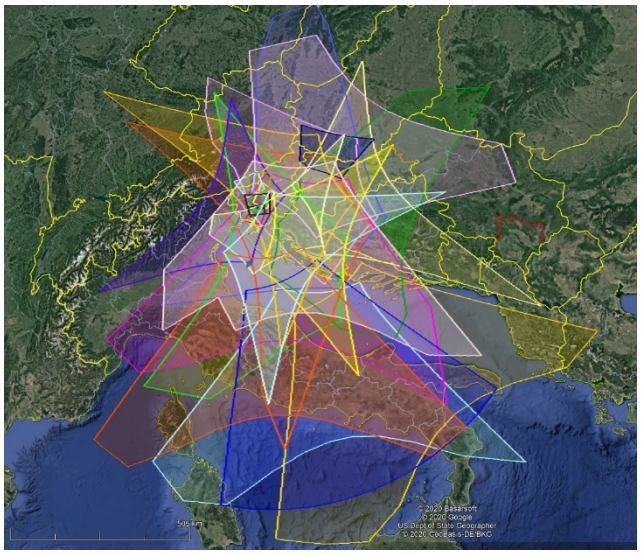

Figure 1 – Global Meteor Network camera fields intersected at 100km elevation, for cameras installed in Croatia, Slovenia and Italy.

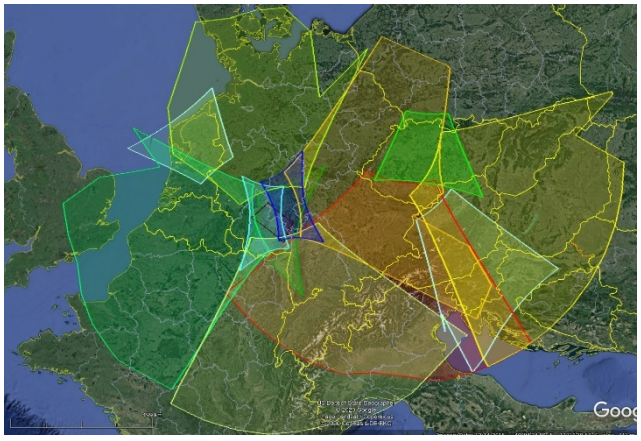

Figure 2 – Global Meteor Network camera fields intersected at 100km elevation, for cameras installed in Czech Republic, Germany and Poland.

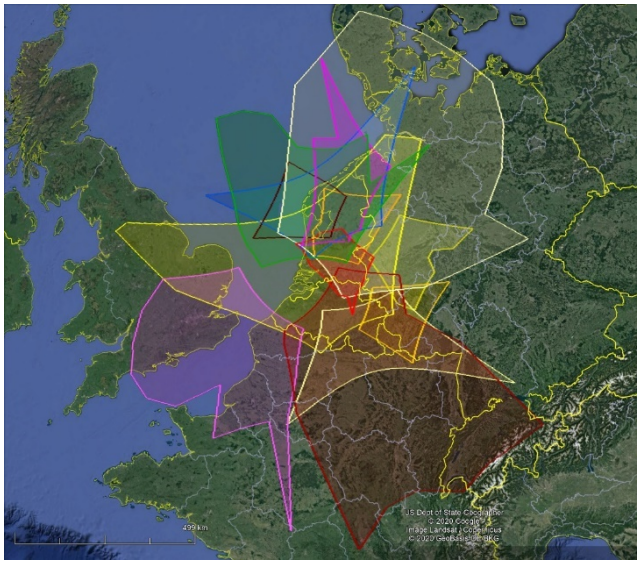

Figure 3 – Global Meteor Network camera fields intersected at 100km elevation, for cameras installed in Belgium and the Netherlands.

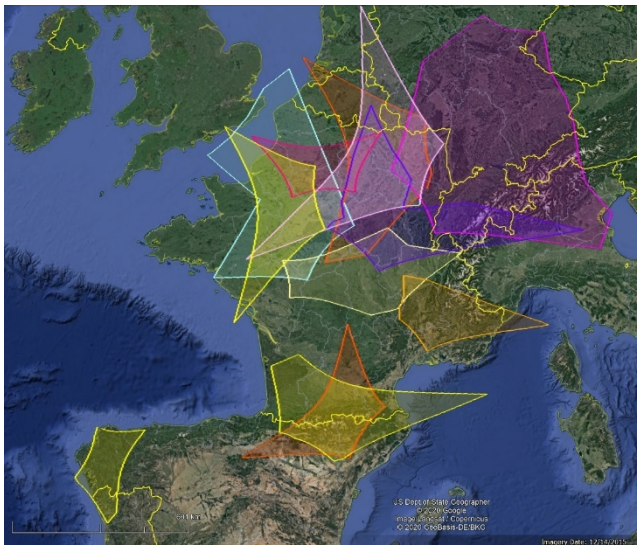

Figure 4 – Global Meteor Network camera fields intersected at 100km elevation, for cameras installed in France and Spain.

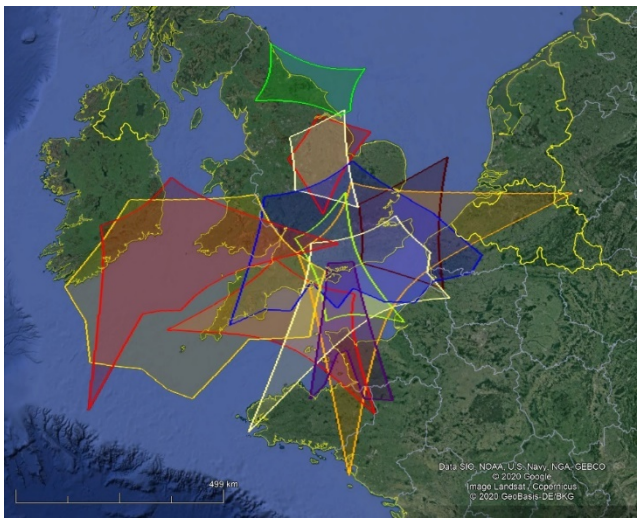

Figure 5 – Global Meteor Network camera fields intersected at 100km elevation, for cameras installed in Ireland and the UK.

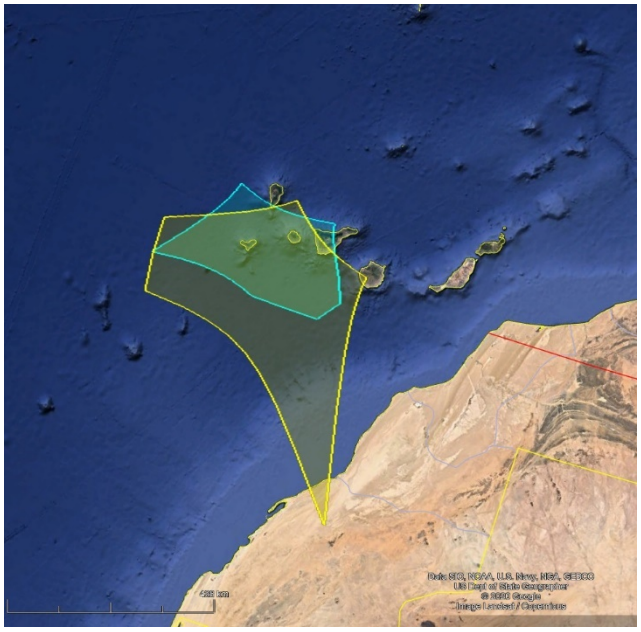

Figure 6 – Global Meteor Network camera fields intersected at 100km elevation, for cameras installed at the Canary Islands.

Figure 7 – Global Meteor Network camera fields intersected at 100km elevation, for cameras installed in Israel.

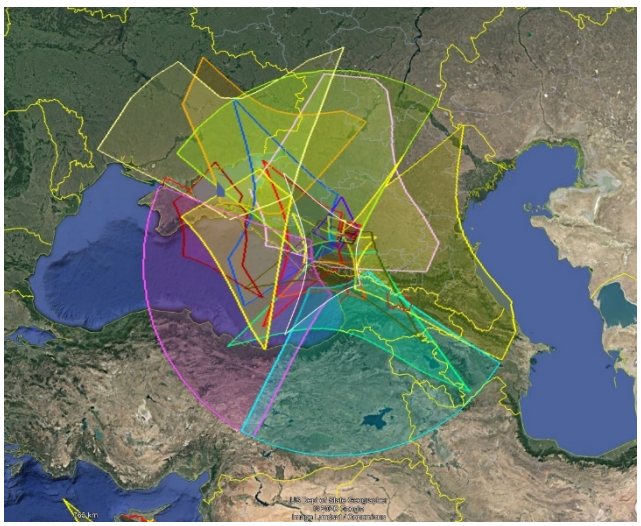

Figure 8 – Global Meteor Network camera fields intersected at 100km elevation, for cameras installed in Russia.

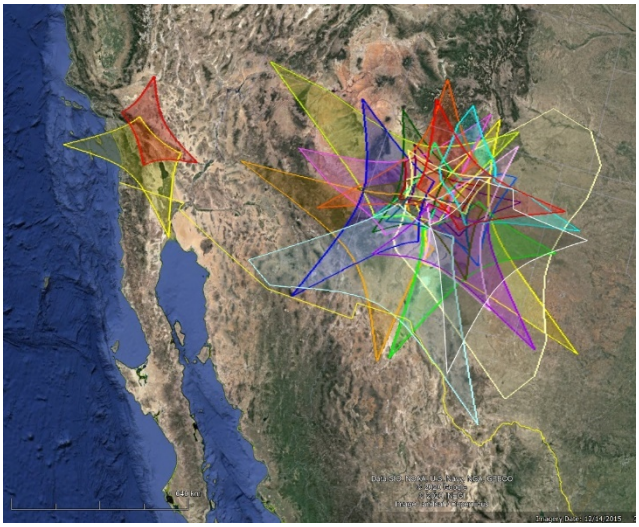

Figure 9 – Global Meteor Network camera fields intersected at 100km elevation, for cameras installed in the USA.

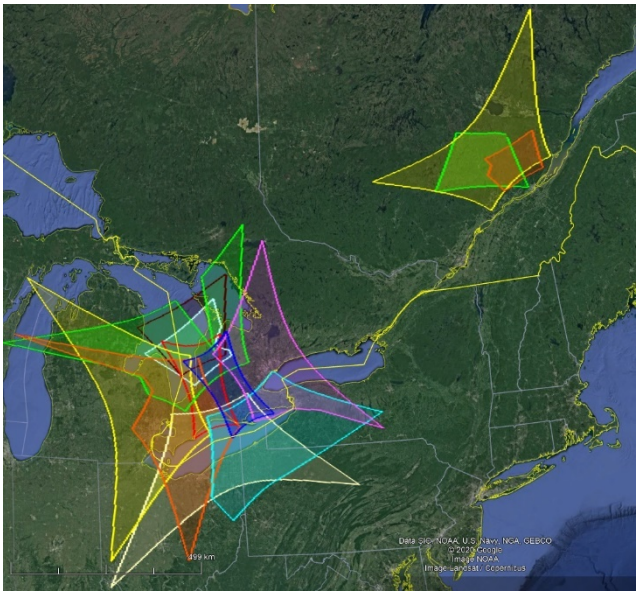

Figure 10 – Global Meteor Network camera fields intersected at 100km elevation, for cameras installed in Canada.

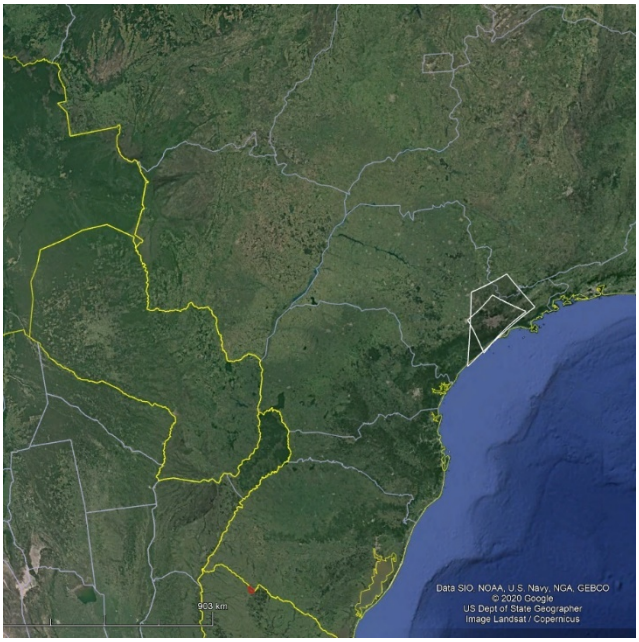

Figure 11 – Global Meteor Network camera fields intersected at 100km elevation, for cameras installed in Brazil.

Hopefully the RMS cameras will find their way to the far East and the Southern hemisphere to obtain a real global coverage.

More information about purchasing or building RMS[21] cameras can be found on the website[22].

References

Gural P. and Šegon D. (2009). "A new meteor detection processing approach for observations collected by the Croatian Meteor Network (CMN)". *WGN, the Journal of the IMO*, **37**, 28–32.

Jenniskens P., Gural P. S., Grigsby B., Dynneson L., Koop M. and Holman D. (2011). "CAMS: Cameras for All-sky Meteor Surveillance to validate minor meteor showers". *Icarus*, **216**, 40–61.

Jenniskens P., Nénon Q., Albers J., Gural P. S., Haberman B., Holman D., Morales R., Grigsby B. J., Samuels D. and Johannink C. (2016). "The established meteor showers as observed by CAMS". *Icarus*, **266**, 331–354.

Kornoš L., Koukal J., Piffl R., and Tóth J. (2014). "EDMOND Meteor Database". In: Gyssens M., Roggemans P., Zoladek, P., editors, *Proceedings of the International Meteor Conference*, Poznań, Poland, Aug. 22-25, 2013. International Meteor Organization, pages 23–25.

Roggemans P. (2020). "RMS cameras as alternative for Watec in CAMS". *eMetN*, **5**, 330–335.

SonotaCo (2009). "A meteor shower catalog based on video observations in 2007-2008". *WGN, Journal of the International Meteor Organization*, **37**, 55–62.

Zubović D., Vida D., Gural P. and Šegon D. (2015). "Advances in the development of a low-cost video meteor station". In: Rault J.-L. and Roggemans P., editors, *Proceedings of the International Meteor Conference*, Mistelbach, Austria, 27-30 August 2015. IMO, pages 94–97.

[21] https://docs.google.com/document/d/18TT-Jm7z9kYskl5ua07jQWD91OiyBemBnOosiNdW6nY/edit?usp=sharing

[22] https://globalmeteornetwork.org/

October 2020 report CAMS BeNeLux

Paul Roggemans

Pijnboomstraat 25, 2800 Mechelen, Belgium
paul.roggemans@gmail.com

A summary of the activity of the CAMS BeNeLux network during the month of October 2020 is presented. October 2020 had exceptional poor weather conditions. Despite the uncooperative weather a total of 20135 meteors has been recorded of which 45% was multi-station, resulting in 3305 good quality orbits.

1 Introduction

The long October nights with high meteor activity are probably the most promising month for the CAMS BeNeLux network. Unfortunately, most years it remains with "promising". Overcast and misty weather is most common during this autumn month in the BeNeLux. Would 2020 bring some good luck with October?

2 October 2020 statistics

3305 orbits could be collected which is the lowest number of orbits for October since 2015 when 8 camera stations less and 43 cameras less were available than this year. 2020 brought really the worst-case weather scenario for the month October with not a single complete clear night for the entire network, worse than previous year. Weather wise we probably got the worse month of October since many years.

This month counted 12 nights with more than 100 orbits. The best October night was 22–23 with as many as 461 orbits in a single night. Only two nights remained without any orbits, but most nights meteors got registered between the clouds. In total 20135 meteors were registered of which only 9042 were multi-station or 45% with a successful solution for an orbit. The statistics of October 2020 are compared in *Figure 1* and *Table 1* with the same month in previous years since the start of CAMS BeNeLux in 2012. In 9 years, 228 October nights allowed to obtain orbits with a grand total of 28790 orbits collected during the month of October during all these years together.

Some CAMS stations were not operational due to technical problems or other reasons. October 2019 had a maximum of 76 cameras at 20 CAMS stations, 67.5 on average available while October 2020 had 90 cameras at 23 CAMS stations and 70.9 on average. Even in October 2016 when at best 54 cameras at 19 stations and on average 41.3 cameras were available, some more orbits could be collected.

Again, no really favorable weather occurred for the Orionids apart from some partial clear sky 21–22–23 October. Next year will be the tenth year for CAMS BeNeLux to hope for a first year with lucky weather for the Orionid activity.

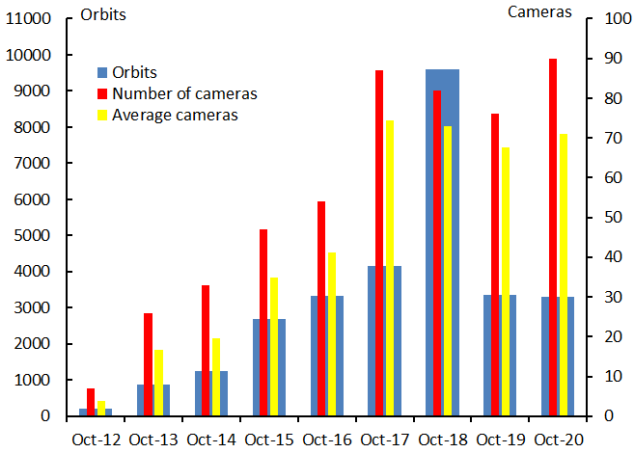

Figure 1 – Comparing October 2020 to previous months of October in the CAMS BeNeLux history. The blue bars represent the number of orbits, the red bars the maximum number of cameras running in a single night and the yellow bar the average number of cameras running per night.

Table 1 – October 2020 compared to previous months of October.

Year	Nights	Orbits	Stations	Max. Cams	Min. Cams	Mean Cams
2012	16	220	6	7		3.9
2013	20	866	10	26		16.8
2014	22	1262	14	33		19.7
2015	24	2684	15	47		34.8
2016	30	3335	19	54	19	41.3
2017	29	4163	22	87	45	74.4
2018	29	9611	21	82	52	73.0
2019	29	3344	20	76	47	67.5
2020	29	3305	23	90	52	70.9
Total	228	28790				

3 Conclusion

The weather made October 2020 the poorest since the start of CAMS BeNeLux. The large number of operational cameras running Auto CAMS still allowed to record a very nice number of orbits under these very unfavorable circumstances.

Acknowledgment

Many thanks to all participants in the CAMS BeNeLux network for their dedicated efforts. This report is based on the data from the CAMS-website[23] with thanks to *Martin Breukers* for providing some extra information and corrections.

The CAMS BeNeLux team was operated by the following volunteers during the month of October 2020: *Hans Betlem* (Leiden, Netherlands, CAMS 371, 372 and 373), Felix Bettonvil (Utrecht, Netherlands, CAMS 376 and 377), *Jean-Marie Biets* (Wilderen, Belgium, CAMS 379, 380, 381 and 382), *Martin Breukers* (Hengelo, Netherlands, CAMS 320, 321, 322, 323, 324, 325, 326 and 327, RMS 328 and 329), *Guiseppe Canonaco* (Genk, RMS 3815), *Bart Dessoy* (Zoersel, Belgium, CAMS 397, 398, 804, 805, 806 and 888), *Jean-Paul Dumoulin, Dominique Guiot and Christian Walin* (Grapfontaine, Belgium, CAMS 814 and 815, RMS 003814), *Uwe Glässner* (Langenfeld, Germany, RMS 3800), *Luc Gobin* (Mechelen, Belgium, CAMS 390, 391, 807 and 808), *Tioga Gulon* (Nancy, France, CAMS 3900 and 3901), *Robert Haas* (Alphen aan de Rijn, Netherlands, CAMS 3160, 3161, 3162, 3163, 3164, 3165, 3166 and 3167), *Robert Haas* (Texel, Netherlands, CAMS 810, 811, 812 and 813), *Robert Haas / Edwin van Dijk* (Burlage, Germany, CAMS 801, 802, 821 and 822), *Kees Habraken* (Kattendijke, Netherlands, RMS 000378), *Klaas Jobse* (Oostkapelle, Netherlands, CAMS 3030, 3031, 3032, 3033, 3034, 3035, 3036 and 3037), *Carl Johannink* (Gronau, Germany, CAMS 311, 314, 317, 318, 3000, 3001, 3002, 3003, 3004 and 3005), *Hervé Lamy* (Dourbes, Belgium, CAMS 394 and 395), *Hervé Lamy* (Humain Belgium, CAMS 816), *Hervé Lamy* (Ukkel, Belgium, CAMS 393), *Koen Miskotte* (Ermelo, Netherlands, CAMS 351, 352, 353 and 354), *Steve Rau* (Zillebeke, Belgium, CAMS 3850 and 3852), *Paul and Adriana Roggemans* (Mechelen, Belgium, CAMS 383, 384, 388, 389, 399 and 809, RMS 003830 and 003831), *Hans Schremmer* (Niederkruechten, Germany, CAMS 803) and *Erwin van Ballegoij* (Heesch, Netherlands, CAMS 347 and 348).

[23] http://cams.seti.org/FDL/index-BeNeLux.html

September observations of the CCY (#757), SPE (#208) and STA (#002) from Norway

Kai Gaarder

Søndre Ålsvegen 698A, N-2740 Roa, Norway
kai.gaarder@gmail.com

A report is presented with the observational results obtained by the author during visual observations in September 2020.

1 Introduction

Not being able to observe meteors since August 15, I was eager to monitor the descending period of the September epsilon Perseids, and check for any signs of the minor chi Cygnids. Weather and moon conditions allowed a total of 9.53 hours of visual observing, yielding a total of 108 visual meteors, and 10 meteors photographed with my DSLR camera. Activity from the CCY was observed, but no more than can be explained by chance lined-up sporadics. Activity from the SPE was clearly detected with some bright meteors. Meteors from the STA were also detected from mid-September, taking over the activity from the Antihelion complex.

2 Observation September12–13, 2020

With the exciting news of the return of the chi Cygnids in my head, I decided to make some observations from my observing site on a small hill in the forest, some 300 meters from my house. The forest protects from any direct light pollution, but the relative proximity to Oslo and nearby small towns, makes the limiting magnitude never exceeding 6.3. This evening sky was clear and transparent, with *Lm* around 6.15 to 6.20. I started observations 19^h40^m UT, and after only 3 minutes I observed a +4 magnitude, slow moving meteor in Cygnus, matching perfectly with the predicted CCY radiant! Inspired by this, I continued to look for further signs of activity. During the next hour I saw a couple of possible candidates, but both were dismissed as sporadics using strict criteria for shower association. Highlights of the hour was a +2 mag SPE in Perseus, and a 0 mag Sporadic low near the horizon in the west.

19^h40^m–20^h40^m T_{eff}: 1.00, *F*: 1.00, *Lm*: 6.14, RA: 315, Dec: +45

- Spo: 0, +2, +3(2), +4(2), +5(2) – 8 meteors
- SPE: +2 – 1 meteor
- CCY: +4 – 1 meteor

The next hour gave no clear CCY candidates, but the SPE delivered a couple of nice meteors. The best one being a 0 magnitude, yellow, fast moving meteor in Andromeda. The meteor left a smoke train lasting 2–3 seconds. 20 minutes later a white +2 mag SPE was seen just above the Pegasus Square. Worth mentioning is also a +1 mag, red, slow moving sporadic meteor moving from Pegasus into Andromeda. The sporadic activity was quite good for evening observation with 12 meteors. A couple of the observed sporadics may in fact have been early Southern Taurids.

20^h40^m–21^h40^m T_{eff}: 1.00, *F*: 1.00, *Lm*: 6.19, RA: 315, Dec: +45

- Spo: +1, +2(3), +3, +4(3), +5(3), +6 – 12 meteors
- SPE: 0, +2 – 2 meteors
- CCY: No meteors

After a 5 minutes break, I was able to observe for one more hour before the descending moon would climb into the sky. Some drifting clouds were also moving in from the north/west, but large areas of the sky were still free of clouds, making observations useful. Meteor activity this hour was a bit lower, with 7 sporadics and 1 SPE seen. The 2 best meteors seen, were both slow moving sporadics. The first one near alpha Andromeda at 22^h40^m, and the next one just above Deneb 12 minutes later. There was no sign of activity from the CCY radiant this hour.

21^h45^m–22^h45^m T_{eff}: 1.00, *F*: 1.05, *Lm*: 6.14, RA: 330, Dec: +45

- Spo: +2(3), +3(2), +5(2) – 7 meteors
- SPE: +3 – 1 meteor
- CCY: No meteors

3 Observations September 16–17, 2020

September 16. came with clear skies, and I decided to follow up my observations of the CCY. Although the sky was apparently cloud free, observing conditions were not optimal. A bad layer of haze was visible in the photos, making the *Lm* reduced to around 6.0. The first 15 minutes went by without any meteors, before a short, white, slow moving sporadic lit up between alpha and gamma Cygni. 45 minutes into the observation, I saw my first "official" Southern Taurid of the year, a +4 mag in Andromeda. At the end of the period, a really good +2 magnitude candidate for the CCY shower was seen in Cygnus.

19^h30^m–20^h50^m T_{eff}: 1.283, *F*: 1.00, *Lm*: 5.95, RA: 330, Dec: +45

- Spo: –1, +3(2), +4(5) – 8 meteors
- SPE: 0 meteors
- STA: +4 – 1 meteor
- CCY: +2 – 1 meteor

In the next period both meteor activity and observing conditions improved a bit. At 21^h03^m a really nice +1 mag SPE lit up in Auriga. Next out was a +4 mag STA, before a yellow, fast, 0 mag Sporadic flashed up in the constellation of Delphinus. In the 3-minute period between 21^h27^m and 21^h30^m, two nice meteors showed up. The first one being a +2 mag, very long-pathed, reddish STA, moving from Pegasus into Andromeda. This one was shortly followed up by a white sporadic of medium speed near the double cluster of Perseus. Right before the end of the observation, a fast moving, yellow/green, 0 mag sporadic lit up in Cassiopeia, rounding off another 2.5 hours of successful observations.

20^h50^m–22^h05^m T_{eff}: 1.250, *F*: 1.00, *Lm*: 6.05, RA: 345, Dec: +45

- Spo: 0(2), +1, +2(2), +3, +4(3), +5(2) – 11 meteors
- SPE: +1, +5 – 2 meteors
- STA: +2, +4 – 2 meteors
- CCY: No meteors

4 Observations September 19–20, 2020

The last night with clear skies in September came on September 19–20. The night was warm and clear, and the observing conditions had improved from my last observing session. I started my observations 20^h00^m UT, and 8 minutes later a very short, yellow sporadic of medium speed lit up in Cassiopeia. This proved to be the brightest meteor of the hour, followed by sporadics in the magnitude range +2 to +5. A +3 magnitude SPE at 20^h25^m, proved this shower still to be active. 3 minutes before the end of the period, I also saw a +3 mag, slow moving CCY in Delphinus.

20^h00^m–21^h00^m T_{eff}: 1.00, *F*: 1.00, *Lm:* 6.14, RA: 330, Dec: +45

- Spo: +1, +2(2), +3(2), +4(2), +5(2) – 9 meteors
- SPE: +3 – 1 meteor
- STA: No Meteors
- CCY: +3 – 1 meteor

The next hour continued with an absence of bright meteors. Sporadic activity was nevertheless quite steady, with 11 observed meteors. A nice +2 mag CCY was observed 7 minutes into the period, ending its path near kappa Cygni. A +5 mag SPE was also seen 21^h48^m UT. Like the previous hour, the STA were absent, and I found this a little surprising due to the clear activity observed earlier in September.

21^h00^m–22^h00^m T_{eff}: 1.00, *F*: 1.00, *Lm*: 6.19, RA: 330, Dec: +45

- Spo: +2, +3(4), +4(3), +5(3) – 11 meteors
- SPE: +5 – 1 meteor
- STA: 0 meteors
- CCY: +2 – 1 meteor

Like the previous hours, the third period had no surprises. Sporadic rates were steady with 9 meteors. A nice –1 Sporadic was seen in the outskirts of my field of view, before a yellow, slow moving STA glided through Aquarius 7 minutes later. A +3 mag SPE was also observed, but no CCY meteors was seen this hour. After 3 hours of observations, I decided to take a 15 minutes break to get some food, and change the battery in my camera.

22^h00^m–23^h00^m T_{eff}: 1.00. *F*: 1.00, *Lm*: 6.23, RA: 345, Dec: +45

- Spo: –1, +1, +2, +3, +4(3), +5, +6 – 9 meteors
- SPE: +3 – 1 meteor
- STA: +1 – 1 meteor
- CCY: 0 meteors

My final period that night lasted from 23^h15^m to 00^h15^m UT. Driven by newly gained powers from a chocolate bar, I was ready for some late-night action! After 11 minutes of observation a nice +2 mag SPE was seen in Andromeda. 9 minutes later another +3 mag SPE trailed through Perseus. 35 minutes into the hour a really beautiful +1 Mag CCY was gliding from Cygnus into Lacerta. Being a little disappointed with STA activity this night, the shower woke up the last 10 minutes of observation, with two +4 mag meteors in Andromeda. A rewarding 4 hours of observation had come to an end, with a total of 51 meteors observed visually.

23^h15^m–00^h15^m T_{eff}: 1.00, *F*: 1.00, *Lm*: 6.23, RA: 0.00, Dec: +45

- Spo: +1, +2(2), +3(2), +4(3), +5(3) – 11 meteors
- SPE: +2, +3 – 2 meteors
- STA: +4(2)
- CCY: +1 – 1 meteor

October observations from Norway

Kai Gaarder

Søndre Ålsvegen 698A, N-2740 Roa, Norway
kai.gaarder@gmail.com

A report is presented with the visual observations carried out by the author in Norway during the month October 2020.

1 Introduction

During the ascending phase of the Orionids, a stable high-pressure system was established over the southern parts of Norway. This provided a rare opportunity to make observations for 5 nights in a row between October 13–14 and October 17–18. A total of 164 meteors were observed visually in 20.67 hours of effective observing time. The dominant showers in this period were the Orionids and the Southern Taurids. Stable and consistent activity from the Southern Taurids were observed, together with rising activity from the Orionid shower towards maximum. In the night of October 14–15, noticeable activity from the minor shower the October Ursa Majorids were observed, also with some bright shower members. Occasional meteors from the delta Aurigids, epsilon Geminids and Leo Minorids were also observed, but nothing out of the ordinary. In the night of October 17–18, two sporadic fireballs of magnitude –4 were observed.

2 Observations October 13–14

A report is given of my observations on October 13–14. A total of 70 meteors were observed, during 5.08 hours of effective observing time. A total of 10 meteors were also photographed with my DSLR camera. A number of sources were active this night, and meteors from the DAU, EGE, LMI, ORI, STA and OCU were observed. The most active shower this night was the Southern Taurids with a total of 13 meteors, followed by the Orionids with 7 meteors.

I started observations under good sky conditions at 22^h00^m UT. The weather forecast was good for the rest of the night, and I was excited to see what the following hours would bring. The first hour started out with good sporadic activity, with 4 meteors in the magnitude range +2 to +5 seen in 15 minutes. Also, a nice +2 mag DAU in Triangulum was seen in that period. Activity kept up for the next quarter, with 3 sporadics and 1 STA in the magnitude range of +4 to +6. After that a rather dull period followed, with only 2 sporadics and 1 STA the next half hour.

22^h00^m–23^h00^m T_{eff}: 1.00, F: 1.00, Lm: 6.23, RA: 45, Dec: +50

- Spo: 0, +2, +3, +4(4), +5, +6 – 9 meteors
- STA: +5, +6 – 2 meteors
- ORI: 0 meteors
- EGE: 0 meteors
- DAU: +2 – 1 meteor
- LMI: 0 meteors
- OCU: 0 meteors

The weak sporadic activity from the last 30 minutes continued into the second hour, with only 5 meteors seen. The hour was saved by the STA with 3 meteors, among them a nice +1 mag into Cygnus. At 23^h41^m a +1 mag, white, fast meteor streaked into Gemini, matching all the criteria to be an October Ursa Majorid.

23^h00^m–00^h05^m T_{eff}: 1.017, F: 1.00, Lm: 6.23, RA: 45, Dec: +50

- Spo: +3(2), +4, +5, +6 – 5 meteors
- STA: +1, +4, +5 – 3 meteors
- ORI: 0 meteors
- EGE: 0 meteors
- DAU: 0 meteors
- LMI: 0 meteors
- OCU: +1 – 1 meteor

With the rising altitude of the Orionid radiant, I was hoping the third hour of observation would reveal the first Orionid of the year. While waiting for this, a beautiful reddish +1 mag sporadic slowly glided through the arm of Perseus. 20 minutes later the STA decided to join in, revealing a yellow 0 mag meteor far from the radiant in UMA. This was quickly followed by another weak STA in Andromeda. A really active period then followed. A +5 mag Orionid in Auriga was almost immediately followed by a +4 mag STA in Taurus. Minutes later a +4 mag OCU was seen, making it the second shower member of the night. At 00^h50^m the battery of my camera went dead, but I decided to continue visual observations for a full hour before changing it. I was kind of hoping no bright meteors would appear in the now abandoned camera field, but of course it had to happen! 2 minutes before the full hour, a beautiful –1 mag Orionid flashed up in Taurus, right where the camera field would have been. Another +2 mag Orionid was also seen low in Gemini in the last 5 minutes of the period.

00^h05^m–01^h05^m T_{eff}: 1.00, F: 1.00, Lm: 6.23, RA: 60, Dec: +50

- Spo: +1, +2, +3(2), +4, +5(4) – 9 meteors

- STA: 0, +4(2) – 3 meteors
- ORI: –1, +2, +5 – 3 meteors
- EGE: 0 meteors
- DAU: 0 meteors
- LMI: 0 meteors
- OCU: +4 – 1 meteor

After a short break with some food and battery change, both my body and my camera were loaded with new energy. With rising radiant positions for most of the observed showers, I was hoping the next hour would bring some rewarding moments. 3 minutes into the period a +3 mag OCU was seen on the Lynx – Auriga border. This meteor was soon followed by a +4 mag STA, and my first LMI for the night, a +5 mag in Auriga. 5 minutes later another nice +1 mag STA was observed in Cassiopeia. Taurid rates were really steady throughout the night, with 2 or 3 meteors observed each hour. Sporadic rates were also steady with 10 meteors this hour, with +1 and 0 mag meteors as highlights. The Orionids provided 2 meteors this hour, and I also saw my first EGE of the night, a +3-mag shooting up between Auriga and Gemini.

01^h05^m–02^h15^m T_{eff}: 1.066, *F*: 1.00, *Lm*: 6.18, RA: 60, Dec: +50

- Spo: 0, +1(2), +3(3), +4(2), +5, +6 – 10 meteors
- STA: +1, +2, +4 – 3 meteors
- ORI: +2, +4 – 2 meteors
- EGE: +3 – 1 meteor
- DAU: +4 – 1 meteor
- LMI: +5 – 1 meteor
- OCU: +3 – 1 meteor

In the last hour a crescent moon and Venus was climbing, making a beautiful couple in the eastern morning sky, but reducing the Lm a little. There were no surprises this final morning hour. Sporadic rates were slightly reduced to 8 meteors, and both the Orionids and the Taurids yielded 2 meteors each. The highlight of the hour was a stunning –2 mag Orionid low in the southern sky. A successful 5-hour long observation period had come to an end, with a total of 70 meteors observed. And best of all, the weather forecast promised clear skies also for the coming nights.

02^h15^m– 03^h15^m T_{eff}: 1.00, *F*: 1.00, *Lm*: 6.13, RA: 75, Dec: +45

- Spo: +2(2), +3, +4(2), +5(2), +6 – 8 meteors
- STA: +2, +5 – 2 meteors
- ORI: –2, +3 – 2 meteors
- EGE: +3 – 1 meteor
- DAU: 0 meteors
- LMI: +4 – 1 meteor
- OCU: 0 meteors

3 Observations October 14–15

On October 14–15, 2020 I observed meteors for 4.57 hours under good sky conditions. A total of 75 meteors were observed, and 10 meteors were photographed with my DSLR camera. Activity from a number of sources were observed, among them noticeable activity from the minor shower called the October Ursa Majorids. A total of 12 meteors were observed during the night, making them one of the strongest sources of activity in the sky.

After a successful previous night of meteor observations, I was eager to check out what another clear night would bring. I started observations from my usual observation site at 22^h30^m UT. The sky was as dark as it gets here, with a Lm of 6.23, so everything looked promising for a long night with meteor observations. After only 3 minutes a beautiful +1 mag EGE appeared close to the radiant in Auriga, looking reddish and rather slow moving for being an EGE. This meteor was photographed with my Nikon D3100 camera with a Samyang 16mm F 2.0 lens, looking green and a lot brighter on the photo than it appeared visually. 2 minutes later a +5 mag DAU followed, shortly before a white +2 mag OCU lit up near Alpha Andromeda. The sporadic activity was on the low side, with 7 meteors observed in the 1.2-hour period. By the end of the period, I had also seen a +4 mag ORI, a +5 mag STA, and another +5 mag EGE and a +5 mag OCU.

22^h30^m–23^h45^m T_{eff}: 1.200, *F*: 1.00, *Lm*: 6.23, RA: 45, Dec: +50

- Spo: +2(2), +3, +4(2), +5(2) – 7 meteors
- STA: +5 – 1 meteor
- EGE: +1, +5 – 2 meteors
- ORI: +4 – 1 meteor
- DAU: +5 – 1 meteor
- LMI: 0 meteors
- OCU: +2, +5 – 2 meteors

5 minutes into the second period, a beautiful, white 0 mag OCU appeared in Taurus. 27 minutes later another white +2 mag meteor met all the criteria for being an OCU. 15 minutes then went by before another +4 mag OCU was seen, followed by a +3 mag OCU 9 minutes later. I was surprised by this activity and was now starting to feel that a real shower was going on in Ursa Major! Other highlights this period was a 0 mag LMI, a +1 mag ORI, and another +1 mag EGE.

23^h45^m–01^h00^m T_{eff}: 1.250, *F*: 1.00, *Lm*: 6.23, RA: 60, Dec +50

- Spo: +2(3), +3(2), +4(2), +5 – 8 meteors
- STA: +6 – 1 meteor
- EGE: +1 – 1 meteor
- ORI: +1, +3 – 2 meteors
- DAU: +6 – 1 meteor
- LMI: 0 – 1 meteor
- OCU: 0, +2, +3, +4 – 4 meteors

The third period started with some weak sporadic meteors and a +5 mag STA. 32 minutes into the period a nice +1 mag OCU lit up between Perseus and Auriga, followed by a 0-mag sporadic one minute later. A very active period then followed. A +2 mag, red STA glided slowly through

Perseus, before a yellow, 0 mag EGE shot out from Auriga into Camelopardalis. 11 meteors followed in the next 20 minutes, among them a +2 mag OCU, a +5 mag LMI, a +5 mag EGE and a +3 and +4 mag STA. At 02^h09^m a +4 mag OCU appeared close to Capella. Almost simultaneously I became aware of a bright –3 mag OCU moving fast from Lynx into Cancer, leaving a smoke train for several seconds! The period was rounded off by a +5 mag ORI. The OCU activity was similar to the previous period, with 4 meteors in 1.117 hours.

01^h00^m–02^h15^m T_{eff}: 1.117, *F*: 1.00, *Lm*: 6.23, RA: 60, Dec: +50

- Spo: 0(2), +2(3), +3(2), +4(2), +5, +6 – 11 meteors
- STA: +2, +3, +4, +5 – 4 meteors
- EGE: 0, +5 – 2 meteors
- ORI: +5 – 1 meteor
- DAU: 0 meteors
- LMI: +5 – 1 meteor
- OCU: –3, +1, +2, +4 – 4 meteors

In the final period the ORI took over the show from the OCU, although the latter one still delivered 2 meteors in one hour. The first one being a yellow +1 mag in Taurus, and then a +6 mag in Perseus. 5 Orionids were seen this hour, among them two nice +1 mag meteors. A +1 mag LMI in Auriga, was also among the highlights this hour. Another morning was now approaching rapidly, and I had to prepare for another day at work with very little sleep! That is however a small price to pay for many memorable moments! I will especially remember the noticeable OCU activity this night, which I think was too high to be explained utterly by chance line-up sporadics. It would be interesting to know if any camera networks can confirm activity from the OCU this night.

02^h15^m– 03^h15^m T_{eff}: 1.00, *F*: 1.00, *Lm*: 6.18, RA: 75, Dec: +45

- Spo: +2(2), +3, +4(4), +5(2) – 9 meteors
- STA: +3 – 1 meteor
- EGE: +5 – 1 meteor
- ORI: +1(2), +2, +3(2) – 5 meteors
- DAU: 0 meteors
- LMI: +1, +4 – 2 meteors
- OCU: +1, +6 – 2 meteors

Observed showers:

- Southern Taurids (STA)
- epsilon Geminids (EGE)
- Orionids (ORI)
- delta Aurigids (DAU)
- Leo Minorids (LMI)
- October Ursa Majorids (OCU)

4 Observations October 15–16

The night both started and ended with clouds, but a 1.53-hour period after local midnight provided good observing conditions. I was especially eager to see if the noticeable activity from the October Ursa Majorids (OCU) observed the previous night, would persist for a second night. Observations proved this not to be the case, with only one shower member observed through the entire period. The far most active shower this night was the Southern Taurids (STA), with 6 meteors in the magnitude range +3 to +5 observed. Activity from the Orionids (ORI) was also on the low side, with only 3 meteors observed. The total meteor count for the night was 25, with 2 meteors photographed with my DSLR camera.

Observations

22^h50^m–00^h25^m T_{eff}: 1.530, *F*: 1:00, *Lm*: 6.23, RA: 45, Dec: +50

- Spo: –1, 0, +1(2), +2(2), +3(2), +4(3), +5 – 12 meteors
- STA: +3, +4(3), +5(2) – 6 meteors
- EGE: +3, +4 – 2 meteors
- ORI: +3, +5(2) – 3 meteors
- DAU: 0 meteors
- LMI: +1 – 1 meteor
- OCU: +6 – 1 meteor

Break between 23^h50^m and 23^h53^m.

Observed showers:

- Southern Taurids (STA)
- epsilon Geminids (EGE)
- Orionids (ORI)
- delta Aurigids (DAU)
- Leo Minorids (LMI)
- October Ursa Majorids (OCU)

5 Observations October 16–17

On October 16–17 I was observing meteors from my homeplace in the south-eastern parts of Norway. The sky was clear with a limiting magnitude of 6.23, and the night was calm and a bit moisty. Showers of interest this night were the Orionids, Southern Taurids, epsilon Geminids, delta Aurigids, and the Leo Minorids. A total of 78 meteors were observed in 4.62 hours of effective observing time, and 9 meteors were photographed with my DSLR camera.

22^h45^m–23^h55^m T_{eff}: 1.167, *F*: 1.00, *Lm*: 6.23, RA: 45, Dec: +50

I started observations 22^h45^m UT, and after only 6 minutes a beautiful, yellow, 0 magnitude Taurid meteor slowly glided through my camera field in Auriga. This meteor was probably a Northern Taurid, but since the working list of the IMO does not consider this shower to be active before October 20, all NTA's observed this night were recorded as being Southern Taurids. Activity from the Taurids continued to be good throughout the first 1.17-hour period, with 3 more meteors observed, making a total of four. 7 sporadic meteors were observed during this first period, and also the ORI, EGE and DAU showers showed up with one meteor each.

- Spo: +3(3), +4(2), +5, +6 – 7 meteors
- STA: 0, +3(2), +4 – 4 meteors
- DAU: +4 – 1 meteor
- EGE: +4 – 1 meteor
- ORI: +4 – 1 meteor
- LMI: 0 meteors

23^h55^m–01^h05^m T_{eff}: 1.167, *F*: 1.00, *Lm*: 6.23, RA: 60, Dec: +45

In the next period sporadic rates were up to 9 meteors, but no meteors were brighter than magnitude +2. The climbing Orionid radiant also contributed to an increase in Orionid rates to 3 meteors observed. Taurid rates were down to 2 observed meteors, both of magnitude +5. I had an impression that meteors belonging to the southern branch of the Taurid shower, were weaker than the ones I considered belonging to the northern branch.

- Spo: +2(2), +3(3), +4(3), +6 – 9 meteors
- STA: +5(2) – 2 meteors
- DAU: 0 meteors
- EGE: +3 – 1 meteor
- ORI: +2, +5, +6 – 3 meteors
- LMI: 0 meteors

01^h05^m–02^h20^m T_{eff}: 1.116, *F*: 1.00, *Lm*: 6.23, RA: 60, Dec: +45

The third period started with an 8 minutes break to change battery in my camera, and to fill up with energy from a chocolate bar. The trend from the previous period continued with rising sporadic activity of mainly faint meteors. 15 meteors were observed during the 1.116-hour long period, with no meteor being brighter than magnitude +2. Orionid rates also climbed to 5 meteors and Taurid rates were back to 4 meteors. All in all, this was an exciting period because of the high overall meteor activity, even though no bright meteors were seen.

- Spo: +2(3), +3(3), +4(4), +5(4), +6 – 15 meteors
- STA: +2, +3(2), +5 – 4 meteors
- DAU: +2 – 1 meteor
- EGE: 0 meteors
- ORI: +2, +4(2), +5, +6 – 5 meteors
- LMI: +5 – 1 meteor

02^h20^m–03^h30^m T_{eff}: 1.167, *F*: 1.00, *Lm*: 6.23, RA: 75, Dec: +40

The last period of the night was pretty much a continuation of the former. A slight decrease in sporadic activity was observed, with 11 meteors in 1,167 hours. 6 Orionids were seen in the same period, along with 5 Southern Taurids and 1 epsilon Geminid. During this period only one meteor brighter than magnitude +3 was seen, a nice, slow +2 magnitude sporadic between Gemini and Procyon. During the whole night only one meteor brighter than magnitude +2 was seen, but the session was not boring after all! Sometimes I feel a great satisfaction in observing faint meteors. It tells me that observing conditions are really good, and it leaves me with an exclusive feeling, knowing that I probably was the only one in the world seeing that elusive +5 magnitude meteor in Andromeda!

- Spo: +2, +3(3), +4(2), +5(4), +6 – 11 meteors
- STA: +3(2), +4(3) – 5 meteors
- DAU: 0 meteors
- EGE: +3 – 1 meteor
- ORI: +3(3), +4(2), +5 – 6 meteors
- LMI: 0 meteors

6 Observations October 17–18

A presentation is given of my observations on October 17–18, 2020. A total of 86 meteors were observed in a total of 4.87 hours effective observing time, and 13 meteors were photographed with my DSLR camera. Two beautiful fireballs were also observed visually this night. One of them was caught on video by the Norwegian Meteor Network, the other one was photographed with my DSLR camera.

Observations:

22^h25^m–23^h45^m T_{eff}: 1.283, *F*: 1.00, *Lm*: 6.23, RA: 45, Dec: +50 – 3 minutes break

- Spo: –4, –1, +2(2), +3(2), +4(2), +5(2) – 10 meteors
- STA: +2, +3 – 2 meteors
- DAU: 0 meteors
- EGE: 0 meteors
- ORI: +1 – 1 meteor
- LMI: +2 – 1 meteor

After a long run with clear nights, the weather forecast indicated that this night would be my last chance to observe this year's Orionids. I was therefore hoping for an increase in the Orionid activity, and hopefully more bright meteors than the night before, which only yielded one meteor brighter than +2 during the whole night. After only 12 minutes of observations my prayers were heard, with a beautiful, slow moving, –1 magnitude sporadic radiating out of Draco and moving into Ursa Major. Fifteen minutes later I became aware of a slow-moving light in the outskirts of my observation field. I turned my head and could follow a very slow-moving fireball low in the southern horizon for several seconds. The meteor appeared to be white in color and had several flares along its path. The fireball was photographed by the Norwegian Meteor Network, and any remnants would have fallen into the sea just north of Denmark. More information and videos about this meteor can be found online[24].

23^h45^m–01^h00^m T_{eff}: 1.250, *F*: 1.00, *Lm*: 6.23, RA: 60, Dec: +45

- Spo: –4, +2(2), +3(3), +4(4), +5, +6 – 12 meteors
- STA: +3(3) – 3 meteors

[24] http://norskmeteornettverk.no/meteor/20201017/225143/

- DAU: +1 – 1 meteor
- EGE: +2, +4, +5 – 3 meteors
- ORI: +2, +3(3), +4(2), +5, +6 – 8 meteors
- LMI: +4 – 1 meteor

With rising radiant elevation, the Orionids became more active. 8 meteors were seen during this 1.25-hour period, all in the magnitude range between +2 and +6. Also, the epsilon Geminids and the Southern Taurids showed some nice activity, with 3 meteors each. Together with 12 sporadics, 1 DAU and 1 LMI, the total meteor count for the period was 28. An entertaining and rewarding period reached its climax at 00^h25^m UT. On the border between Lynx and Ursa Major a bright yellow light started to emerge, gaining brightness as it slowly moved through Cancer, before ending in a bright flash near the horizon in Hydra. The fireball reached magnitude –4, maybe even brighter at its final flare. I was lucky to catch this meteor in the outskirts of my camera field but missing its endpoint in Hydra.

01^h00^m–02^h20^m T_{eff}: 1.167, *F*: 1.00, *Lm*: 6.23, RA: 60, Dec: +45 – 10 minutes break

- Spo: +1, +3(2), +4(3), +5(3), +6 – 10 meteors
- STA: 0 meteors
- DAU: 0 meteors
- EGE: 0 meteors
- ORI: +1(2), +2(2), +3(4) – 8 meteors
- LMI: +1 – 1 meteor

Orionid activity kept up in the third period with a total of 8 meteors, with a couple of nice +1 magnitude meteors. A decent +1 magnitude LMI was also seen in Ursa Major, but activity from the STA, EGE and DAU showers were absent. With 10 sporadic meteors seen, the total count in this period came in at 19 meteors.

02^h20^m–03^h30^m T_{eff}: 1.167, *F*: 1.00, *Lm*: 6.23, RA: 75, Dec: +40

- Spo: +1, +2, +3, +4(4), +5(3), +6(2) – 12 meteors
- STA: +2(2), +4(3), +5, +6 – 7 meteors
- DAU: 0 meteors
- EGE: +3 – 1 meteor
- ORI: +3, +4(2) – 3 meteors
- LMI: 0, +3 – 2 meteors

Meteor activity picked up a little in the last period. A total of 25 meteors were seen, most of them in the magnitude range +3 to +5. After a quiet period, the Taurids were on the rise again, with 7 meteors observed. For some reason Orionid activity fell to 3 meteors, even though the radiant now was high in the sky. Another successful night of meteor observing was rounded off with a beautiful 0 magnitude LMI in Auriga.

Figure 1 – Photo taken with a Nikon D3100 camera, with a Samyang 16mm F 2.0 lens. Exposure time was 20 seconds, with ISO 1600 settings. The brightest star in the upper middle of the photo is Capella.

November 2020 observations from Norway

Kai Gaarder

Søndre Ålsvegen 698A, N-2740 Roa, Norway
kai.gaarder@gmail.com

A report is presented with the visual observations carried out by the author in Norway during the month November 2020.

1 Introduction

November is usually a month dominated by clouds and fog at my homeplace in eastern Norway. So also this year, but the author was able to conduct 3 observing sessions during the Leonid shower. A total of 9.10 hours of effective observing time was yielding a total of 117 visual meteors, and 21 meteors photographed with my DSLR camera. An overview of my observation each night is given.

2 Observations 2020 November 17–18

21^h35^m–22^h35^m T_{eff}: 1.00, *F*: 1.00, *Lm*: 6.25, RA: 60, Dec: +50

- SPO: –1, 0, +1, +2, +3(2), +4(4), +5, +6 – 12 meteors
- STA: +4, +5 – 2 meteors
- NTA: +2, +5 – 2 meteors
- LEO: 0 – 1 meteor
- NOO: 0 meteors

The one-week weather forecast for the maximum of the Leonids did not look good this year. As maximum approached it became clear that the night of November 16–17 would be clouded out. The same story was seemingly about to happen to November 17–18, when a short possible clearing around midnight appeared in the weather charts. The clearing came as predicted, but fog created by lakes in the lowlands, was pushing up against my observing site at 460 meters altitude. I decided to jump in my car and drive to an alternative observing site at 630 meters altitude. This proved to be a right decision, and I was able to start observing at 21^h35^m UT, with the Leonid radiant very low in the eastern sky.

I had no expectations for the Leonids this first hour, due to the low radiant position. Anyway, I was hoping that good sporadic rates, and maybe some Taurids would be possible under the good sky conditions at this observing site. In the second minute of observation a +2 magnitude NTA lit up just west of the Pleiades. 4 minutes later a +6 mag SPO confirmed the good observing conditions, before a +5 mag NTA was slowly gliding towards beta Tauri. Satisfied with the start, I suddenly became aware of a long pathed, 0 mag meteor streaking quite slowly from the eastern horizon through Ursa Major. No doubt this was an Earth grazing Leonid, and it left a smoke train hanging in the sky for about 3 seconds!

The sporadics continued in a steady flow, and at 22^h01^m a nice slow moving 0 mag SPO appeared in the outskirts of my observing field. 15 minutes later an even brighter –1 mag SPO started out in Ursa Major and glided slowly into Draco. At the end of the period, two weak Southern Taurids of mag +4 and +5, added to the activity from the Taurid complex.

22^h35^m–23^h35^m T_{eff}: 1.00, *F*: 1.00, *Lm*: 6.18, RA: 75, Dec: +50

- SPO: +2, +3, +4, +5(3), +6(2) – 8 meteors
- STA: 0 meteors
- NTA: +6 – 1 meteor
- LEO: –2, +3, +4 – 3 meteors
- NOO: +2 – 1 meteor

The clearing was supposed to last for 2 to 3 hours, so I was hoping for at least one more hour of clear skies. Another exciting factor was whether the rising Leonid radiant would lead to more activity from this source. I had to wait just 5 minutes before the Leonids proved to be alive and kicking! At 22^h40^m a yellow –2 mag Leonid was streaking from Leo Minor all the way into Cassiopeia, leaving a clear smoke train for at least 5 seconds! Then a quiet period followed with no meteors seen the next 15 minutes. Some dispersed lower clouds also appeared near the horizon, together with a thin layer of higher clouds in parts of the sky, making a slight deterioration of the observing conditions.

Despite this, a more active period started just before 23^h00^m with a couple of sporadics, a +6 mag NTA and 2 Leonids of mag 3 and 4 in just 5 minutes! A +2 mag November Orionid glided through Gemini at 23^h08^m, followed by some more sporadics towards the end of the period. At this time clouds had moved in, making serious meteor observations difficult. While packing down my observation gear, I still saw a couple of Leonid meteors through gaps in the clouds, giving a testimony of higher activity towards the morning.

Figure 1 – Picture taken from the observation site at 630 metres height at Gullenhaugen after ending observations on November 18. Skies still clear in the northern horizon, but clouds quickly moving in from south-west.

3 Observations 2020 November 19–20

01^h25^m–02^h25^m T_{eff}: 1.00, *F*: 1.00, *Lm*: 6.19, RA: 105, Dec: +50

- SPO: +1(2), +2, +3(2), +4(4), +5(3) – 12 meteors
- LEO: –2, +1, +2, +3 – 4 meteors
- STA: 0 meteors
- NTA: +2, +5 – 2 meteors
- NOO: +1 – 1 meteor

A small but elusive high-pressure system was suddenly appearing over the southern parts of Norway on November 19. The uplifting weather forecast made me go to bed early, planning to get some early morning observations before going to work the next day. After some hours of good sleep, I was out in the observation field and ready to start observing at 01^h25^m UT. The session was initiated with a couple of sporadic meteors, before a nice +1 mag November Orionid lit up in Auriga eight minutes into the period. Another eight minutes went by before the first Leonid of the night, a +3 mag in Ursa Major appeared. This was followed by a nice +2 mag Northern Taurid the next minute, before a beautiful yellow +1 Mag Leonid streaked into Auriga six minutes later.

This ignited a really active period with a lot of bright meteors! At 01^h52^m a white +2 mag Leonid shot into Ursa Major. Two minutes later two sporadic meteors of mag +1 appeared nearly simultaneous, one in Ursa Major and one in Gemini. Then it was time for the Leonids to show some muscles! At 01^h56^m a yellow –2 mag Leonid lit up in Ursa Major, leaving a smoke train for several seconds! This was the fourth Leonid of the hour, showing that the Leonids shower still is able to produce decent activity two nights after maximum. The hour was rounded off with some weaker sporadics and a +5 mag NTA, leaving the sporadic rate of the hour at 12 meteors.

02^h25^m–03^h30^m T_{eff}: 1.033, *F*: 1.00, *Lm*: 6.19, RA: 120, Dec: +50 – 3 minutes break.

- SPO: +1, +2(2), +3(2), +4(2), +5, +6 – 9 meteors
- LEO: +2, +3, +5 – 3 meteors
- STA: 0 meteors
- NTA: 0 meteors
- NOO: 0 meteors

The next hour started with a nice +2 mag Leonid two minutes into the period. After a flying start, activity started to decline. The action with bright meteors from the first hour was over, but the Leonids still produced two more meteors of mag +3 and +5. Also, the Taurid complex and the November Orionids went into hibernation this hour, with no meteors seen. The sporadic activity was still decent but declining to 9 meteors of mostly weaker magnitudes.

03^h30^m–04^h30^m T_{eff}: 1.00, *F*: 1.00, *Lm*: 6.19, RA: 120, Dec: +50

- SPO: +1, +3, +4(3), +5(2), +6 – 8 meteors
- LEO: –1, +3(2) – 3 meteors

- STA: 0 meteors
- NTA: +1, +2 – 2 meteors
- NOO: +1 – 1 meteor

First out this hour was a white, slow moving, +2 mag NTA in Leo. Second later a yellow, fast moving sporadic of mag +1 appeared in Ursa Major. Two minutes later the Leonids had a final show of force, with a beautiful, yellow, –1 mag meteor in Draco. The hour continued with two nice +1 mag meteors from the NTA and NOO respectively. The Leonids produced two more +3 mag meteors during the hour, and the sporadic rate ended at 8 meteors. A successful 3-hour session had come to an end, showing that the Leonids were still quite active and able to produce some really bright meteors! A total of 45 meteors were seen in 3.03 hours of observation, and 8 meteors were photographed with my DSLR camera.

4 Observations 2020 November 21–22

23^h45^m–00^h45^m T_{eff}: 1.00, F: 1.05, Lm: 6.19, RA. 90, Dec: +50

- SPO: +2(2), +3, +4 – 4 meteors
- STA: +3 – 1 meteor
- NTA: +4 – 1 meteor
- LEO: 0 meteors
- AMO: +5 – 1 meteor
- NOO: 0 meteors

Another clear night was predicted in the weather forecast, and I was eager to see if the Leonids still could have some surprises. Arriving at the observation field, I became aware of some drifting clouds and a weak northern light making the sky conditions a little worse. I was anyway able to start observing 23^h45^m, but it soon became evident that meteor activity was weak. Only 4 sporadic meteors were seen this first hour, all in the magnitude range +2 to +4. No meteors were seen from the Leonids, but the radiant was still quite low in the sky. Two meteors were seen from the Taurid complex, together with one AMO of mag +5. This sums up a rather dull first hour, where the drifting clouds alone cannot explain the low sporadic activity.

00^h45^m–01^h50^m T_{eff}: 1.033, F: 1.00, Lm: 6.19, RA: 105, Dec: +50 – 3 minutes break

- SPO: 0, +3(2), +4(2), +5 – 6 meteors
- STA: +2 – 1 meteor
- NTA: +5 – 1 meteor
- LEO: +4, +5 – 2 meteors
- AMO: +4 – 1 meteor
- NOO: +4 – 1 meteor

At the start of the second period the drifting clouds had disappeared from the observation field, and I was hoping the activity would pick up a bit. After a while it was clear that activity was still on the dull side with mainly faint meteors. The two Taurid branches produced one meteor each, and the AMO and NOO showers also came in with one +4 mag meteor each. The climbing Leonid radiant resulted in two meteors of mag +4 and +5. The hour was rounded off with the highlight of the hour, a beautiful, yellow, slow moving, 0 mag sporadic meteor in Ursa Major.

01^h50^m–03^h00^m T_{eff}: 1.033, F: 1.03, Lm: 6.19, RA: 120, Dec: +50 – 8 minutes break

- SPO: +1, +2(3), +3, +4, +5, +6 – 8 meteors
- STA: +5 – 1 meteor
- NTA: +1, +3, +4 – 3 meteors
- LEO: +4(2) – 2 meteors
- AMO: 0 meteors
- NOO: 0 meteors

In the third hour some drifting clouds were back again, but not more than that useful observations could be carried out. First out was a nice +1 mag NTA in Ursa Major, followed by some weaker sporadics and a +5 mag STA. Half an hour into the period the first +4 mag Leonid appeared, with another +4-mag following 20 minutes later. The Northern Taurids made a good impression this hour with 3 meteors, and the sporadic activity ended at a more decent number of 8 meteors.

03^h00^m–04^h00^m T_{eff}: 1.00, F: 1.00, Lm: 6.19, RA: 135, Dec: +50

- SPO: +3(2), +4(2), +5 – 5 meteors
- STA: 0 meteors
- NTA: +5 – 1 meteor
- LEO: –1, +2, +3 – 3 meteors
- AMO: 0 meteors
- NOO: 0 meteors

The last hour confirmed the general low sporadic activity of the night with 5 meteors. The Leonids made a decent appearance with 3 meteors, with the highlight being a yellow –1 mag near Procyon. Despite some frustrating periods with clouds and low meteor activity, another successful session had come to an end. A total of 42 meteors were observed in 4.07 hours of observation, and 11 meteors were photographed with my DSLR camera.

Showers observed in November:

- LEO – Leonids
- STA – Southern Taurids
- NTA – Northern Taurids
- NOO – November Orionids
- AMO – Alpha Monocerotids

Figure 2 – Picture taken at the start of my observing session on November 21, showing the Northern lights and some clouds threathening in the horizon.

Observations December 6–8 in Belarus

Ivan Sergei[1] **and Yuri Goryachko**[2]

[1] **Mira Str.40-2, 222307, Molodechno Belarus**
seriv76@tut.by

[2] **Derazhnoye, Belarus**
astronominsk@gmail.com

The authors describe their visual and photographic efforts during 6-7 and 7-8 December 2020.

1 Introduction

I present the results of visual and photographic meteor observations between December 6 to 8, 2020. VISDAT and RADIANT were used to analyze the observations

2 Observations

Observations were made at a private astronomical observatory in Polanyi, 8 km from the city of Molodechno. On the northeastern side there is a slight illumination of the sky from the city. There is some obstruction of the sky in the northern sector (up to a height of 30–35 degrees) and slight obstruction in the eastern and southern directions, which does not interfere with observations. For the comfort of the observations, I created my own special observing chair with adjustable backrest (*Figure 1*).

Figure 1 – Homemade chair for observing meteors.

The average stellar limiting magnitude at the zenith is about 5.5. All paths of meteors were plotted on copies of star charts, printouts from the StarCalc planetarium program. Photographic observations were made with a Canon 350D camera with an MC 3.5/8A lens mounted at a height of 8 meters (on the dome of the astronomical observatory). For lens heating against freezing and fogging we used a hair dryer controlled by an electronic timer-socket "Electraline" in a mode of 1 hour of heating and a 30 minutes break. The camera would start 20 minutes after sunset and stop recording 10 minutes before sunrise every night from December 6 to 7, 7 to 8. Photographs were taken with an exposure of 30 seconds, ISO 1600. From December 6 to 8, 8 bright meteors in the –4 to +2 magnitude range were photographed. Of these, 6 are classified as sporadic, two were identified as probably associated with the December alpha Draconids (DAD#334)[25].

Figure 2 – DAD – meteor registered by all-sky camera.

[25] https://www.ta3.sk/IAUC22DB/MDC2007/Roje/pojedynczy_obiekt.php?kodstrumienia=00334&colecimy=0&kodmin=00001&kodmax=01049&sortowanie=0

One of them was a fireball in Cassiopeia, the second one appeared at 00^h24^m UT on December 8 in the constellation of Orion (*Figure 2*). Another one of interest, at 00^h58^m UT appeared in Cam, a beautiful yellow meteor (SPO) with a double flash (*Figure 3*).

Figure 3 – Beautiful meteor with a double flash in Cam.

3 Analysis of the observations

The purpose of the visual observations was to check the activity of the Geminids (GEM) and the minor showers (Rendtel J.,2020) NOO, HYD, MON, and some others. The second goal was to determine the radiant coordinates of those streams showing sufficient activity to define a radiant. The third aim was to look for new radiant positions for the meteoroid streams. The goal of the all-sky camera photo-patrols was to record bright meteors and bolides. The coordinates of the starting and ending points of the flight were determined from printouts from the StarCalc planetarium program. All data together with the characteristics of the meteors were entered into VISDAT. The table of active meteoroid streams from the IMO Meteor Calendar, VMDBRAD.DBF and a table with daily radiant drifts DRIFT.DBF were preconfigured in this program. VISDAT automatically classifies meteor shower associations based on criteria developed by IMO, and calculates activity – zenithal hour numbers *ZHR*. The Radiant positions were calculated using RADIANT software which reads VISDAT database files: vmdata20.dbf (table with information about meteors: time, brightness, angular velocity, accuracy of plotting, etc.) and vmhead20.dbf (the table with the observing conditions: interval, Lm, coordinates of the center of observed sky area, correction factor for cloudiness). The radiant locations are computed by three methods; however, two methods are most relevant for the analysis of observations: the "Tracing back" method and the Probabilities method. Each track on the photos was checked if it was caused by artificial satellites by the program HeavenSat. Data from the photographic observations were entered into the VISDAT program with an average meteor velocity of 15 degrees per second. Note that a correction was made to the showasso.txt file for autoclassification of meteors, just as with the visual observations. The correction was that a meteor not falling within the required velocity range by 1 degree per second was considered as belonging to a given meteor shower. For example, let VISDAT set the velocity range as 10–15 degrees per second for a given meteor while the real angular velocity which was entered into the database was 16 degrees per second. Without the correction, the program would classify this meteor as a sporadic, whereas after correction the meteor would be classified as a December Monocerotids (MON#19), for example. The radiant locations were calculated based on visual and photographic observations together, the data were imported from VISDAT (Richter J. ,1999) into RADIANT (Arl R.2001).

4 Results

During the first observation interval on December 06, I noticed some meteor activity from the polar region. Attempts to find the December alpha Draconids (DAD#334) radiant from my visual observations of December 6–7 by Probabilities was unsuccessful – the RADIANT program persistently "pops up" a radiant in Ursa Minor (*Figure 4*). Such radiant is not listed in the Meteor Data Center database. On December 8, a possible bolide, classified by VISDAT as belonging to DAD (*Figure 5*), was seen by a camera.

The same bolide (–3.8 mag) was recorded by a video camera of Yuri Goryachko in Minsk (*Figure 6*).

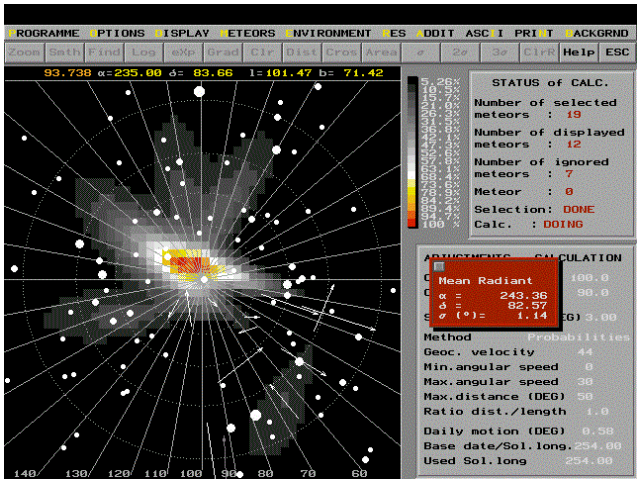

Figure 4 – Results of radiant position calculations for the December 6 and 7 meteors in the RADIANT program.

On the video (SonotaCo,2009), Yuri saw another faint meteor, as if a part of the main fireball had split off. His calculation gives the location of the radiant of the fireballs at the position of the DAD radiant (*Figure 7*). The fireball and the faint meteor on the camera of Yuri appeared almost simultaneously, these are on the same video.

Figure 5 – Fireballs recorded by an all-sky camera in Polanyi at 02^h44^m UT on December 8, 2020.

Figure 6 – Fireball recorded by Yuri Goryachko (Minsk, Belarus) at 02^h44^m UT on December 8, 2020.

Table 1 – The activity of the meteors of the different streams, based on the processing of observations in the program-VISDAT.

Date	Interval (UT)	Shower	Field	*Lim*	T_{eff}	*F*	*N*
06.12.20	15^h55^m–16^h50^m	2DAD, 1GEM, 3 SPO	52 +50	5.60	0.90	1	6
	18^h10^m–19^h10^m	1MON, 2SPO	80 +50	5.5	0.98	1	3
	20^h25^m–21^h25^m	1SPO	60+30	5.4	1	1	1
07.12.20	15^h35^m–16^h36^m	4SPO	52+50	5.4	1	1	4
	17^h00^m–18^h01^m	1DAD, 1GEM, 1SPO	52+50	5.6	1	1	3

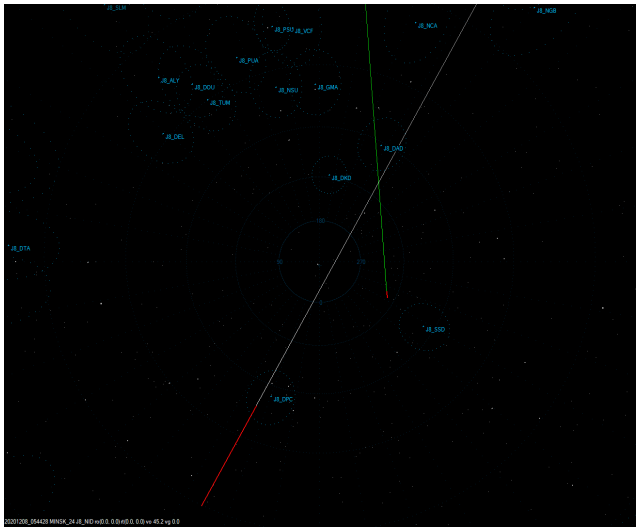

Figure 7 – Calculation of the location of the bolide and a faint meteor by the program UFOOrbit for December 08, 2020, performed by Yuri Goryachko.

But most interestingly, CMOR radar (Jones, 2005) shows a prominent short-lived radiant in the area on December 8, e.g., it has been active only one day, and then disappeared (*Figure 8*).

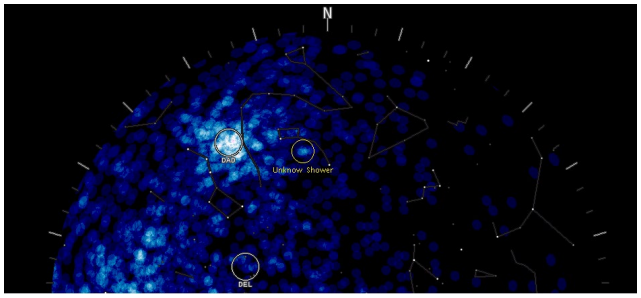

Figure 8 – Location of the unknown radiant in Ursa Minor on the CMOR radar on December 08, 2020

The Tracings method seems to indicate a possible radiant for the fireballs between UMa and Dra, suggesting it may belong to the DAD meteor shower (*Figure 9*).

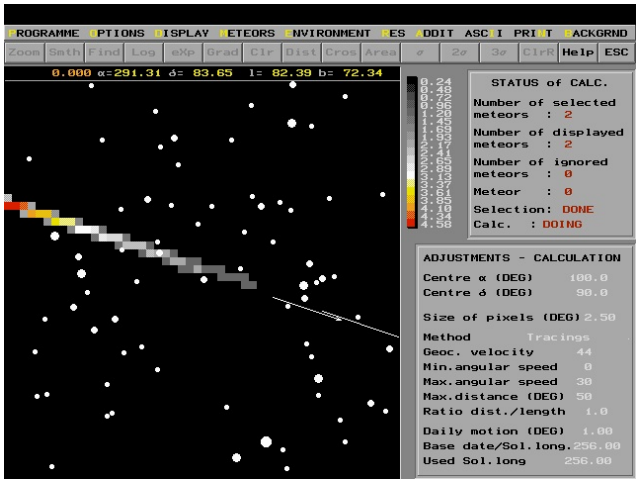

Figure 9 – Calculation of the position of the bolide from photographic observations I.Sergey and video observations Y. Goryachko December 08, 2020 by Tracings method.

5 Conclusion

Meteors belonging to DAD are classified by VISDAT on the basis of criteria developed by IMO. Here the situation is somewhat contradictory. RADIANT "shows" a radiant in Umi if calculated with Probabilities, while VISDAT classifies some meteors as DAD. Radiant, on the other hand, shows a probable radiant in the DAD region when calculating with the Tracing method. Most likely DAD meteors appear before as well as after the peak date. CMOR radar shows a variable and complex DAD meteor shower structure. There are probably several sub centers. Whether some minor DAD shower activity has been detected, or some meteor shower activity from an unknown radiant in Umi, is not clear. Visual observations have the evidence that the observer sees what is happening at the sky, while the video observer only learns about their results the next day or even later. A second advantage of visual observations over video observations is that fainter meteors can be captured. The third advantage is aesthetic – direct "communication" of the observer with the starry sky is very fascinating and an exciting awareness that is beneficial for science. No observable, reliably detectable radiants have been recorded between December 6 and 8. There is some hint of faint meteor activity with a possible radiant near Capella, but there is no confirmation of this from the CMOR radar. So, the exact identity of the fireball is a mystery.

Acknowledgments

I thank Yuri Goryachko for providing video observation materials and the analysis of his data, and Paul Roggemans for proofreading the article. Thanks to Konstantin Morozov (Minsk) for his recommendations on working with the program HeavenSat.

References

Arlt R. (2001). "The RADIANT Software – Details and Problems Scrutinized". In, Arlt R., Triglav M., Trayner C., editors, *Proceedings of the International Meteor Conference*, Pucioasa 2000. International Meteor Organization, pages 10–17.

Jones J., Brown P., Ellis K. J., Webster A. R., Campbell-Brown M., Krzemenski Z., and Weryk R. J. (2005). "The Canadian Meteor Orbit Radar: system overview and preliminary results". *Planetary and Space Science*, **53**, 413–421.

Rendtel J. (2019). "Meteor Shower Calendar". IMO.

Richter J. (1999). "VISDAT: a database system for visual meteor observations". *WGN, Journal of the International Meteor Organization*, **27**, 2–4.

SonotaCo (2009). "A meteor shower catalog based on video observations in 2007-2008". *WGN, Journal of the International Meteor Organization*, **37**, 55–62.

Radio meteors October 2020

Felix Verbelen

Vereniging voor Sterrenkunde & Volkssterrenwacht MIRA, Grimbergen, Belgium
felix.verbelen@skynet.be

An overview of the radio observations during October 2020 is given.

1 Introduction

The graphs show both the daily totals (*Figure 1 and 2*) and the hourly numbers (*Figure 3 and 4*) of "all" reflections counted automatically, and of manually counted "overdense" reflections, overdense reflections longer than 10 seconds and longer than 1 minute, as observed here at Kampenhout (BE) on the frequency of our VVS-beacon (49.99 MHz) during the month of October 2020.

The hourly numbers, for echoes shorter than 1 minute, are weighted averages derived from:

$$N(h) = \frac{n(h-1)}{4} + \frac{n(h)}{2} + \frac{n(h+1)}{4}$$

Local interference and unidentified noise remained moderate during most of the month and only on 3 days lightning activity was detected.

Due to a technical problem the beacon power was reduced from 12 till 17 October. This is clearly seen in the plot of "all" reflections which are counted automatically, but hardly affected the manually counted overdense and longer reflections.

Although the Draconids and Orionids often produce a nice show, this time they were hardly eye-casting. The most striking activity increase happened on October 16th (solar longitude 203.1°) with a clear increase of reflections longer than 10 seconds.

This month 15 reflections longer than 1 minute were observed here. A selection of these, together with some other interesting reflections are included (*Figures 5, 6, 7, 8, 9, 10, 11 and 12*).

If you are interested in the actual figures, or in plots showing the observations as related to the solar longitude (J2000) rather than to the calendar date. I can send you the underlying Excel files and/or plots, please send me an e-mail.

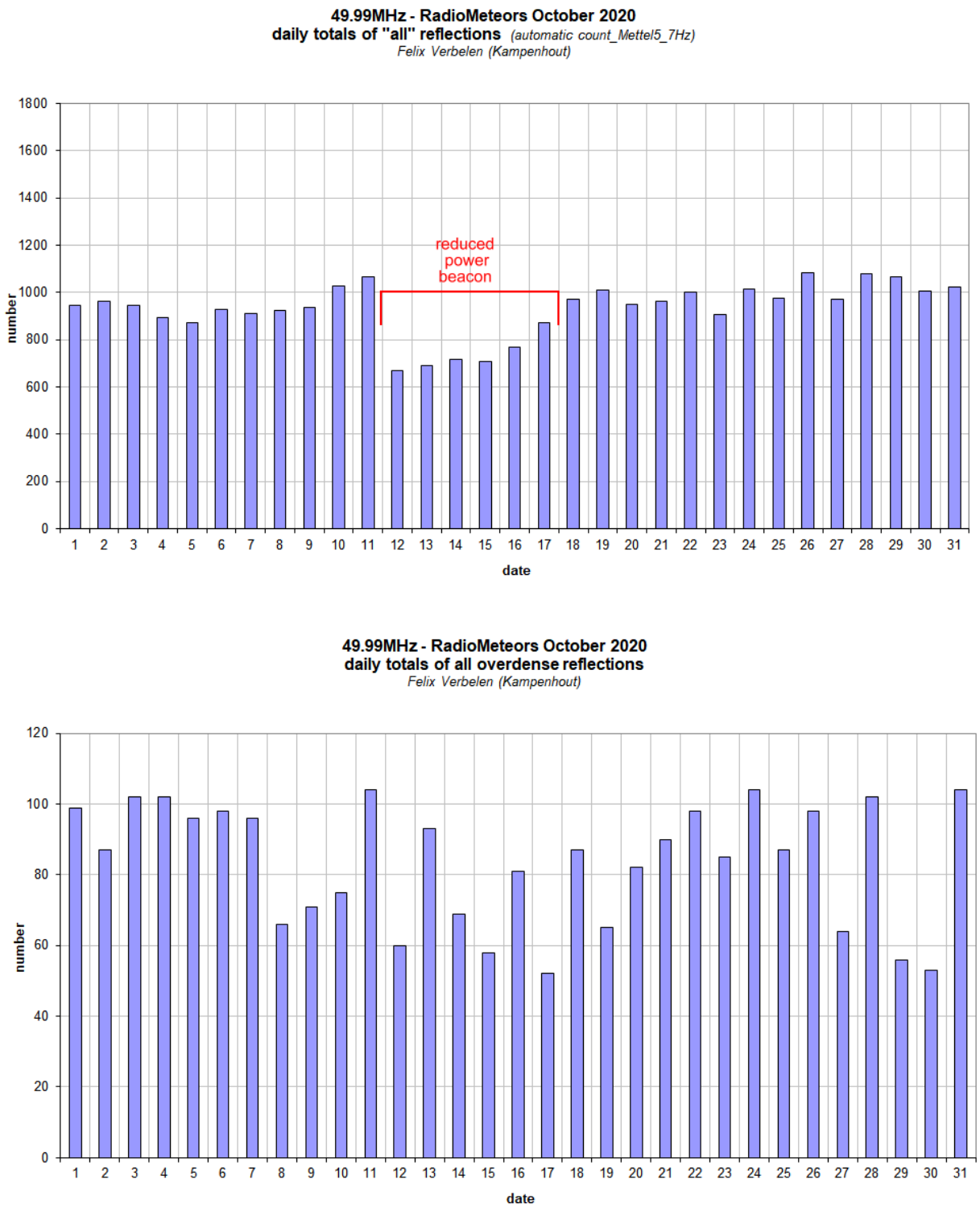

Figure 1 – The daily totals of "all" reflections counted automatically, and of manually counted "overdense" reflections, as observed here at Kampenhout (BE) on the frequency of our VVS-beacon (49.99 MHz) during October 2020.

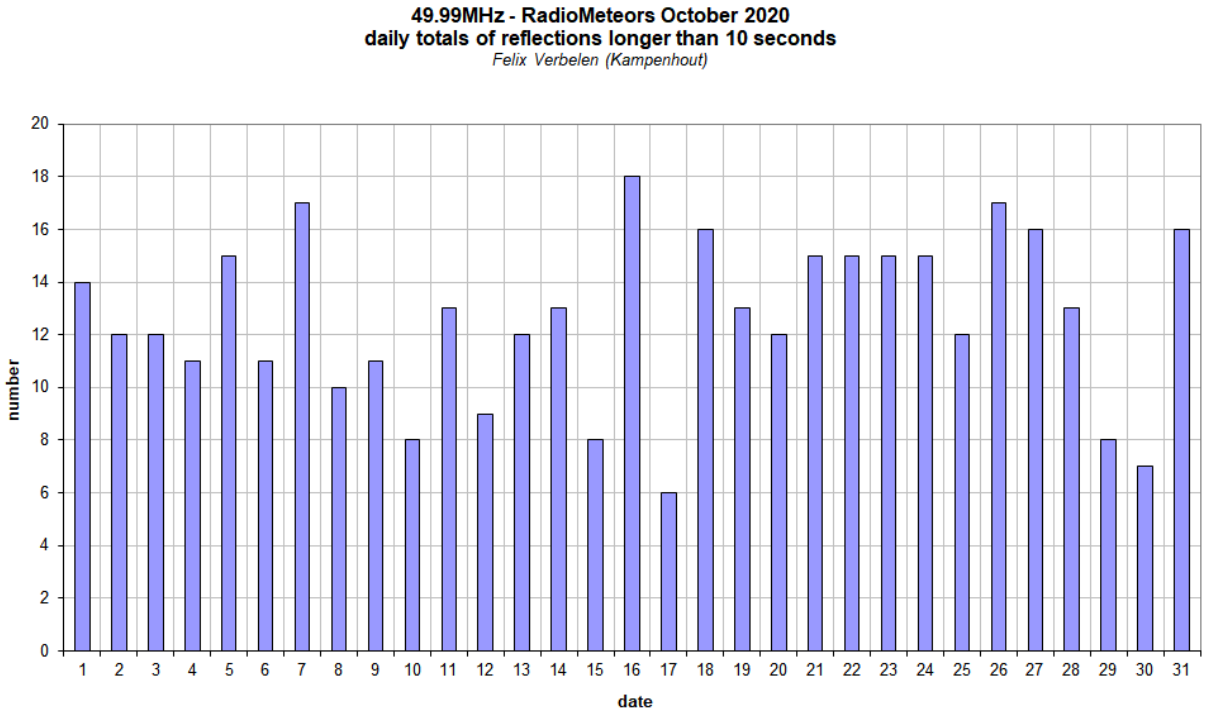

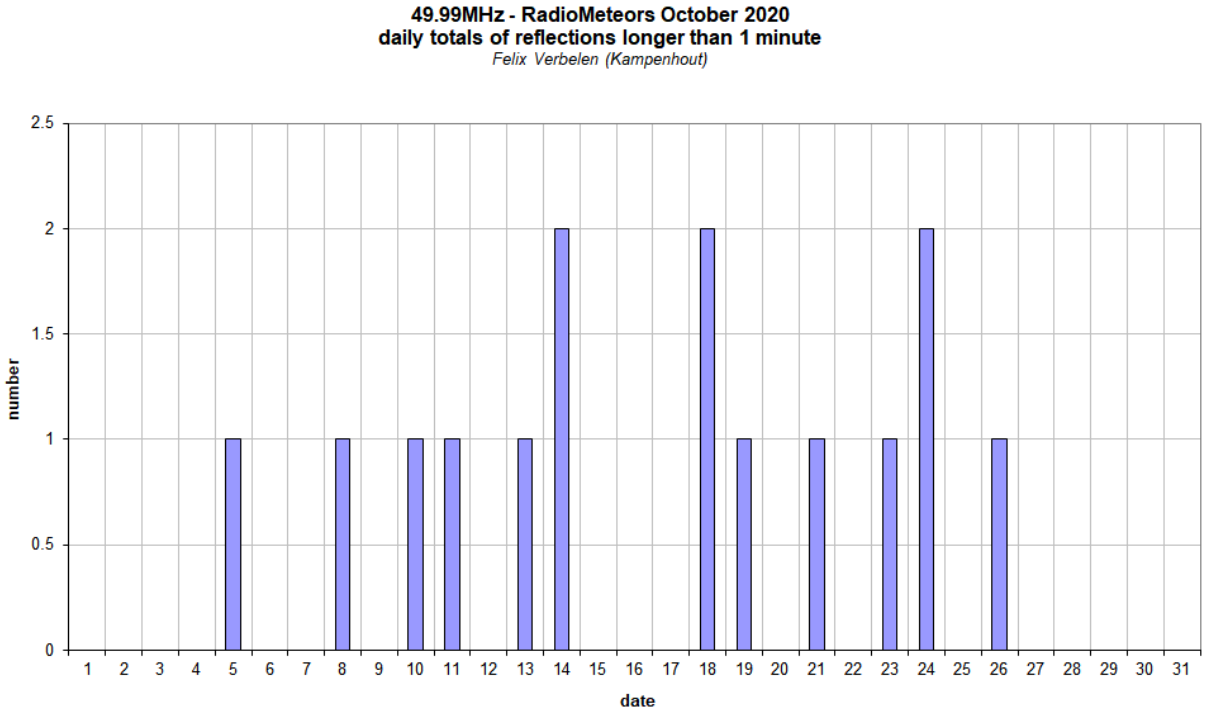

Figure 2 – The daily totals of overdense reflections longer than 10 seconds and longer than 1 minute, as observed here at Kampenhout (BE) on the frequency of our VVS-beacon (49.99 MHz) during October 2020.

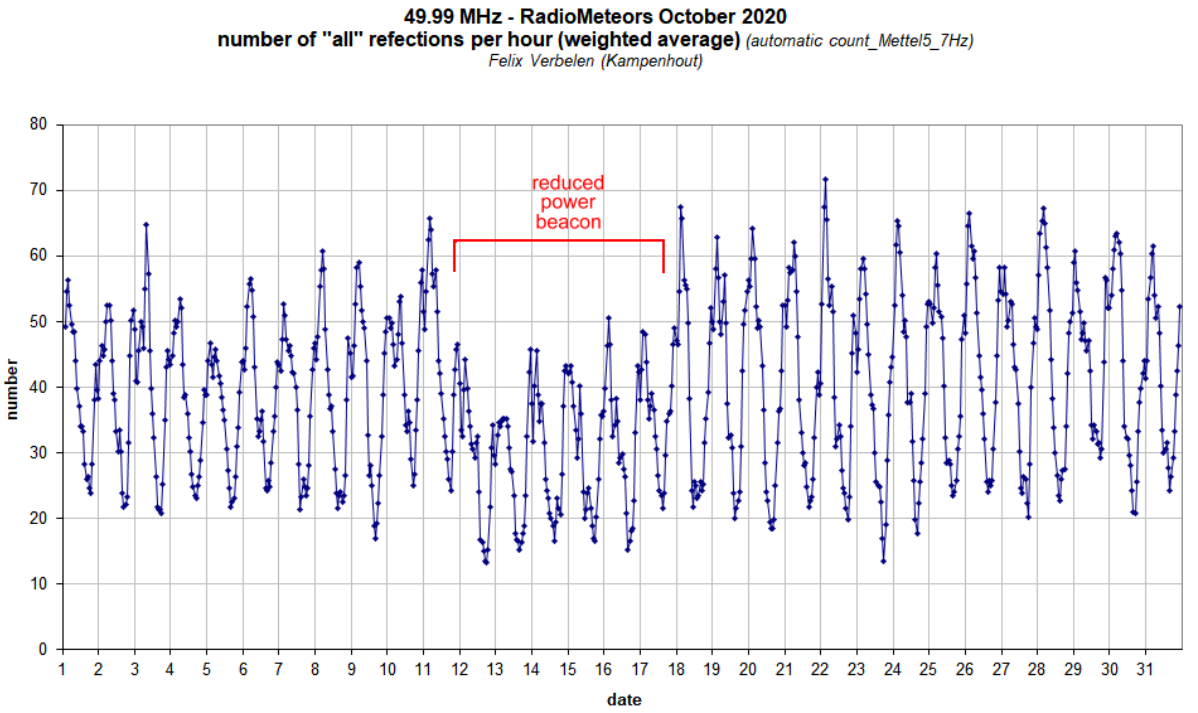

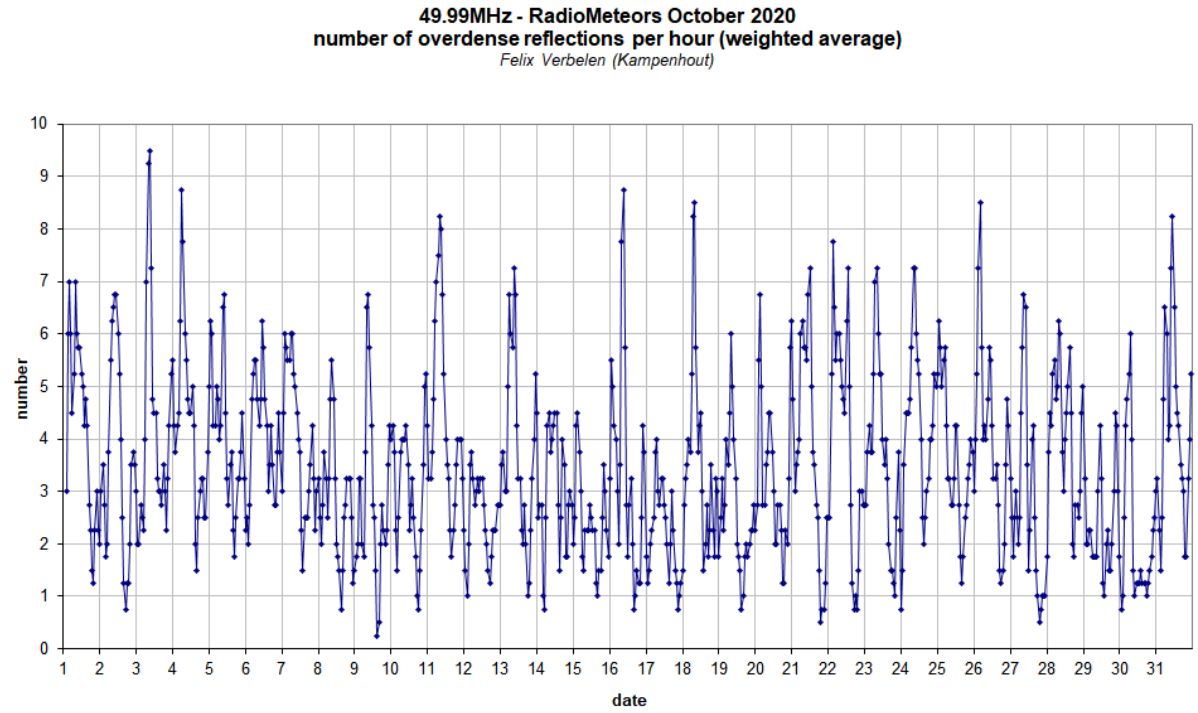

Figure 3 – The hourly numbers of "all" reflections counted automatically, and of manually counted "overdense" reflections, as observed here at Kampenhout (BE) on the frequency of our VVS-beacon (49.99 MHz) during October 2020.

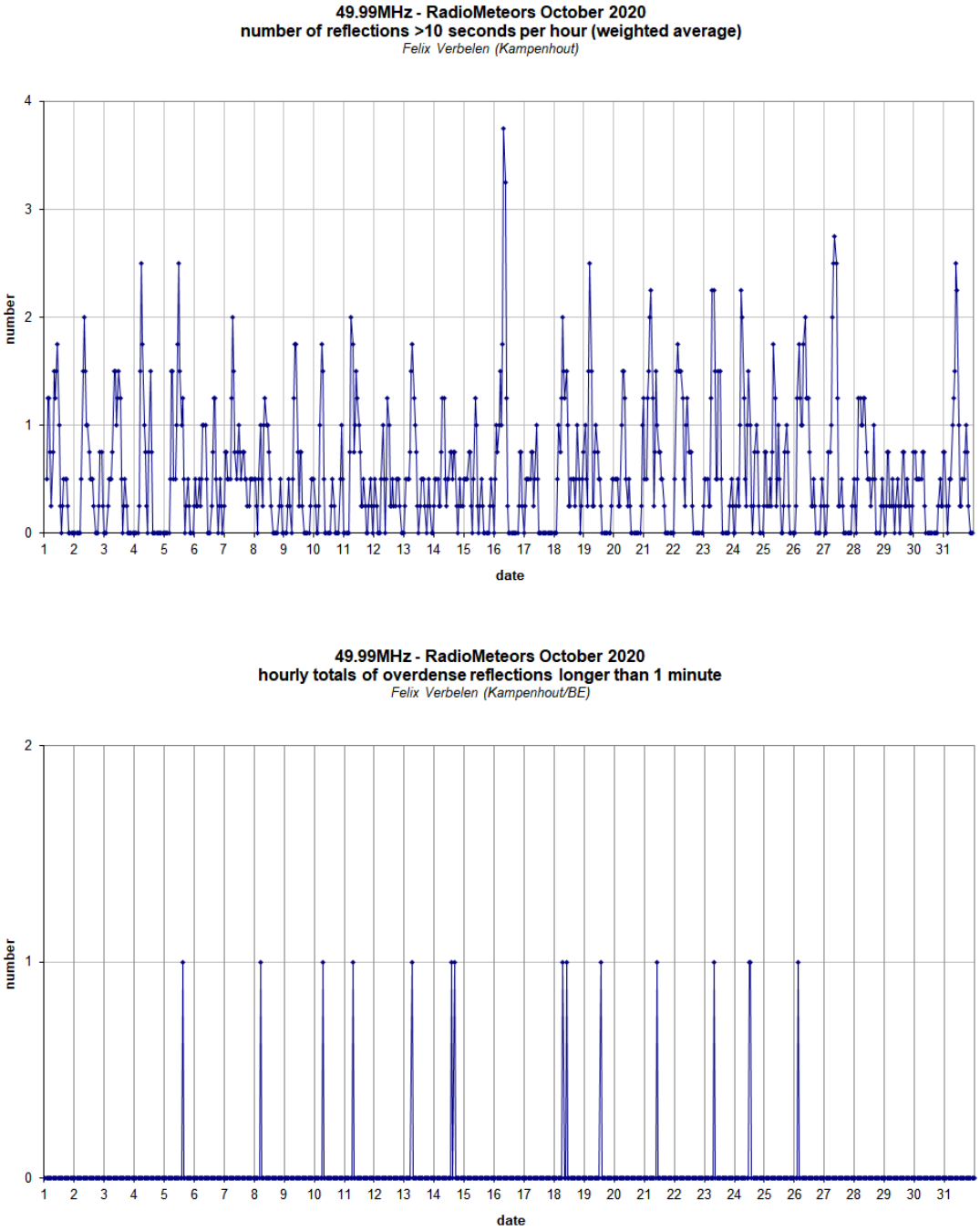

Figure 4 – The hourly numbers of overdense reflections longer than 10 seconds and longer than 1 minute, as observed here at Kampenhout (BE) on the frequency of our VVS-beacon (49.99 MHz) during October 2020.

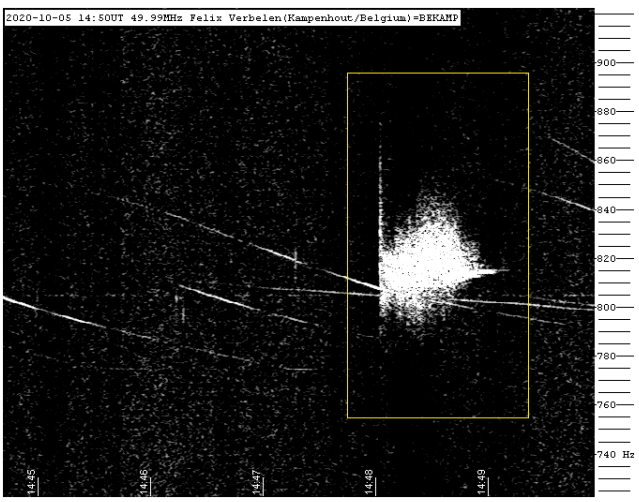

Figure 5 – 2020 October 05 at 14^h50^m UT.

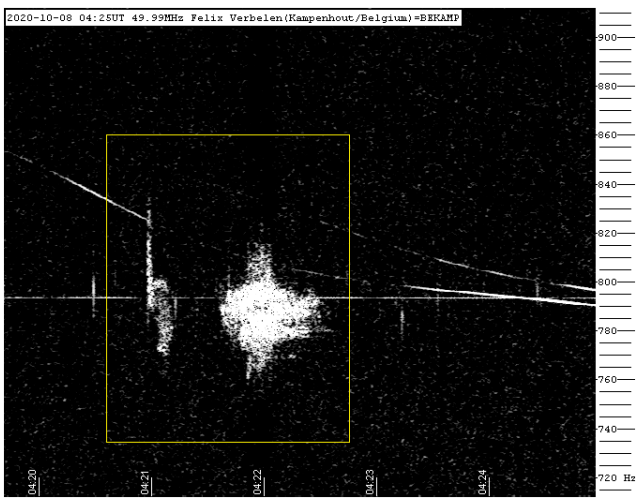

Figure 6 – 2020 October 08, 04^h25^m UT.

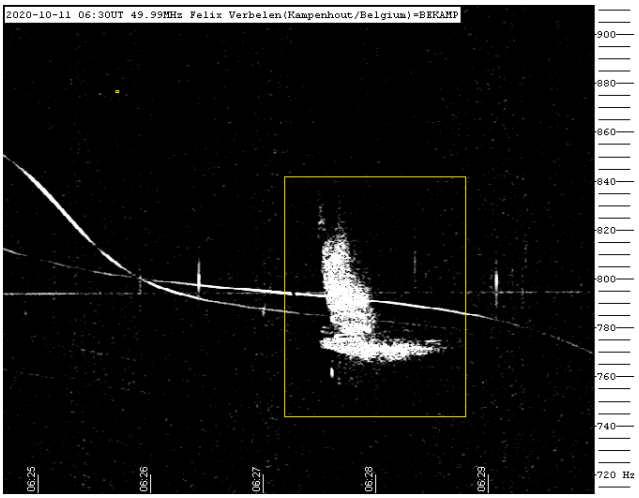

Figure 7 – 2020 October 11, 06^{h}30^{m} UT.

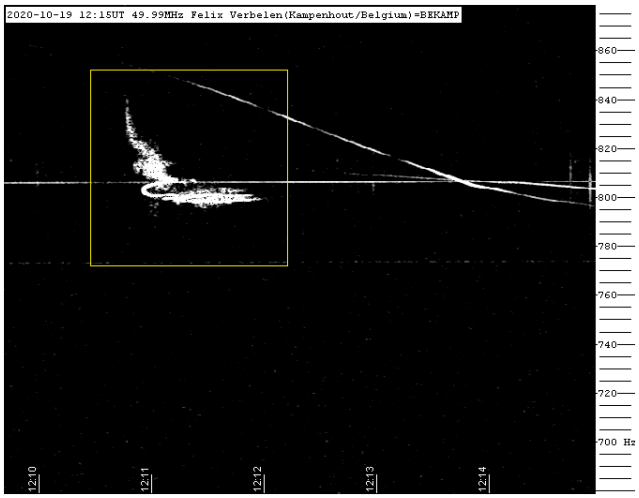

Figure 10 – 2020 October 19, 12^{h}15^{m} UT.

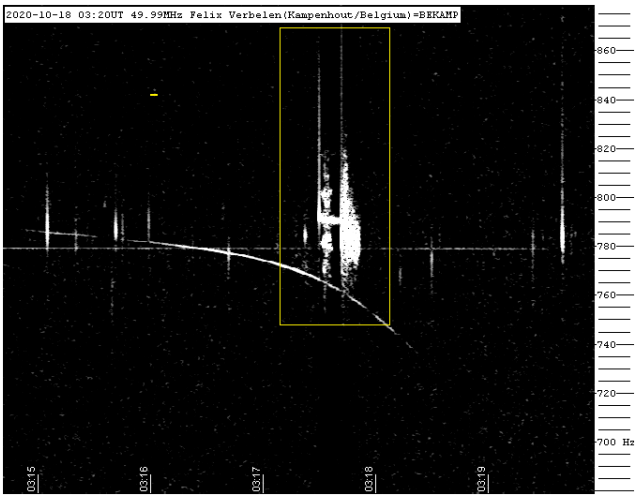

Figure 8 – 2020 October 18, 03^{h}20^{m} UT.

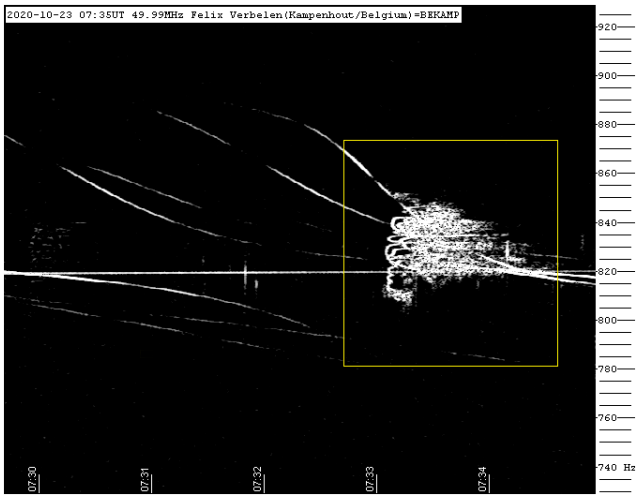

Figure 11 – 2020 October 23, 07^{h}35^{m} UT.

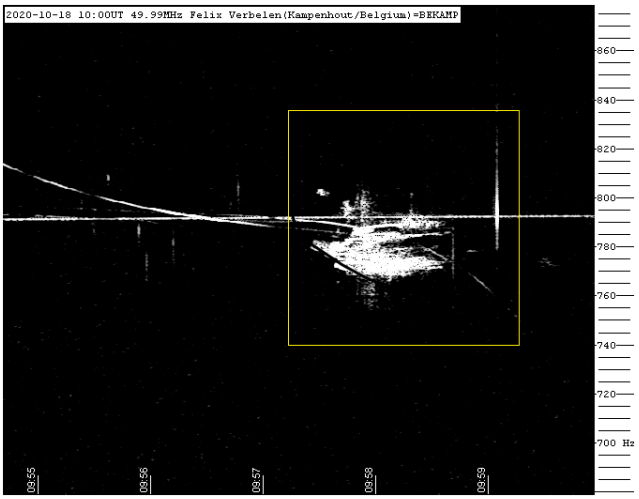

Figure 9 – 2020 October 18, 10^{h}00^{m} UT.

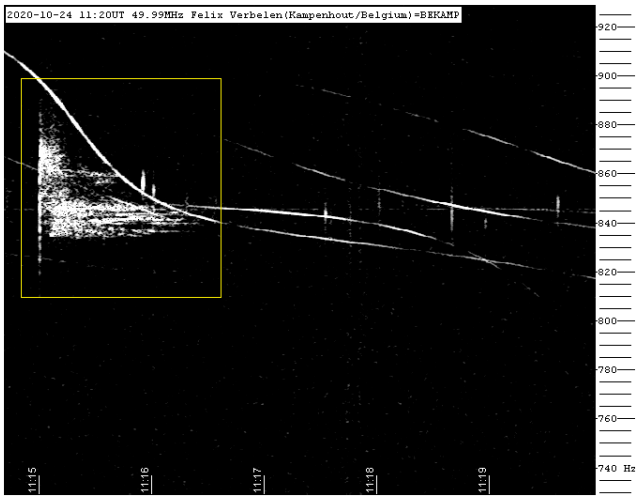

Figure 12 – 2020 October 24, 11^{h}20^{m} UT.

Radio meteors November 2020

Felix Verbelen

Vereniging voor Sterrenkunde & Volkssterrenwacht MIRA, Grimbergen, Belgium
felix.verbelen@skynet.be

An overview of the radio observations during November 2020 is given.

1 Introduction

The graphs show both the daily totals (*Figure 1 and 2*) and the hourly numbers (*Figure 3 and 4*) of "all" reflections counted automatically, and of manually counted "overdense" reflections, overdense reflections longer than 10 seconds and longer than 1 minute, as observed here at Kampenhout (BE) on the frequency of our VVS-beacon (49.99 MHz) during the month of November 2020.

The hourly numbers, for echoes shorter than 1 minute, are weighted averages derived from:

$$N(h) = \frac{n(h-1)}{4} + \frac{n(h)}{2} + \frac{n(h+1)}{4}$$

Local interference and unidentified noise remained moderate during most of the month and no lightning activity was detected.

The meteor activity was surprisingly strong this month, especially on November 4th (solar longitude 220°) and from November 15th till the 21st (solar longitude 233° till 240°), these periods being clearly linked to the Taurid complex and the Leonids. It is interesting to notice that the strongly increased activity is only evident for long overdense reflections and hardly seen in the underdense figures.

This month 34 reflections longer than 1 minute were observed here. A selection of these, together with some other interesting reflections are included (*Figures 5, 6, 7, 8, 9, 10, 11, 12, 13, 14, 15, 16, 17, 18, 19, 20 and 21*).

If you are interested in the actual figures, or in plots showing the observations as related to the solar longitude (J2000) rather than to the calendar date. I can send you the underlying Excel files and/or plots, please send me an e-mail.

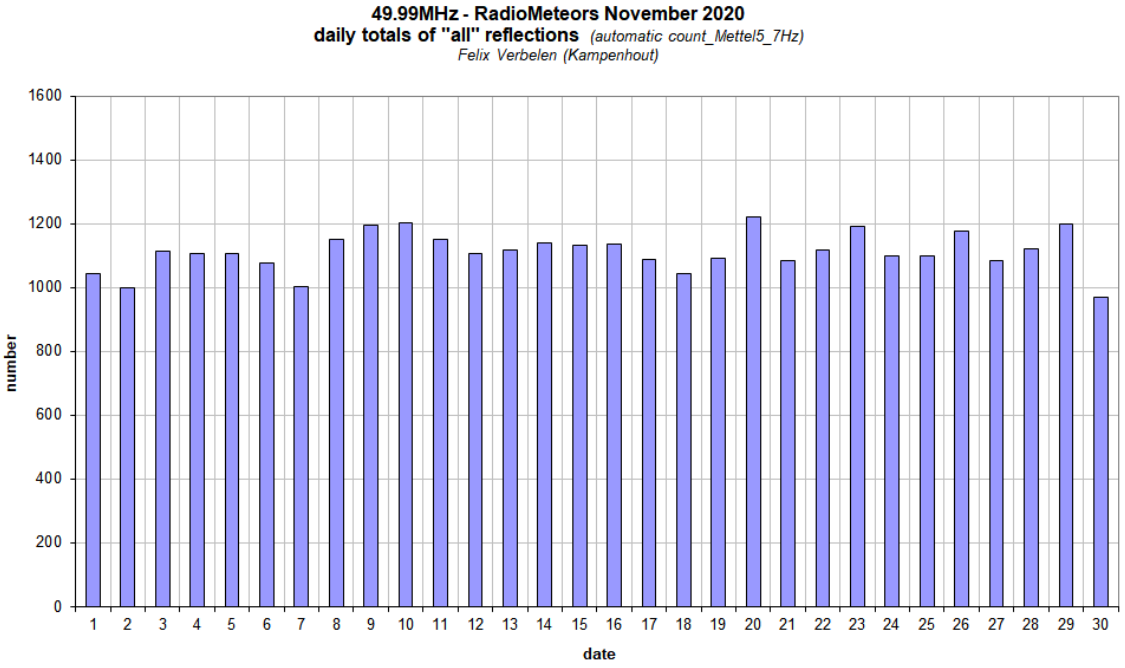

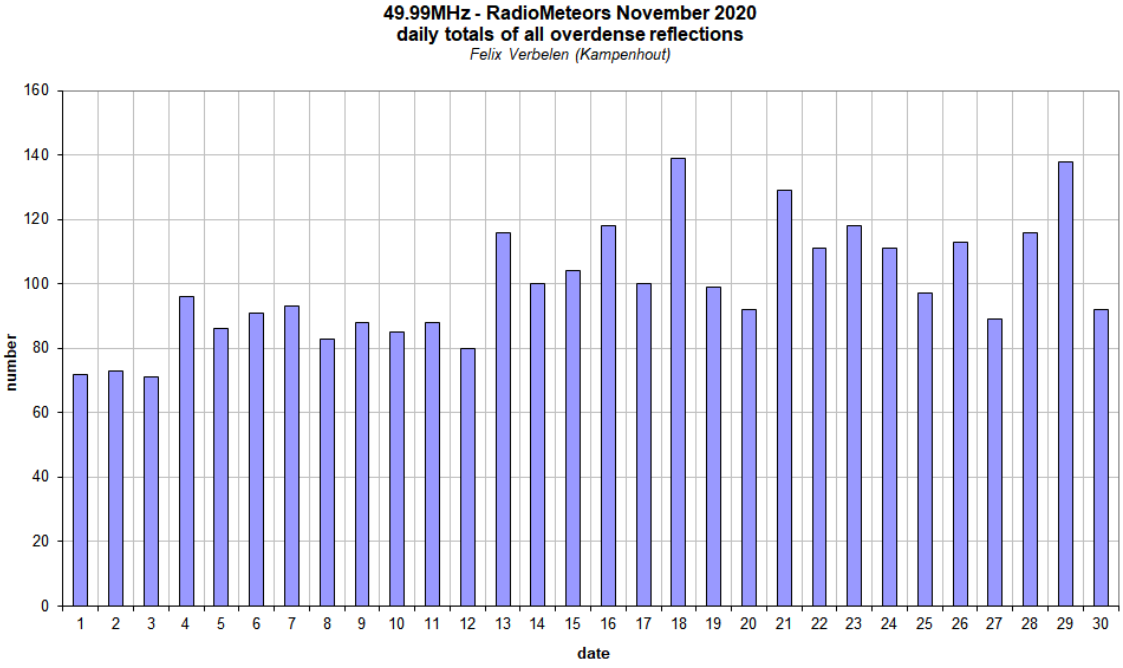

Figure 1 – The daily totals of "all" reflections counted automatically, and of manually counted "overdense" reflections, as observed here at Kampenhout (BE) on the frequency of our VVS-beacon (49.99 MHz) during November 2020.

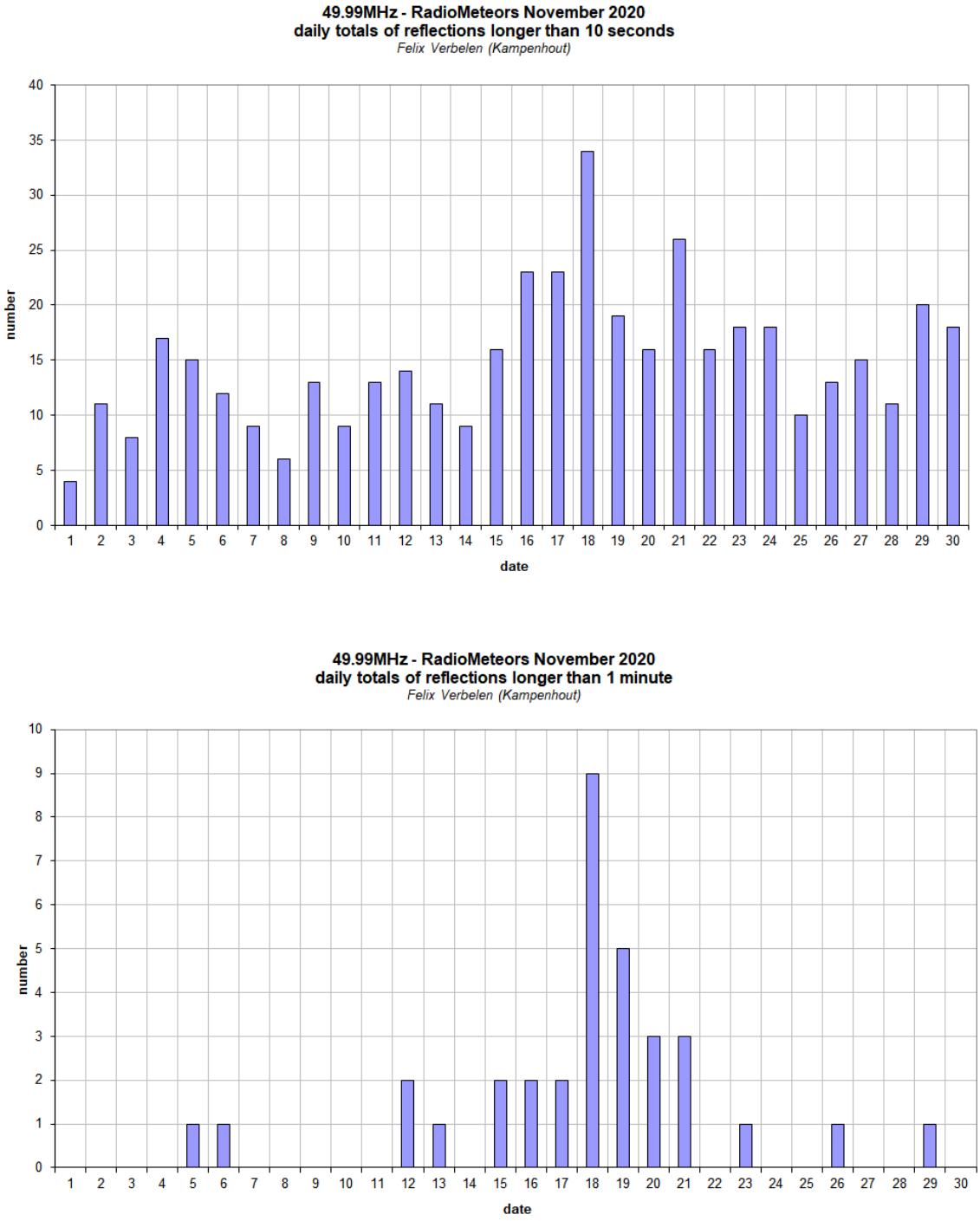

Figure 2 – The daily totals of overdense reflections longer than 10 seconds and longer than 1 minute, as observed here at Kampenhout (BE) on the frequency of our VVS-beacon (49.99 MHz) during November 2020.

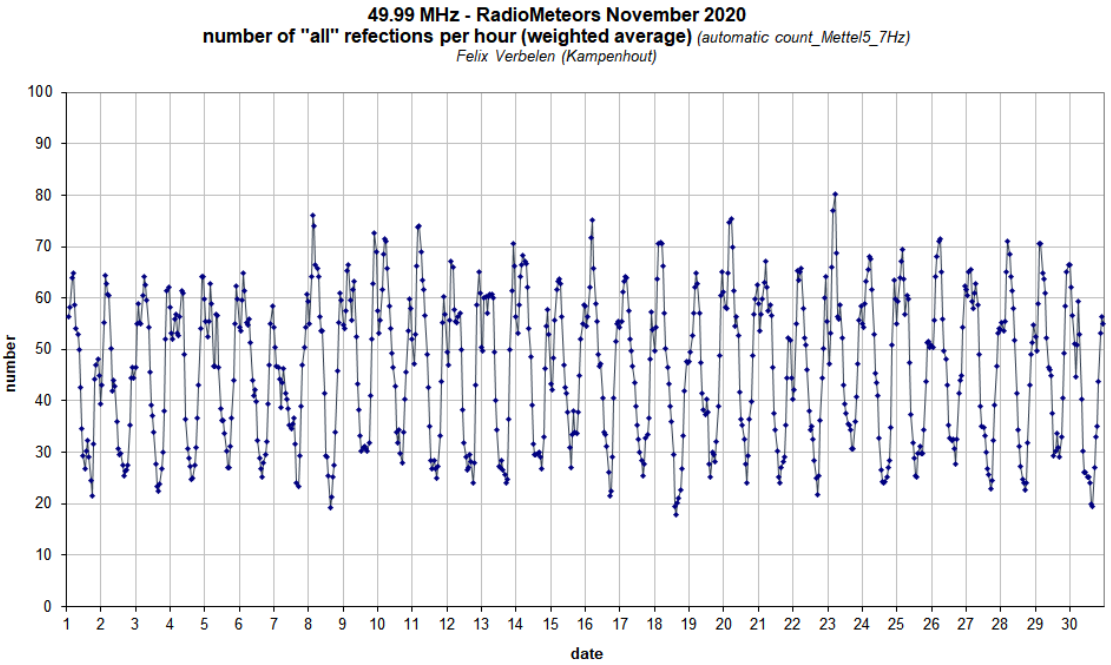

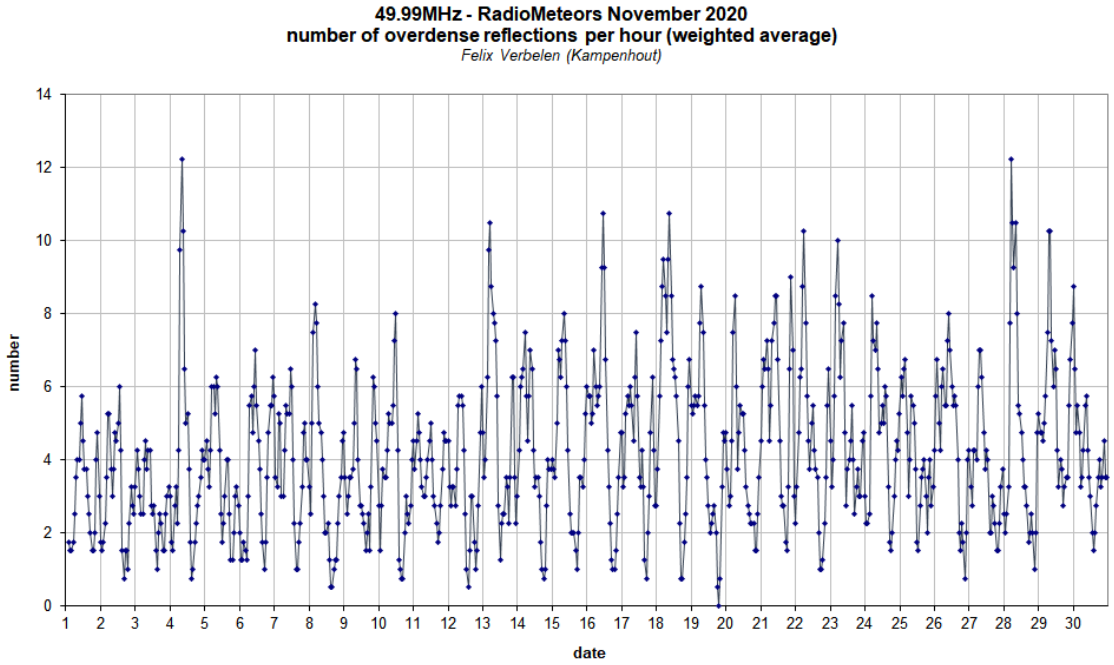

Figure 3 – The hourly numbers of "all" reflections counted automatically, and of manually counted "overdense" reflections, as observed here at Kampenhout (BE) on the frequency of our VVS-beacon (49.99 MHz) during November 2020.

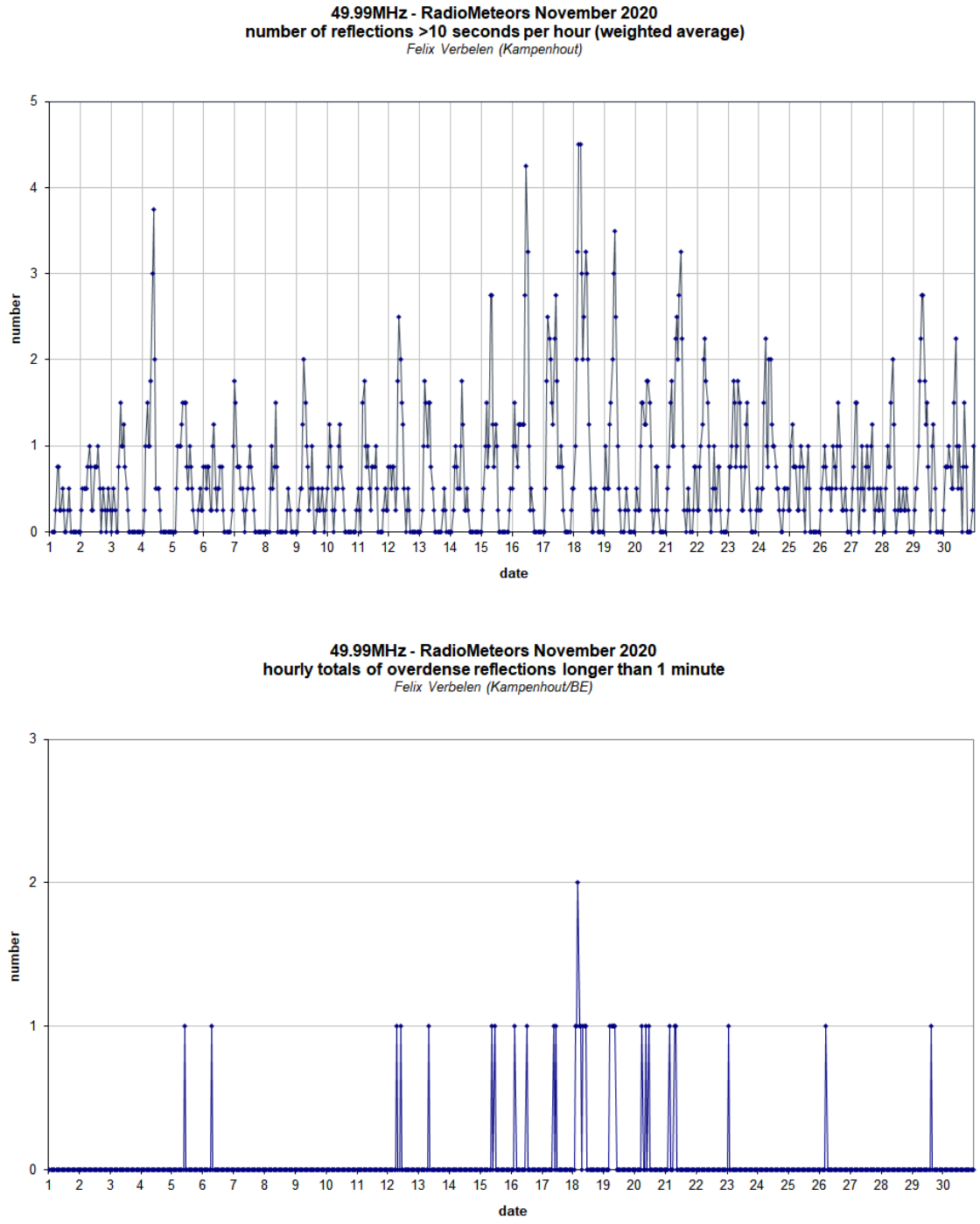

Figure 4 – The hourly numbers of overdense reflections longer than 10 seconds and longer than 1 minute, as observed here at Kampenhout (BE) on the frequency of our VVS-beacon (49.99 MHz) during November 2020.

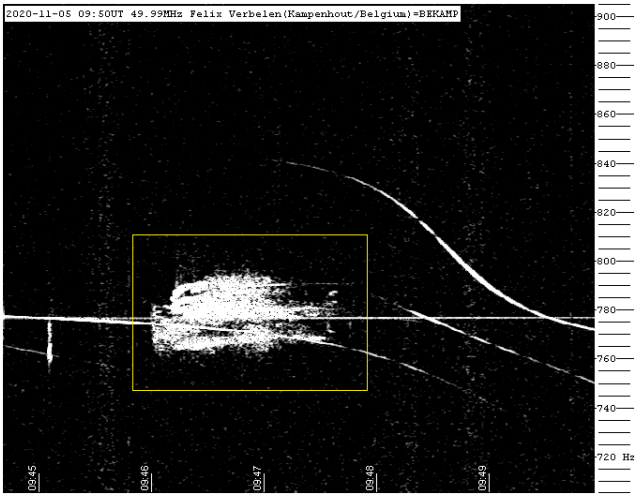

Figure 5 – 2020 November 05, 09^{h}50^{m} UT.

Figure 6 – 2020 November 12, 06^{h}35^{m} UT.

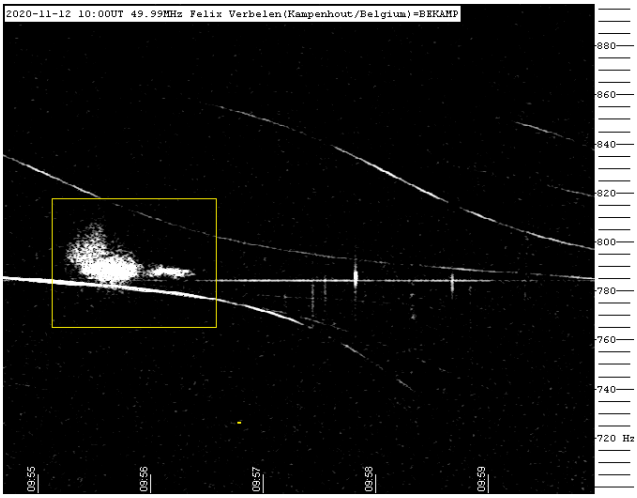

Figure 7 – 2020 November 12, 10^{h}00^{m} UT.

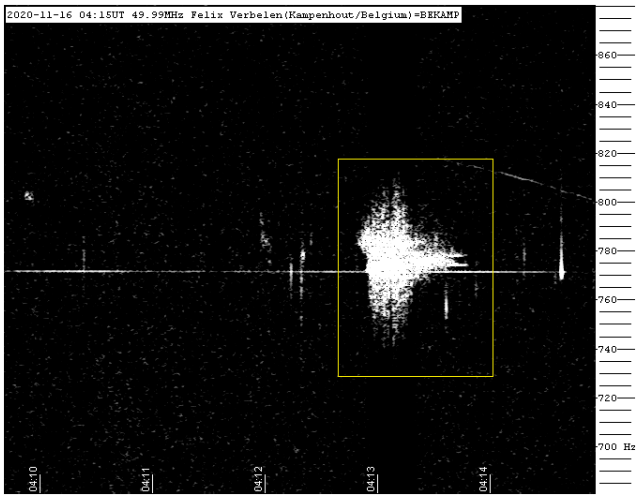

Figure 8 – 2020 November 16, 04^{h}15^{m} UT.

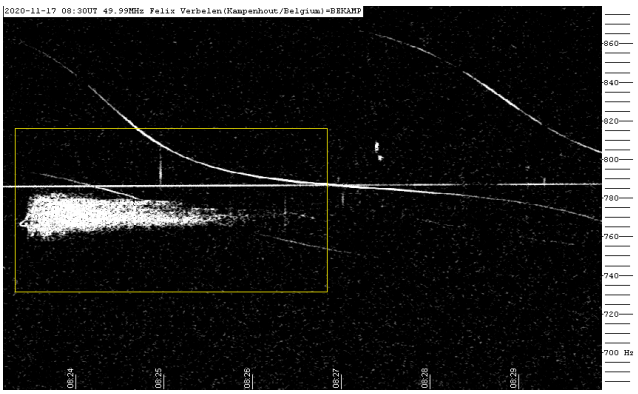

Figure 9 – 2020 November 17, 08^{h}30^{m} UT.

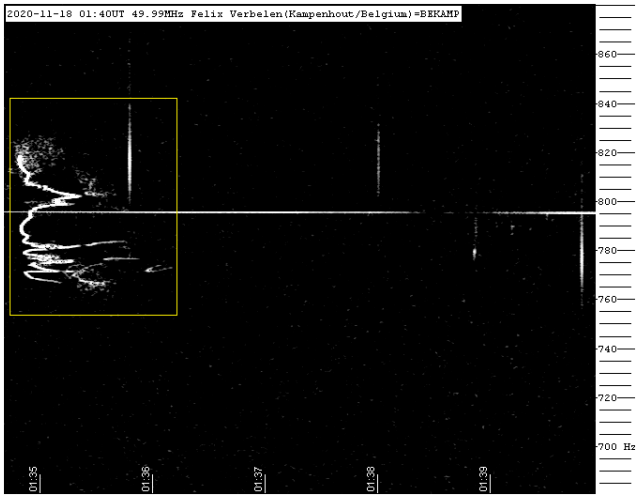

Figure 10 – 2020 November 18, 01^{h}40^{m} UT.

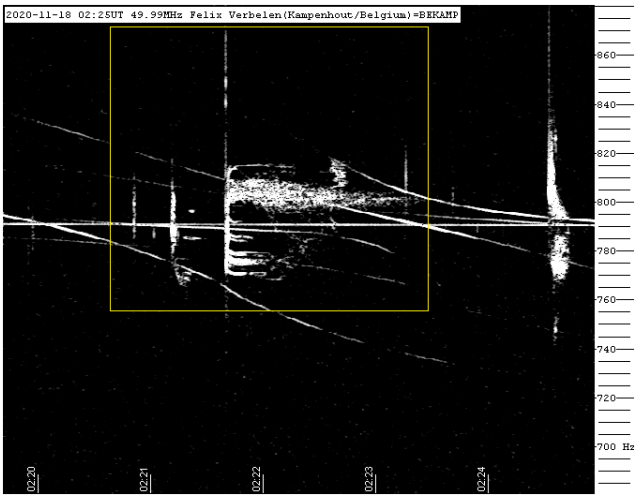

Figure 11 – 2020 November 18, 02^{h}25^{m} UT.

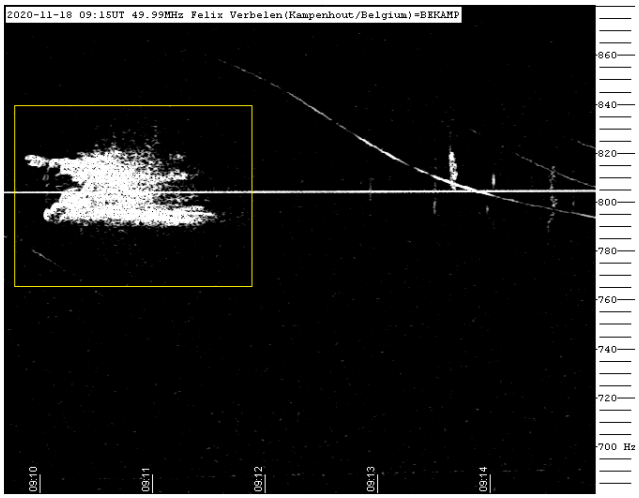

Figure 14 – 2020 November 18, 09^{h}15^{m} UT.

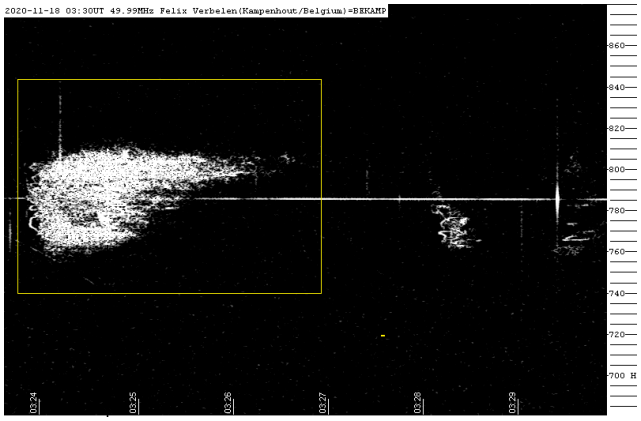

Figure 12 – 2020 November 18, 03^{h}30^{m} UT.

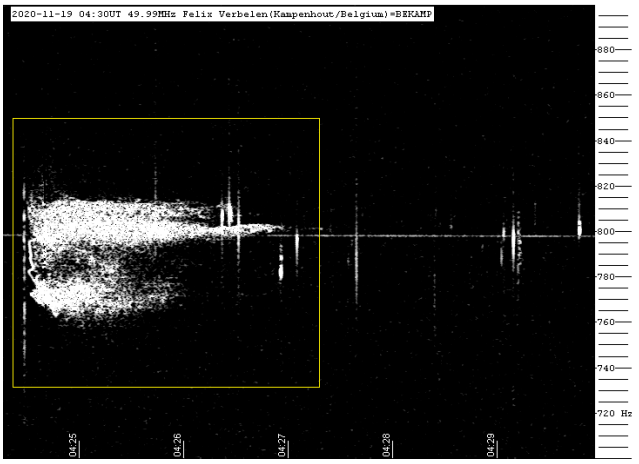

Figure 15 – 2020 November 19, 04^{h}30^{m} UT.

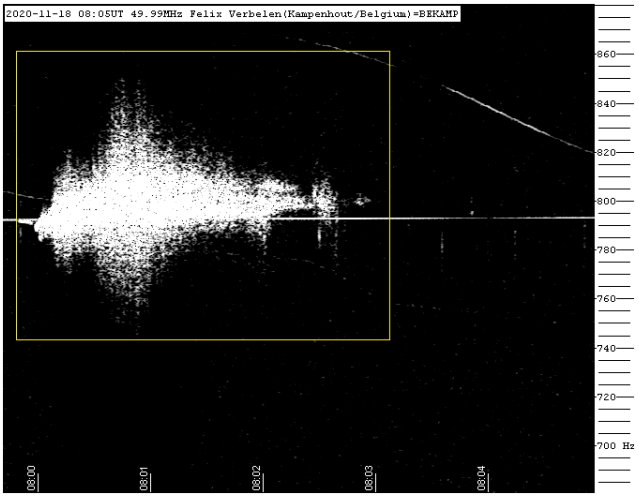

Figure 13 – 2020 November 18, 08^{h}05^{m} UT.

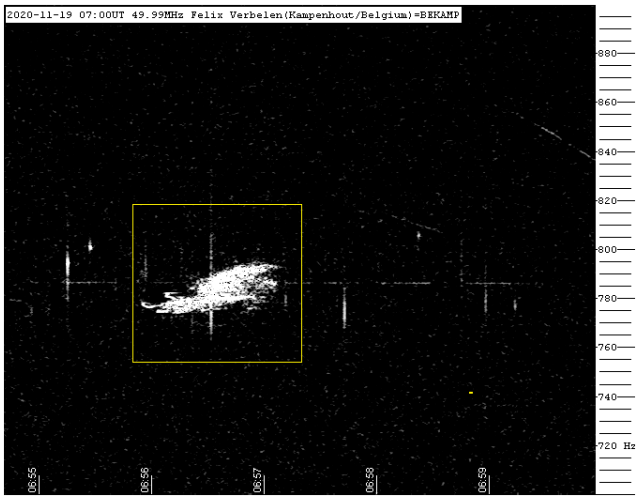

Figure 16 – 2020 November 19, 07^{h}00^{m} UT.

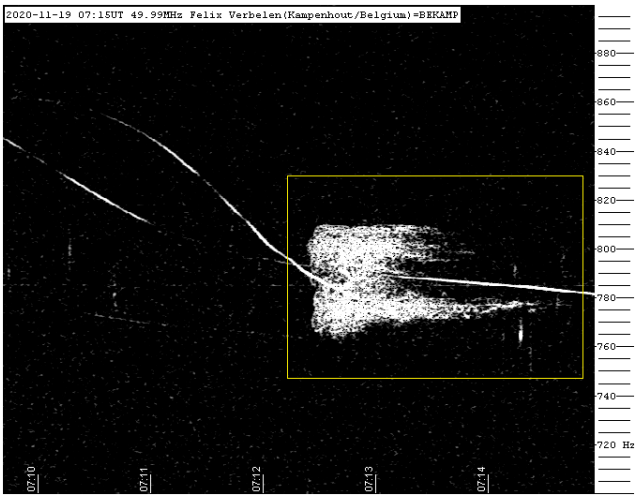

Figure 17 – 2020 November 19, 07^{h}15^{m} UT.

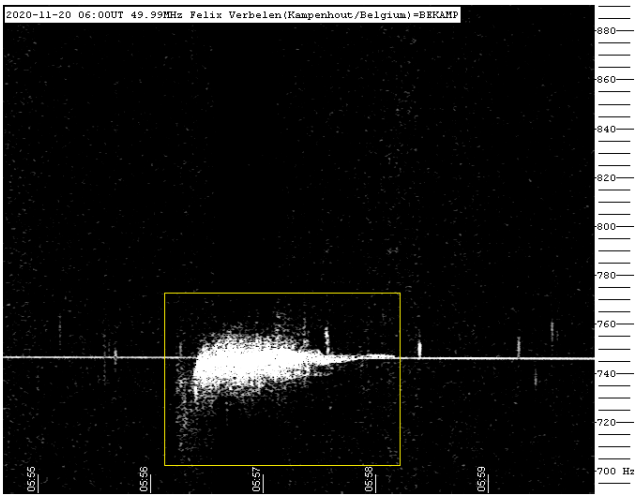

Figure 18 – 2020 November 20, 06^{h}00^{m} UT.

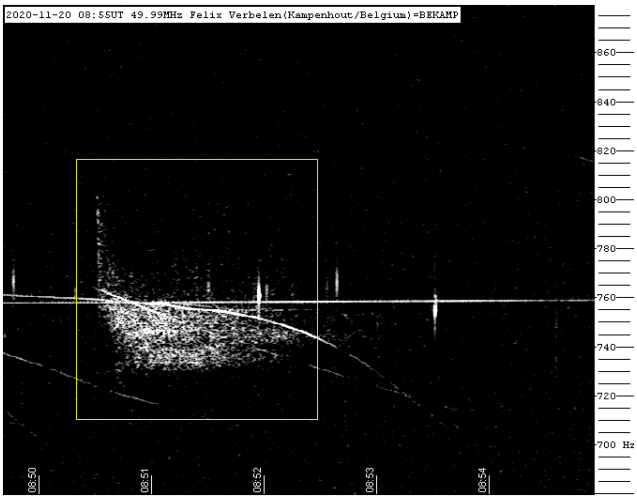

Figure 19 – 2020 November 20, 08^{h}55^{m} UT.

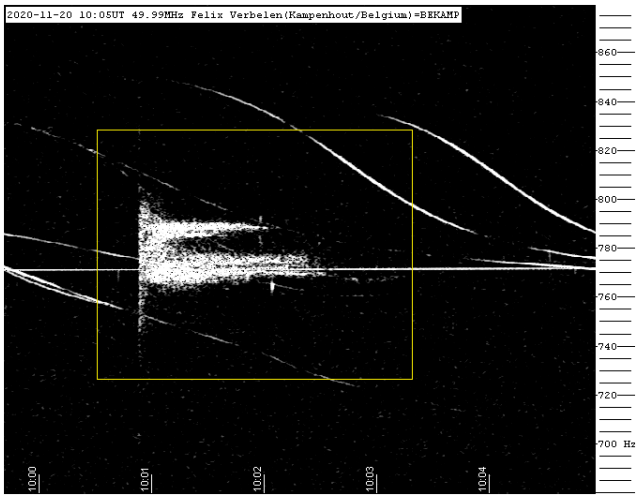

Figure 20 – 2020 November 20, 10^{h}05^{m} UT.

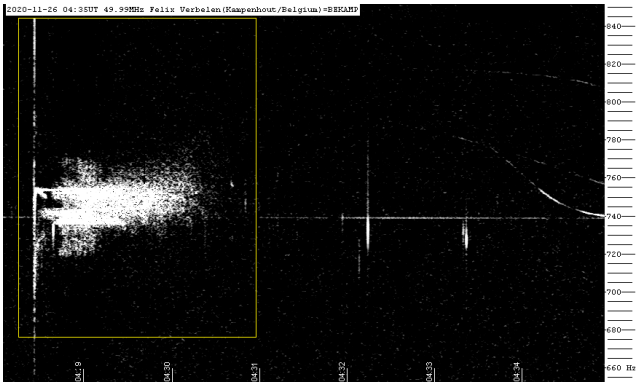

Figure 21 – 2020 November 26, 04^{h}35^{m} UT.

Earth grazing meteoroid recorded by GMN above the Czech Republic and Germany

Milan Kalina

Global Meteor Network, Czech Republic
milank2010@gmail.com

An Earth grazing meteoroid has been recorded by cameras of the Global Meteor Network on 2020 September 15, 19^h37^m UT. The trajectory and the orbit could be determined, the meteoroid had an orbit type of an undiscovered long periodic comet but no meteor shower association could be proven.

1 Introduction

On 2020 September 15th, at 19^h37^m UTC, Central European GMN cameras in Czech Republic, Germany (see *Figure 1*) and Poland registered an Earth grazer. The automatic procedure reduced only the camera data for the RMS systems CZ0002 and PL0001. A manual analysis was required to include the German camera data. Grazing meteor trajectories have peculiar geometrics which cannot be handled by the automated procedures.

Typically for an Earth grazing meteor the path length is exceptionally long and the ending point can be considerably higher than the point of closest approach relative to the surface of the Earth due to the curvature of the Earth. Such unusual meteor geometrics require a careful manual approach. Earth grazers are rather rare events, but recorded every now and then by all major camera networks.

2 Results

It was not a very bright, but a long duration event caused by a meteoroid, which entered the atmosphere at a height of 122 km with a very low entry angle above northern Czech Republic, and it left the atmosphere at the height of 121 km over southern Germany, close to the Swiss border (*Figure 2*).

During its duration of 7.6 s, the object travelled more than 520 km, thanks to a very high initial speed of about 68 km/s. The point of closest approach with the lowest height relative to the Earth surface did not get below 116 km. Photometry on the visible trajectory has been calculated along the whole path. A small portion with inconsistent data (CZ0002) obtained at a low elevation angle, affected by tropospheric scatter and distant clouds was removed.

An apparent correlation between the peak height and peak magnitude has been obtained (*Figure 3*).

Figure 1 – The Earth grazer at 2020 September 15, at $19^h37^m19^s$ UT registered by RMS camera DE0008 in Germany.

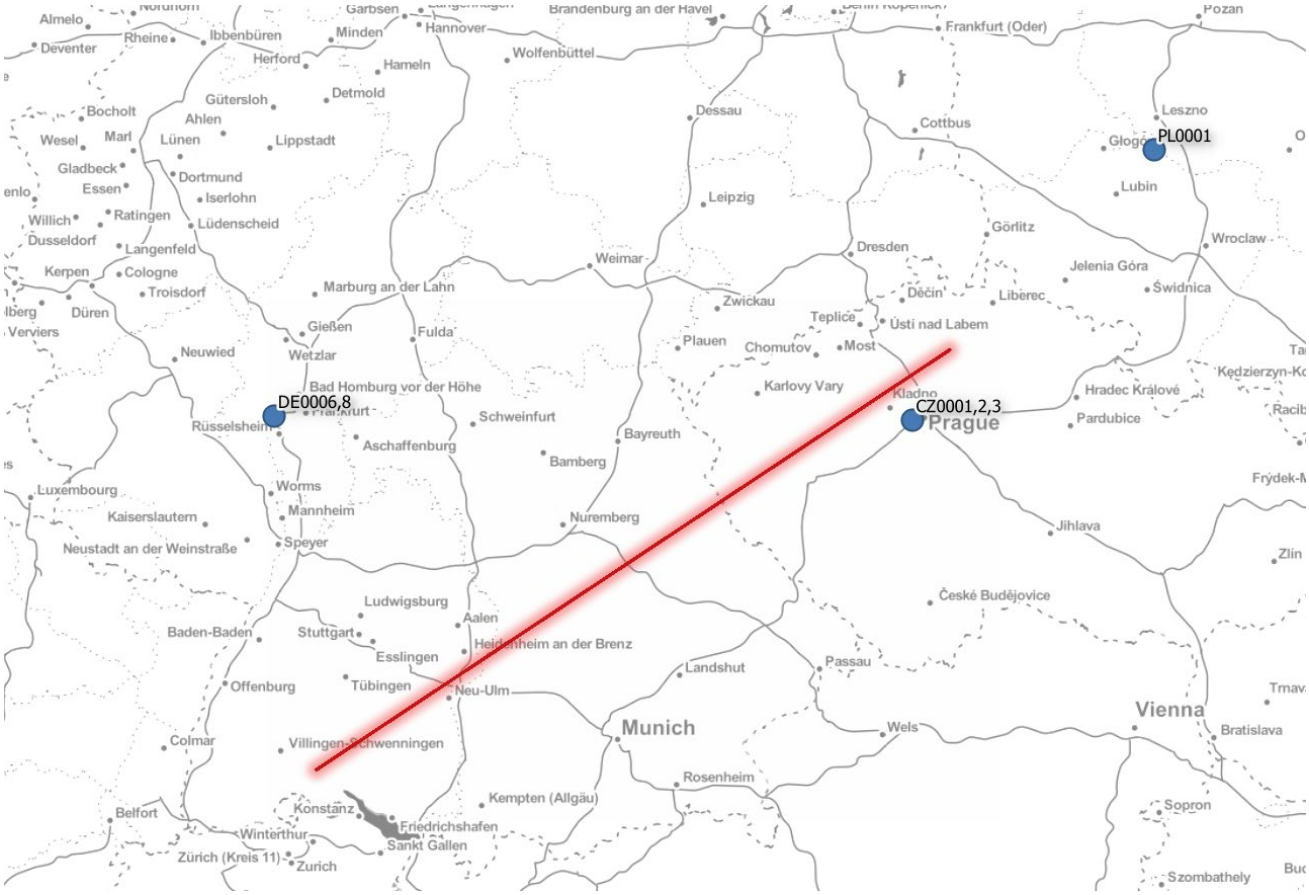

Figure 2 – The positions of the three GMN camera stations and the ground plot of the trajectory of the Earth grazer.

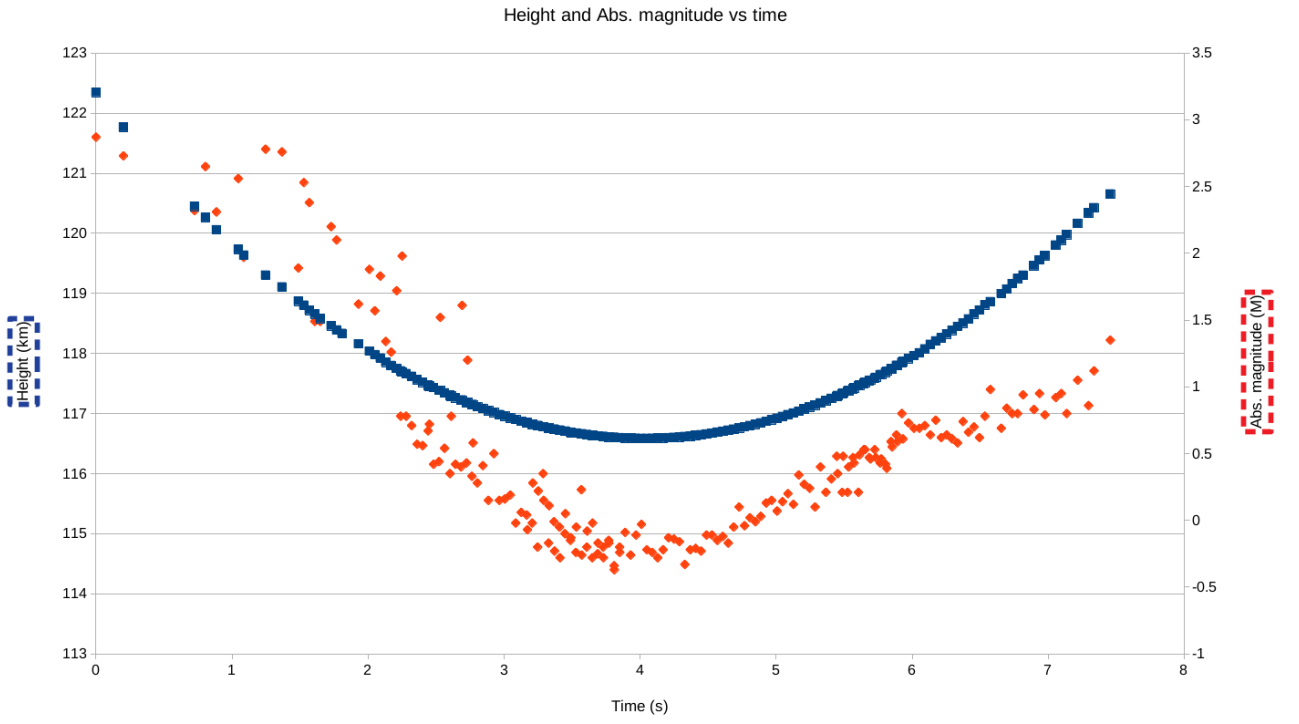

Figure 3 – The height (km) and photometry (absolute magnitude) of the grazing meteor versus time. The curved trajectory reflects the curvature of the Earth.

The GMN trajectory calculation based on data from 4 cameras, which covered the entire trajectory also revealed the origin, most probably a long periodic comet fragment from a yet undiscovered parent body (*Figure 6*).

The following radiant position (*Figure 4*), velocity and orbit has been obtained for this meteor:

- $\lambda_{\odot} = 173.130915°$
- $\alpha_g = 58.06 \pm 0.02°$
- $\delta_g = +20.62 \pm 0.01°$
- $v_g = 67.55 \pm 0.02$ km/s
- $v_{\infty} = 68.45 \pm 0.02$ km/s
- $a = \infty$ AU (hyperbolic)
- $q = 0.60469 \pm 0.0006$ AU
- $e = 1.0073 \pm 0.0008$
- $i = 179.15 \pm 0.03°$
- $\omega = 257.97 \pm 0.08°$
- $\Omega = 172.976 \pm 0.004°$
- $\Pi = 70.95 \pm 0.00°$

The velocity uncertainty is underestimated, probably as much as one order of magnitude. The uncertainty margin for the eccentricity makes the meteor's orbit hyperbolic, which is most certainly not the case.

A check in the IAU MDC working list of meteor showers resulted in no matching known shower, hence this event should be classified as a sporadic meteor. A visual check of the meteor shower list resulted in a poorly documented possible meteor shower listed as the 14 Aurigids (FAR#608)[26]. Although the D criteria reject any likely association, this shower has a retrograde orbit with a similar perihelion distance, high eccentricity and comparable velocity, but recorded 21 days later from a radiant roughly 20° east in Right Ascension and 10° north in declination.

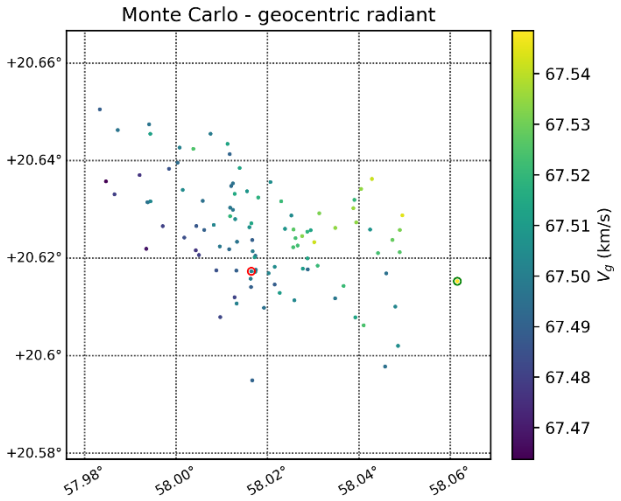

Figure 4 – The Monte Carlo geocentric velocity versus the radiant position.

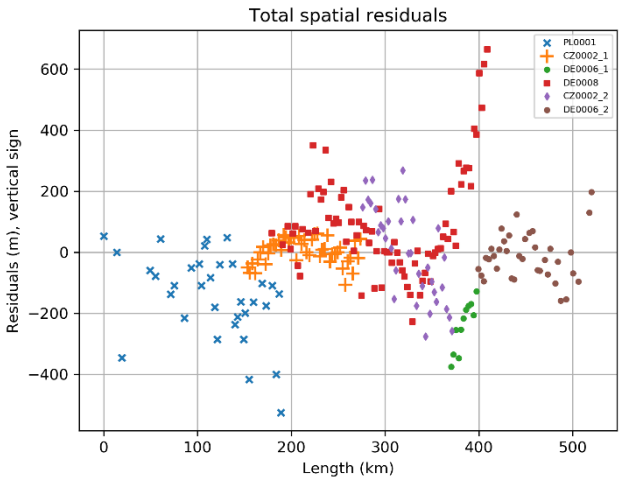

Figure 5 – The plot with the fit residuals for the entire length of the trajectory.

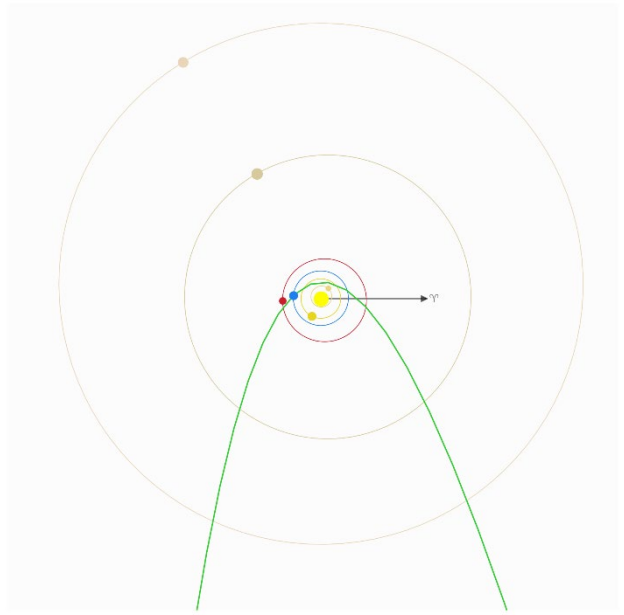

Figure 6 – The orbit plotted relative to the planets.

Acknowledgment

The author thanks the camera operators *Jürgen Dörr* and *Przemek Naganski* and *Denis Vida* for his advices.

The author used the data of the Global Meteor Network[27] which is released under the CC BY 4.0 license[28].

[26] https://www.ta3.sk/IAUC22DB/MDC2007/Roje/pojedynczy_obiekt.php?kodstrumienia=00608

[27] https://globalmeteornetwork.org/data/

[28] https://creativecommons.org/licenses/by/4.0/

Grazing meteor over Belarus and Poland on November 1, 2020

Ivan Sergei[1], Yuri Goryachko[2] and Zbigniew Tymiński[3]

[1] **Mira Str.40-2, 222307, Molodechno Belarus**
seriv76@tut.by

[2] **Derazhnoye, Belarus**
astronominsk@gmail.com

[3] **Otwock, PFN40, Poland**
zbyszek.tyminski@gmail.com

A bright grazing meteor occurred over the territory of Belarus and Poland on 2020 November 1 at $3^h44^m04^s$ UT. The event was recorded by cameras in Belarus and Poland.

1 Introduction

The analysis of the video data has been made by Yuri Goryachko from Minsk for the observational data from Derazhnoye. We could cover different parts of the track but due to a lack of data, having no other registrations for this peculiar meteor, it was not possible the establish a complete picture.

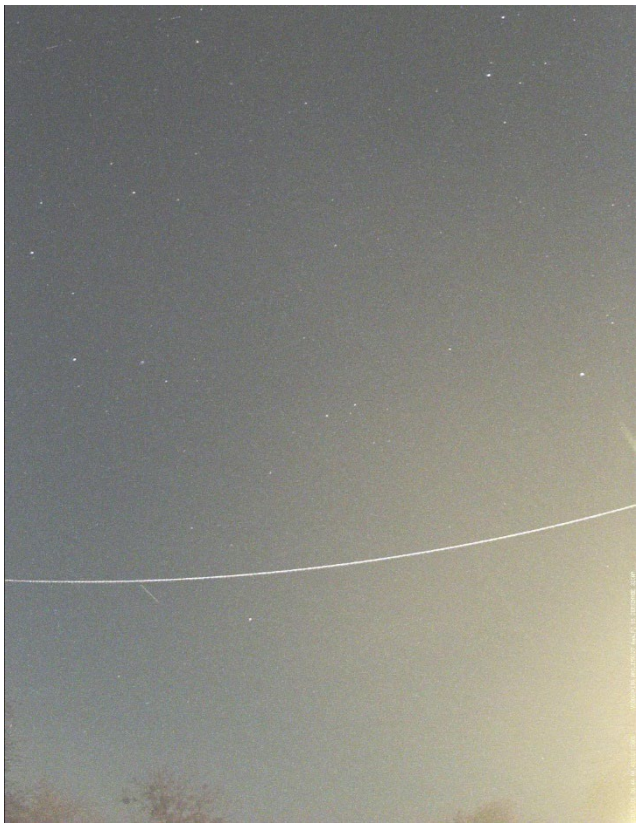

Figure 1 – The path of the grazing meteor registered by the camera of Yuri Goryachko (Belarus).

Also, the beginning and the ending point of the meteor trajectory was outside the field of view of our cameras. For these and some other reasons, the software UFO Orbit[29], for example, could not do calculations for both parts as a whole, but displayed the characteristics for each part separately.

Figure 2 – The trajectory of the grazing meteor recorded by Zbigniew Tymiński, 2020 November 1, $03^h44^m13^s$ (Polish Fireballs Network, Otwock, PFN40, Poland).

2 Some results

The initial survey indicated that the meteor grazer belonged to the Daytime iota Virginids (IVI#251)[30] meteor shower. It is important to note that this is a daytime radiant, which was located about 13 degrees from the Sun. To catch such a meteor is a great rarity and just a huge luck. There is very little data on this meteor shower. The IAU MDC working list of meteor showers list the following data (Sekanina, 1976):

- $\lambda_\odot = 223°$
- $\alpha = 210.4°$
- $\delta = -3.8°$
- $v_g = 29$ km/s
- $a = 1.217$ AU
- $q = 0.985$ AU
- $e = 0.1906$

[29] http://sonotaco.com/soft/UO2/UO21Manual_EN.pdf

[30] https://www.ta3.sk/IAUC22DB/MDC2007/Roje/pojedynczy_obiekt.php?kodstrumienia=00251

- $\omega = 60.7°$
- $\Omega = 224.3°$
- $i = 10.1°$

The brightness varied between +0.3m and –1.0m. According to rough estimates, the duration of the event could be about 15 seconds or even more. The length of the trajectory is about 450–500 km. As for heights and velocities, these were defined more precisely. For each part of the trajectory separately these were:

First part:

- Height from 104 km to 101 km
- $v_o = 30.07$ km/s
- $v_g = 27.63$ km/s
- $v_h = 38.65$ km/s

Second part:

- Height from 101 km to 106 km
- $v_o = 29.46$ km/s
- $v_g = 26.95$ km/s
- $v_h = 38.36$ km/s

With v_o the initial velocity, v_g the geocentric velocity and v_h the heliocentric velocity.

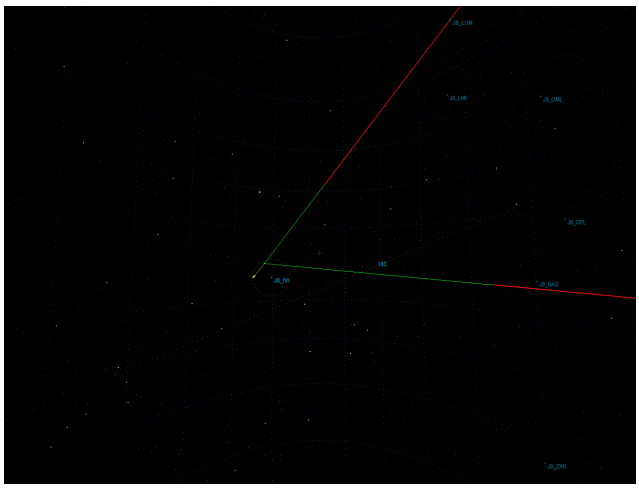

Figure 3 – Calculation of the radiant position obtained with the program UFO.

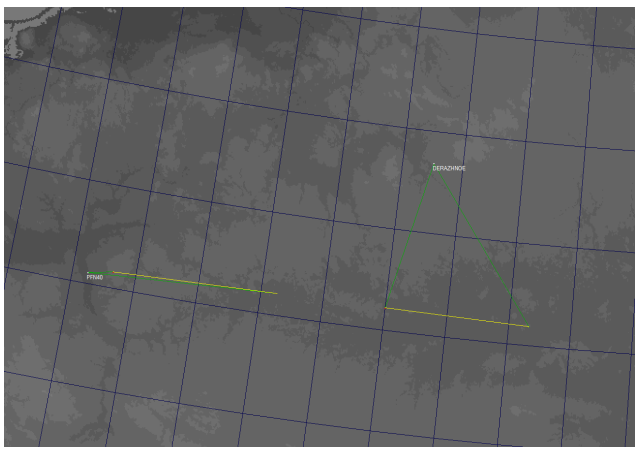

Figure 4 – The basic reconstruction of the meteor grazer trajectory by Belarusian and Polish video cameras.

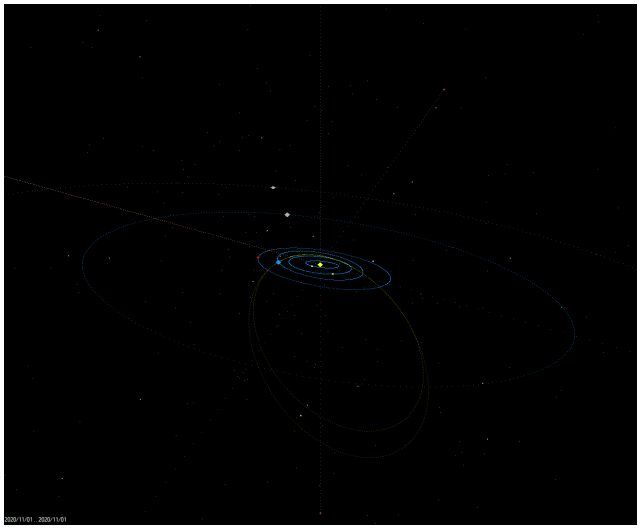

Figure 5 – Determination of the orbit of the meteor grazer in space computed by the UFO software.

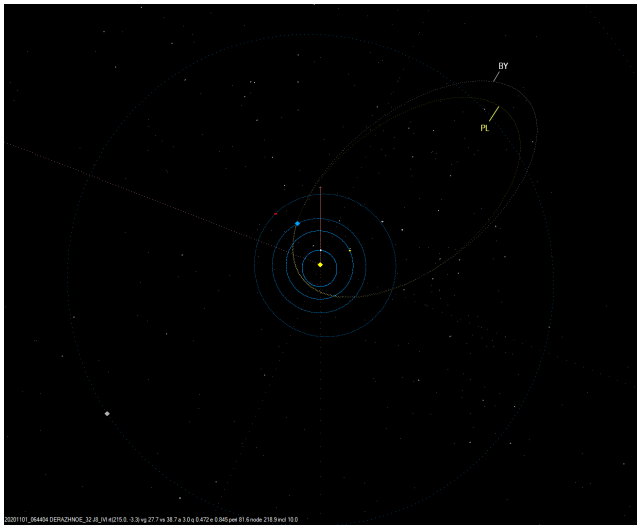

Figure 6 – Projection of the orbit of the meteor grazer in space in the ecliptic plane.

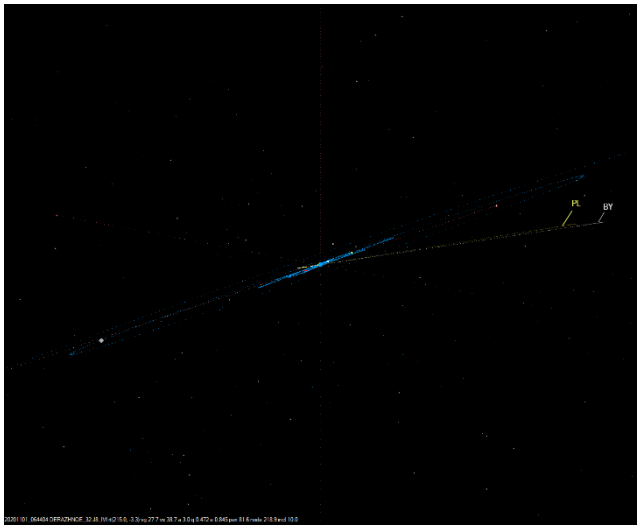

Figure 7 – The orbit of the meteor grazer seen perpendicular to the orbital plane.

The conclusion of Przemysław Żołądek (software PyPN): "*I have the beginning of the Belarusian section at 103.95 km. The end of the Belarusian section at 100.86 km. v_o velocity 30.27 km/s for me, 30.07 km/s for your friend. Very nicely. The beginning of the Polish section was at an*

altitude of 101.12 km. The end of the whole phenomenon for me was 105.37 km, for your friend's 106 km. The starting velocity of the Polish section was 29.11 km/s, for your friend it was 29.46 km/s. The consistency of the results is very satisfactory!"

3 Radio recording

The Radio Meteor System of Ivan Sergey recorded a signal from this grazing meteor on November 1 at 03^h44^m UT lasting about 10 seconds. Of course, I cannot prove 100% this echo signal is caused by this meteor. Have a look at the list of signals during the interval 03^h40^m–04^h00^m UT November 1, 2020 in *Table 1*.

Acknowledgments

Thanks to *Yuri Goryachko* from the astronomical group "Astronominsk[31]" and *Zbigniew Tymiński* of the Polish Fireballs Network[32] for the sending the information about this event and *Przemysław Żołądek* for the analysis of observations. I thank *Paul Roggemans* for correcting this article.

References

Sekanina Z. (1976). "Statistical Model of Meteor Streams. IV. A Study of Radio Streams from the Synoptic Year". *Icarus*, **27**, 265–321.

Table 1 – List of radio echo signals during the interval 03^h40^m–04^h00^m UT November 1, 2020. Bck: Background signal level, Thr: Radio signal triggering (detection) threshold, L: signal duration, A: amplitude signal power, Max: peak signal level, Noise: noise level.

Date and time	Bck	Thr	L	A	Max	Noise
01.11.2020 $3^h41^m00^s$	5680	3000	0.06	908	4370	517
01.11.2020 $3^h41^m23^s$	5600	3000	0.12	1275.3	8607	648
01.11.2020 $3^h41^m49^s$	5700	3000	3.4	13493.98	10727	795
01.11.2020 $3^h42^m19^s$	5412	3000	0.08	936.1	9849	461
01.11.2020 $3^h42^m22^s$	5425	3000	0.14	1127.92	8484	573
01.11.2020 $3^h42^m33^s$	5463	3000	0.42	2528.36	9074	1190
01.11.2020 $3^h43^m54^s$	5595	3000	0.38	2126.44	6904	793
01.11.2020 $3^h44^m06^s$	5888	3000	9.8	37846.32	13683	1301
01.11.2020 $3^h48^m48^s$	5545	3000	0.06	863.82	11337	418
01.11.2020 $3^h50^m23^s$	5454	3000	0.26	1508.7	6744	630
01.11.2020 $3^h54^m46^s$	5405	3000	0.18	2548.82	22743	1104
01.11.2020 $3^h59^m27^s$	5394	3000	0.78	2916.34	7141	1127
01.11.2020 $3^h41^m00^s$	5680	3000	0.06	908	4370	517
01.11.2020 $3^h41^m23^s$	5600	3000	0.12	1275.3	8607	648
01.11.2020 $3^h41^m49^s$	5700	3000	3.4	13493.98	10727	795
01.11.2020 $3^h42^m19^s$	5412	3000	0.08	936.1	9849	461
01.11.2020 $3^h42^m22^s$	5425	3000	0.14	1127.92	8484	573
01.11.2020 $3^h42^m33^s$	5463	3000	0.42	2528.36	9074	1190
01.11.2020 $3^h43^m54^s$	5595	3000	0.38	2126.44	6904	793
01.11.2020 $3^h44^m06^s$	5888	3000	9.8	37846.32	13683	1301
01.11.2020 $3^h48^m48^s$	5545	3000	0.06	863.82	11337	418
01.11.2020 $3^h50^m23^s$	5454	3000	0.26	1508.7	6744	630
01.11.2020 $3^h54^m46^s$	5405	3000	0.18	2548.82	22743	1104
01.11.2020 $3^h59^m27^s$	5394	3000	0.78	2916.34	7141	1127

[31] http://www.astronominsk.org/index_en.htm

[32] https://www.pkim.org/?q=en/node/1583

Possible meteorite fall in Austria

Gábor Kővágó

fotospentax@gmail.com

On 19 November, 2020 at $3^h46^m55^s$ UT a bright meteor lighted up the sky above Austria. Despite the early hour there were many visual observations of the long, low angle flight and the rumbling noise after some seconds. As always, meteorological cameras and dedicated meteor cameras caught the phenomenon across and around the country, additionally some professional and amateur photographs have been taken with great success. Based on the characteristics of the fall and the calculated values, there is a high probability that meteorites reached the ground.

1 Initial data

Firstly, I've seen a picture of this fireball from an Austrian amateur astronomer who was able to photograph the bolide with a clear sky with fine resolution. This has been published on Facebook, from there I could download many others' videos, among them the great montage of the AllSky7 Fireball Network in Germany[34].

Figure 1 – Two all-sky pictures[33]. (author: Rudi Dobesberger).

Of course, some Czech meteorological cameras around the area recorded the event too. The sky was totally cloudy above Slovakia and Hungary so no observations from there. I had to manually calibrate all of the pictures from the different cameras with UFOAnalyser (Sonotaco, 2009).

2 Trajectory

I wrote a program – called Metlab – to help organize, transform, store and export all data to R91 format, which is readable for UFOOrbit (Sonotaco, 2009). Depending on how accurate the calibrated images are, I excluded some of them from the final solution. On the end I kept four different records.

- AllSky7 Fireball Network – Seysdorf, Germany
- AllSky7 Fireball Network – Salzburg, Austria
- Hermann Koberger's image from Fornach, Austria
- 2 images of the meteorological camera of Znojmo, Czech Republic

In all the cases, the maximum calibration error was around or below 0.1 degree, which is acceptable.

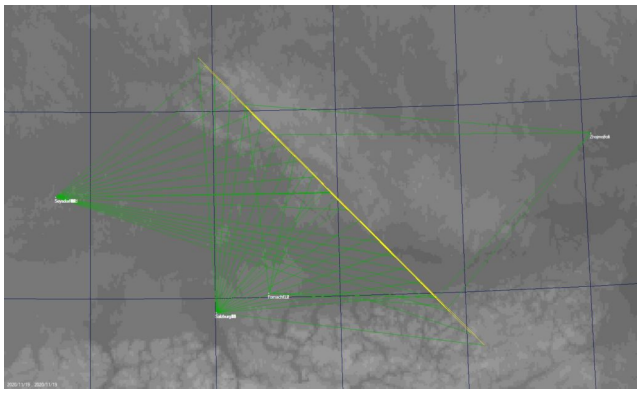

Figure 2 – The ground projection of the fireball path.

[33] https://www.facebook.com/Sternfreunde-Steyr-1682329762060617

[34] https://allsky7.net

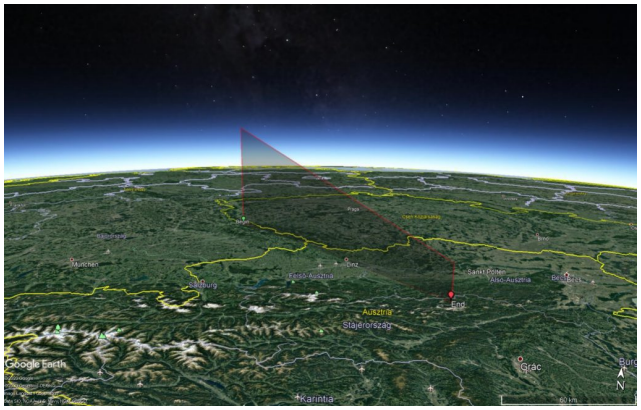

Figure 3 – The fireball trajectory in 3D projection.

The meteor started its luminous path at 89 ± 0.9 km entering the atmosphere with 15.6 ± 0.1° inclination. It moved with an average speed of 13 km/s from Furt im Wald (Germany; N49.2716°, E12.9172°) to Weichselboden (Austria; N47.7026°, E15.1591°) during more than 23 seconds (see *Figures 2 and 3*). The fireball travelled more than 240 km trough the atmosphere and formed a 16 km long cloud of debris at the end of its path. The meteor's fragments decelerated a lot in this phase until less than 2.2 km/s. I could calculate the deceleration by making frame by frame measurements of the Salzburg's and Seysdorf's videos for different heights during the fall. They also contained information about the initial velocity which was greater than 14.3 km/s. The last fragments of the body could penetrate 24.7 ± 0.5 km deep into the Earth's atmosphere. The calculated end of the trajectory was 27.2 km because a program like UFOOrbit tries to approximate the path as a straight line, but with this shallow angle and low speed the gravitational deflection was a whopping 2.5 km! (*Figure 4*).

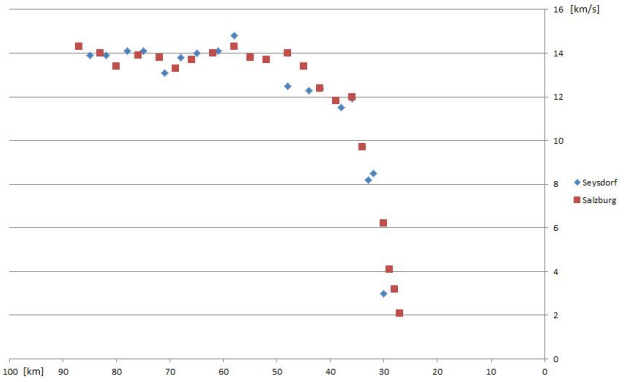

Figure 4 – The velocity and deceleration of the fireball.

3 Dark flight

- The visual observers heard a thunder-like sound after the event.
- The fireball penetrated deeply into the atmosphere.
- The measured velocity slowed down below ablation speed.

All of these suggest that some remaining debris could have reached the ground. I used Metlab – a self-developed program – to calculate the strewn field with the initial data above. Unfortunately, I couldn't find any high atmospheric wind measurement about that date, maybe because of the pandemic. The nearest data came from Munich, I had to use for that. Wind and atmospheric data can be retrieved from the University of Wyoming (Department of Atmospheric Science) website[35]. Taking into consideration the luminosity of the fall, the strewn field picture contains meteorite sizes from 100 g. to 1 kg. Bluish colors mean that the pieces started their dark flight phase from higher, while whites started at lower altitude.

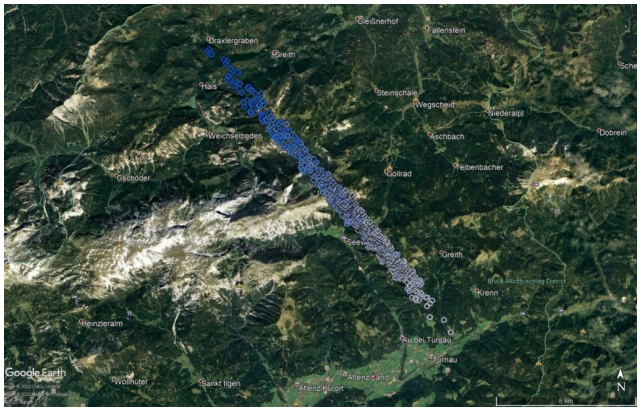

Figure 5 – The strewn field of the fireball.

4 Orbit

As seen from the speed diagram, the deceleration was great along the whole trajectory, so I used only the first three seconds of the flight – where the meteoroid kept its entry velocity quite the same speed – to calculate the orbit of the fireball with the help of UFOOrbit. It's originated from an Apollo type orbit – from the main asteroid belt between Mars and Jupiter – with a very small angle to the plane of the solar system.

The resulting orbital elements are:

- $\alpha = 357.8°$
- $\delta = +22.6°$
- $a = 2$ A.U.
- $q = 0.955$ A.U.
- $e = 0.533$
- $\omega = 205.5°$
- $\Omega = 237°$
- $i = 5°$

Reference

SonotaCo (2009). "A meteor shower catalog based on video observations in 2007-2008". *WGN, Journal of the International Meteor Organization*, **37**, 55–62.

[35] http://weather.uwyo.edu/upperair/sounding.html

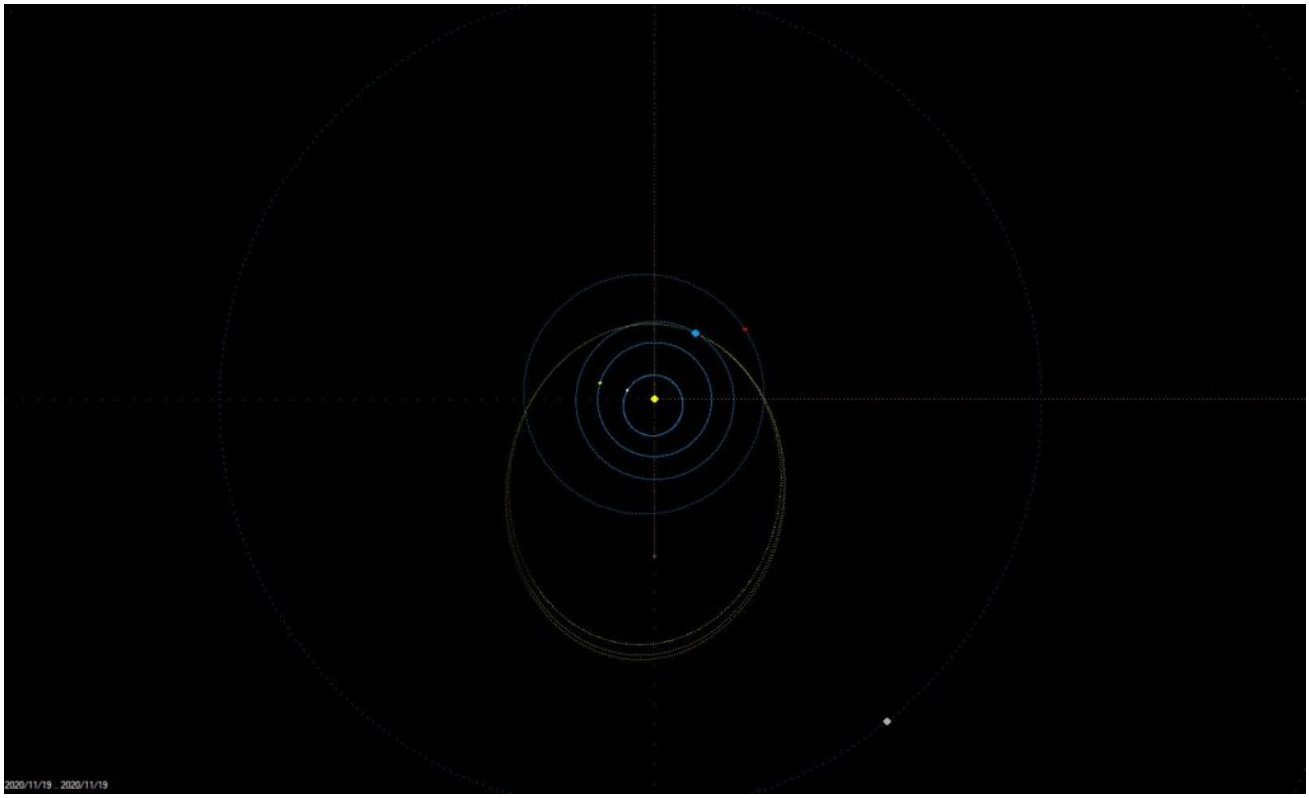

Figure 6 – The orbit plotted in the ecliptic plane

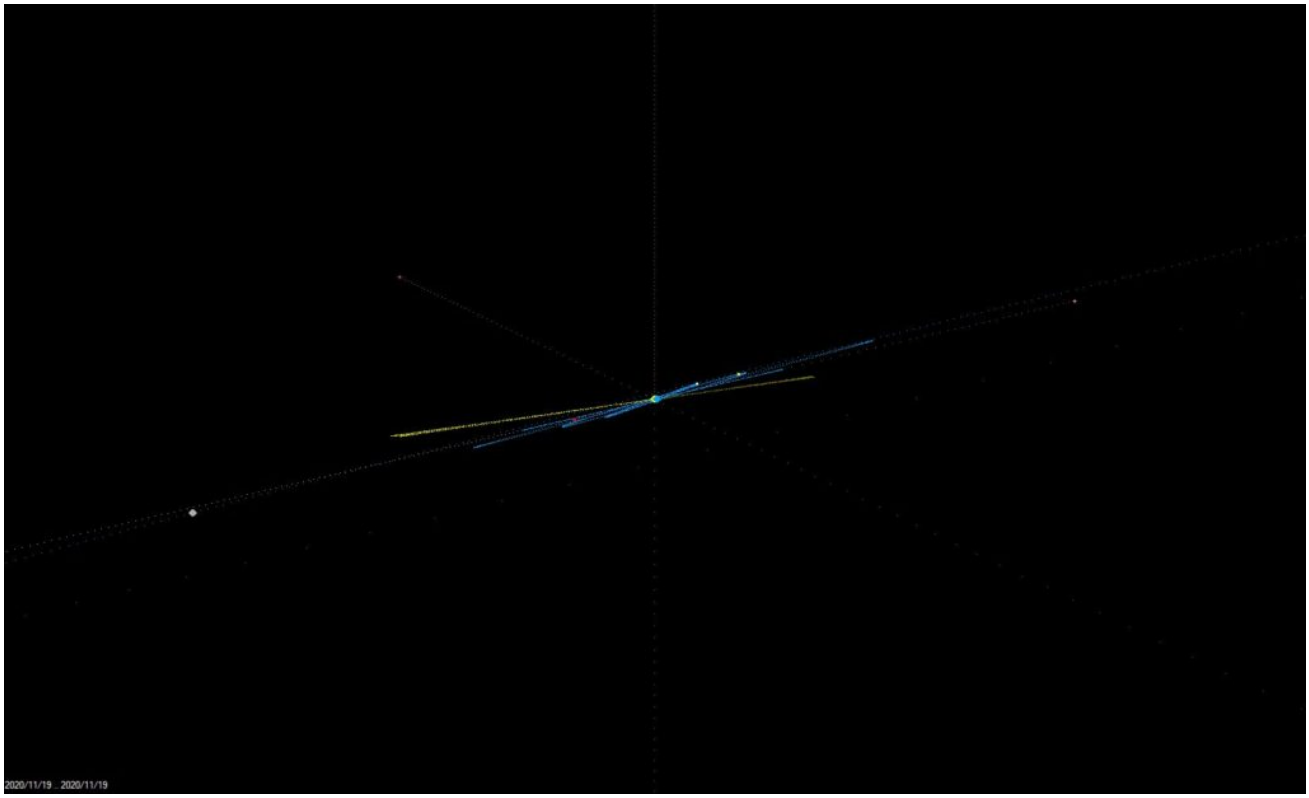

Figure 7 – The orbital plane as seen perpendicular to the ecliptic plane.

Fireball events over Spain in November 2020

José María Madiedo

Instituto de Astrofísica de Andalucía, Spain
madiedo@iaa.es

An overview is presented of the exceptional fireball event by the meteor observing stations operated by the SMART Project from Sevilla and Huelva during November 2020.

1 Introduction

On 16 November 2020, at $2^h49^m09^s$ UT, a beautiful and very bright fireball was spotted over the south of the Iberian Peninsula[36]. The bolide overflew Spain and Portugal. It was generated by a cometary meteoroid that hit the atmosphere at about 227000 km/h. The fireball, which was much brighter than the Full Moon, began at an altitude of about 132 km over Andalusia (south of Spain), and ended at a height of around 61 km over the south of Portugal.

This impressive meteor was recorded in the framework of the SMART project, operated by the Southwestern Europe Meteor Network (SWEMN) from the meteor-observing stations located at Sevilla, La Hita (Toledo) and Calar Alto (Almería). The event has been analyzed by the principal investigator of the SMART project: Dr. Jose M. Madiedo, from the Institute of Astrophysics of Andalusia (IAA-CSIC).

Figure 1 – The exceptionally bright fireball over the south of the Iberian Peninsula on 16 November 2020, at $2^h49^m09^s$ UT.

[36] https://youtu.be/dCnfEIPyP2Y

The mission of MeteorNews is to offer fast meteor news to a global audience, a swift exchange of information in all fields of active amateur meteor work without editorial constraints. MeteorNews is freely available without any fee. To receive a notification: https://www.meteornews.net/newsletter-signup/.

You are welcome to contribute to MeteorNews on a regular or casual basis, if you wish to. Anyone can become an author or editor, send an email to us. For more info read: https://meteornews.net/writing-content-for-emeteornews/

The running costs for website hosting are covered by a team of sponsors. We want to thank Anonymous (3x), Nigel Cunnington, Kai Frode Gaarder, Pierre Tioga Gulon, J Andreas Howell, Koen Miskotte, Paul Roggemans, Mark Upton, Lorenzo Barbieri, Peter Stewart, Carlos Adib and Joseph Lemaire for their financial contributions.

Gifts are welcome to share the maintenance costs. To join the team of sponsors send your donation by PayPal: https://www.paypal.com/pools/c/8ks6DnMamJ

Webmaster & account administrator:

Richard Kacerek (United Kingdom): rickzkm@gmail.com

Contributing to this issue:

- K. Gaarder
- Y. Goryachko
- P. Jenniskens
- R. Kacerek
- M. Kalina
- M. Koseki
- G. Kővágó
- J. M. Madiedo
- K. Miskotte
- E. J. Mroz
- H. Ogawa
- P. Roggemans
- I. Sergei
- H. Sugimoto
- Z. Tymiński
- F. Verbelen
- D. Vida

ISSN 2570-4745 Online publication https://meteornews.net

Listed and archived with ADS Abstract Service: https://ui.adsabs.harvard.edu/search/q=eMetN

MeteorNews Publisher:

Valašské Meziříčí Observatory, Vsetínská 78, 75701 Valašské Meziříčí, Czech Republic